وزارة التعليم العالي والبحث العلمي
Minstry of Higher Education and Scientific Research
جامعة عبدالحميد ابن باديس مستغانم
Abdelhamid Ibn Badis University of Mostaganem
كلية العلوم و التكنولوجيا
Faculty of Sciences and Technology

Order N° : D ...../GC/2015

Thesis Submitted for

DEGREE OF DOCTOR (LMD)

Section: Civil Engineering

Option: Structures & Transportation

Theme

DYNAMIC ANALYSIS OF HIGHWAY BRIDGES UNDER MULTIPLE RANDOM EXCITATIONS

Presented by:

ZELLAT Kaoutar

Presented on: 02/ 06 / 2016 Before a Jury Composed of :

President: Pr. BENDANI KARIM (UMAB Mostaganem)

Examiner: Pr. BRANCI TAIEB (UHBB Chlef)

Examiner: Pr. KASSOUL AMAR (UHBB Chlef)

Supervisor: Pr. KADRI Tahar (UMAB Mostaganem)

Academic Year: 2015 / 2016

Dedication

To my family

Their love and support for that I am grateful

Acknowledgements

This project would not have been possible without the help of Allah, the Most Gracious and the Most Merciful. Then, I would like to gratefully acknowledge the enthusiastic supervision of Pr. KADRI Tahar during the course of research for his support and guidance. He was abundantly helpful and offered invaluable assistance. Deepest gratitude go also to the members of the jury who accept kindly to read this work. I owe an enormous debt of gratitude to Pr. GENEŞ Cemal from the Zirve University (Gazientep, Turkey) for his very helpful contribution.

Special thanks to my friends for sharing literature and information. I would like also to convey thanks to all the members of the administration in the department of Civil Engineering , Sciences and Technology Faculty (Abelhamid Ibn Badis University, Mostaganem), especially Mr. BOUHALOUFA Ahmad for facilitating all the procedures of subscriptions, viva organization and dissertation submission.

I thank also Dr. ZELLAT Imen for her assistance and rectifications of English language, she supplied my thesis with. In addition to the librarians for authorizing all the post grades to consult books in the library at all moment. I wish to express my love and gratitude to my beloved parents and dear family for their understanding and endless love.

Abstract

Many long-span bridges throughout the world are subject to very complicated loading, especially those that are located in wind-prone regions or high seismic zones and that carry both trains and road vehicles. Taking into consideration the multiple types of loading that are concerned and the complexity of the loading combinations, the response analysis of long-span bridges under vehicle, wind loading and seismic forces stand as a great scientific challenge. Moreover, mitigation of the studied vibrations generated by those dynamic loads is of more concern because of their several consequences on the construction components safety.

This thesis focuses on the bridge vibrations and their mitigation under multiple dynamic loads to be: the vehicles, wind and earthquake. The work was divided into two parts; the first was an analytical study of separated coupled systems which are: the bridge-vehicle, the wind-bridge-vehicle and the bridge-seismic with a numerical simulation for each one. In the second part a comparison study was developed between a bridge structure provided by vibrations mitigation mechanism and the same structure without vibrations absorbers under a strong earthquake.

The bridge-vehicle system was modelled as two separated three dimensional subsystems, the equations of motion were established for each model and the interacting forces were determined by the method of moments. A numerical simulation was given to illustrate the analysis using SAP2000 V 16 structural software applied on a cable stayed bridge.

The effect of aerodynamic loads applied on the bridge-vehicle coupled system was studied as a second step, the equations of motion of the three dimensional models were extracted and wind forces acting on the bridge and the vehicle were simulated using analytical approaches. To investigate the dynamic response of the vehicle-bridge system under wind actions an incremental-iterative approach was

used where the nonlinear aerodynamic curves were simulated by a sequence of piecewise connected linearly.

Seismic forces present the most critical loads applied on bridge structure, for that reason, the comparative study on isolated bridges was against earthquake excitation. The study put most emphasis on the time variation of base shear and bearing displacement in order to understand the behaviour of seismically isolated bridges with a comparison between isolated and non isolated bridges. For this purpose seismic forces were applied as a spectrum obtained from recorded strong earthquakes by specialized stations on the three dimensional bridge model using structural software. Three kinds of bearings were studied including N-Z, LRB and FPS since they are considered as the most popular bearings in the field of bridges vibration control.

Résumé

De nombreux ponts à longue travée à travers le monde sont soumis à des chargements très compliqués, en particulier ceux qui sont situés dans les régions menacées par les tourbillons de vent ou zones à séismicité élevée et aussi qui transportent des trains et des véhicules en même temps. Compte tenu des multiples types de chargements concernés et la complexité des combinaisons de chargement, l'analyse de la réponse des ponts à longue travée sous l'effet des véhicules, du vent et des forces sismiques est un grand défi scientifique. En outre, l'atténuation des vibrations étudiées et qui sont générées par ces charges dynamiques est plus pertinente vue leurs nombreuses conséquences néfastes sur la sécurité des éléments de la construction pont.

Cette thèse porte sur les vibrations de la structure pont et leur atténuation dans la présence des charges dynamiques multiples; soit les véhicules, le vent et les tremblements de terre. Le travail a été divisé en deux parties dont la première était une étude analytique des systèmes couplés séparément soient pont-véhicule, vent-pont-véhicule et pont-séisme avec une simulation numérique pour chacun d'eux. Dans la deuxième partie une étude comparative a été établie entre une structure pont munie d'un mécanisme d'atténuation des vibrations et la même structure sans absorbeurs de vibrations sous l'action d'un tremblement de terre.

Le système pont-véhicule a été modélisé comme deux sous-systèmes tridimensionnels séparés, les équations du mouvement ont été établies pour chaque modèle et les forces d'interaction ont été déterminées par la méthode des moments. Une simulation numérique a été établie pour illustrer l'analyse en utilisant le logiciel structurel SAP2000 V 16 appliquée sur un pont à haubans.

L'effet des charges aérodynamiques sur le système couplé pont-véhicule a été étudié dans une deuxième étape, les équations du mouvement des modèles tridimensionnels ont été extraites et les forces du vent appliquées sur le pont et le véhicule ont été simulées à l'aide des approches analytiques. Afin d'analyser la réponse dynamique du système véhicule-pont sous l'action du vent une approche

itérative incrémentale a été utilisée là où les courbes aérodynamiques non linéaires ont été simulées par une séquence de morceaux reliés linéairement.

Les forces sismiques présentent les charges les plus critiques appliquées sur la structure pont, en fonction de cette raison que l'étude comparative sur l'isolation des ponts était sous l'effet de l'excitation de tremblement de terre. L'étude a mis l'accent sur la variation temporelle du cisaillement à la base et du déplacement des appuis afin de comprendre le comportement des ponts isolés sismiquement avec une comparaison entre les ponts isolés et non isolés. A cet effet, les forces sismiques ont été appliquées sous forme d'un spectre obtenu à partir des enregistrements des tremblements de terre établis par les stations spécialisées sur le modèle tridimensionnel de pont en utilisant un logiciel structurel. Trois types d'appuis ont été étudiés, y compris le N-Z, LRB et FPS, car ils sont considérés comme les appuis les plus populaires dans le domaine du contrôle des vibrations des ponts.

ملخص

تخضع العديد من الجسور ذات الفتحات الطويلة في العالم لحمولات معقدة، خاصة تلك التي تقع في المناطق المعرضة للرياح الشديدة أو مناطق ذات شدة زلزالية عالية وأيضا تلك التي تحمل طرقا وسككا حديدية في نفس الوقت. بالنظر إلى الحمولات المتعددة وتراكيبها المعقدة فان تحليل استجابة الجسور ذات الفتحات الطويلة تحت تأثير السيارات، الرياح و القوى الزلزالية يبقى تحديا علميا كبيرا. ولذلك فان تخفيف الاهتزازات المدروسة والناجمة عن هذه الأحمال الديناميكية وثيقة الصلة نظرا لكثرة نتائجها السلبية على سلامة عناصر منشاة الجسر.

ندرس في هذه الأطروحة اهتزازات الجسر وتخفيضاتها بوجود الأحمال الديناميكية المتعددة. وقد جزأنا العمل إلى قسمين حيث في الأول دراسة تحليلية للأنظمة المزدوجة كل واحدة على حدى ليكن: جسر- سيارة, رياح - جسر و جسر - زلزال مع محاكاة رقمية لكل واحد منها .و في الجزء الثاني دراسة مقارنة بين منشأة جسر مزودة بنظام تخفيف الاهتزازات وأخرى عادية تحت تأثير هزة أرضية.

تمت نمذجة النظام جسر - سيارة كنظامين منفصلين، واستخرجنا معادلات الحركة لكل نموذج وحددنا قوى التماس بطريقة العزوم. وأجريت محاكاة رقمية باستعمال برنامج SAP2000 نسخة 16 مطبقة على جسر معلق.

وتمت دراسة تأثير أحمال الرياح الديناميكية على نظام جسر - سيارة كمرحلة ثانية واستنتجنا معادلات الانتقال للنماذج ثلاثية الأبعاد، واستعملت محاكاة أحمال الرياح وفقا لمناهج تحليلية.

تمثل القوى الزلزالية الأحمال الحدية الأكثر تأثيرا على الجسر، ولهذا الغرض أجريت دراسة المقارنة للعزل الزلزالي تحت تأثير الهزات الأرضية. ركزت الدراسة على التغير المؤقت للقص عند القاعدة وعلى انتقال المساند من اجل فهم سلوك الجسور المعزولة زلزاليا مع مقارنة الجسور المعزولة وغير المعزولة.

في هذا الإطار، تم تطبيق القوى الزلزالية على شكل طيف ناجم عن تسجيلات الهزات الأرضية الناتجة عن محطات مخصصة مطبقة على نموذج الجسر الثلاثي الأبعاد باستعمال برنامج حاسوبي.وتمت دراسة ثلاثة أنواع من المساند بما فيها N-Z, LRB, FPS كونها الأنواع الأكثر استعمالا وملائمة في مجال مراقبة اهتزازات الجسور.

Table of Contents

List of Figures

List of Tables

List of Symbols

a: *Amplitude*

α: *Coefficient vector*

$\boldsymbol{A_n(t)}$***:*** *Function of time*

C: *Damping*

E(x): *Variance function*

EI*: Bending Stiffness*

f(t)*: Evolutionary random excitation*

g(t)*: Slowly varying modulation function*

$\boldsymbol{H_y(\omega)}$***:*** *Frequency response function*

$\boldsymbol{\Upsilon_j}$*: Mode participation factor*

K: *Stifness*

M: *Mass*

$\boldsymbol{N_e}$*: Shape function*

$\boldsymbol{n_k}$*: Wave number*

$\boldsymbol{\phi_j}$*: Mass normalized mode*

$\boldsymbol{\Phi_n(x)}$*: Mode shapes*

$\boldsymbol{\Phi_x(\omega,T)}$***:*** *Energy density spectrum*

$\boldsymbol{\omega}$*: Frequency*

$\boldsymbol{\Omega_n}$*: The generalized flexible dynamic frequency*

$\boldsymbol{\Omega_p}$*: The disturbance frequency of the harmonic load*

P(X,t)*: Probability density function*

$\boldsymbol{\psi_j}$*: Eigenpairs*

$\boldsymbol{\psi_k}$*: Basis function*

Q: *Maximum frictional force*

r*: Rank of* $S_{xx}(\omega)$

R*: Radius of curvature*

r(x)*: Road surface profile function*

Rx(τ)*: Cross-correlation function*

Sx(ω)*: Power Spectral Density Function*

t*: Time*

T*: Period*

T_c: *The required time of the harmonic force*

θ_k *:Random phase angle*

V*: Base shear*

W*: Weight*

X*: Random variable*

x(t)*: Time variable function*

$X_T(\omega)$*: Fourier transform function*

$\tilde{x}, \tilde{y}, \tilde{z}$: Response vectors

$\ddot{x}_g(t)$*: Ground acceleration*

$\ddot{\tilde{x}}_g(t)$*: Pseudo ground acceleration*

y*: displacement vector*

y(x, t)*: is the dynamic displacement*

List of Abbreviations

2D: *Two Dimensions*

3D: *Three Dimensions*

AASHTO: *American Association of State of Highway Transportation Officials*

ASD: *Acceleration Spectral Density*

CA: *Cellular Automaton*

CIP/PS: *Cast-In-Place/Prestressed*

CQCA: *Conventional Complete Quadratic Combination Algorithm*

DOF: *Degree of Freedom*

EP: *Error Percentage*

FEM: *Finite Element Method*

FEMs: *Finite Element Models*

FPS: *Friction Pendulum System*

FT: *Fourier Transform*

ISO: *International Organization for Standardization*

LRB: *Lead Rubber Bearing*

MOM: *Method of Moments*

PDF: *Probability Density Function*

PEM: *Pseudo Excitation Method*

PSD: *Power Spectral Density*

PSDF: *Power Spectral Density Function*

NDT: *Non Destructive Testing*

RQPE: *Real Quantity of Percentage Error*

SCMs: *Structural Component Models*

SVD: *Singular Value Decomposition*

ULS: *Ultimate Limit State*

VB: *Vehicle Bridge system*

WVB*:* *Wind Vehicle Bridge system*

Chapter I

Research Background

Introduction

The interaction between bridges, vehicles, winds and earthquakes presents a complicated dynamic problem; a large number of variables controls the dynamic interaction of the system. An insight into the mechanics of this problem is essential to develop an efficient numerical method for its analysis. In this way, a large number of analytical and experimental investigations have been carried out in the past to study the dynamic behaviour of bridge decks that are subjected to time varying loads.

There is growing interest nowadays in the process of designing bridge engineering structures to withstand dynamic loads. Essentially, dynamic analyses focus on evaluation of time dependent displacements, from which the stress state of the structure in question can be computed. The most basic pieces of information needed for this are the natural period which is a function of the structure's mass and stiffness, and the amount of available damping (or, equivalently, the amount of energy that can be absorbed by the structure).

This section gives an overview on the bridges failure under dynamic loads over the world in the last four decades in addition to the progress of scientific research in bridge design and health monitoring using analytical, numerical and experimental methods.

I.1. Bridges Dynamic Loads and Failure

Bridges are an important part of the surface transportation system. Failure in a bridge operation can cause severe economic, environmental and/or social consequence. A considerable number of bridge failures, caused by natural or human-made forces, can be prevented by theoretical studies, updating design criteria, re-evaluating safety and structural maintenance.

Today, about one half of the bridges in the world have aged more than 40 years. On average, about 12% of existing bridges are already structurally deficient and need repairs, strengthening, maintenance and perhaps closure (Kappos,

A.J.2002). The critical situation can be where two or more failure causes happen at the same time. For example, a structurally deficient bridge under overloading conditions can be significantly in danger of collapse. Moreover many highway bridges have been built throughout the world in the past few decades to meet the economic, social and recreational needs of communities. Some of these bridges have main span lengths of more than 1000m, such as the Akashi Kaikyo Bridge (1991m, Japan, 1998), the Xihoumen Bridge (1650m, China, 2009), the Great Belt Bridge (1624 m, Denmark, 1998), and the Run Yang Bridge (1490 m, China, 2005). Some of them carry both road and rail traffic, such as the Tsing Ma Bridge (1377m, Hong Kong, 1997), the Minami Bisan-Seto Bridge (1100m, Japan, 1989), and the 25 de Abril Bridge (1013m, Japan, 1966). Most of these bridges are located in wind-prone regions, and long-span length makes them susceptible to strong crosswinds (Chen, Z.W.2010).

Further, the increases in traffic volume and gross vehicle weight that accompany economic development significantly affect the local dynamic behaviour of such bridges. Most of highway bridges are multi loaded since they are simultaneously suffering from a combination of effects of dynamic loading, such as railway, highway, wind and seismic loading. Multi-load bridges play significant roles in the entire transportation system, and thus it is critically important to protect such immense capital investments and ensure user comfort and bridge safety.

I.1.1. Bridges Failure Meaning

In the broadest sense, failure of a bridge occurs whenever it is unable properly to fulfil its function. It may be found that a bridge is unable to carry its full design loads and, for this reason, a load restriction is placed on the bridge. This is, in a sense, a failure. A gain, the form of the bridge may be such that, in periods of high wind, traffic is unable to cross.

Bridge failures may happen at any stage of the bridge life time. Collapse can be present in older bridges, newly designed bridges, and even those which are under construction. Deterioration of the bridge elements and inadequate design criteria in older codes can be two main reasons for collapse of old bridge structures.

I.1.2. Failure Causes

Beside deterioration and lack of regular inspection and maintenance, design errors and unpredicted loads can also cause collapse of bridges including new and/or old bridge structures. Hydraulic loads, collision, overloading, deterioration, earthquake and construction have been measured as the most destructive causes of bridge failures. For example, deteriorated elements subjected to overloads or earthquake excitations might be a source of damage and possible structural collapse.

In practice, failures occur in different forms in a material and are likely to be different for steel, concrete, and timber bridges. Common types of failure that occur in steel bridges are yielding (crushing, tearing or formation of ductile or brittle plastic hinges), buckling, fracture and fatigue (reduced material resistance, reversal of stress in welds and connections, vibrations), shearing and corrosion. Large deformations due to impact, sway, violent shaking during seismic events, erosion of soil in floods or settlement due to expansive soils may induce failure in both steel and concrete bridges.

The most common causes of bridge failure include: overstress of structural elements due to section loss, design defects and deficiencies, long- term fatigue and fracture, failures during construction, accidental impacts from ships, trains and aberrant vehicles, fire damage, earthquakes, lack of inspection and unforeseen events. The data base of bridges inspection all over the world shows that the most touched types of bridges between the periods 1989 to 2001 are the steel construction and beam/girder bridges due to corrosion and traffic loading (Wesley,C. 2014) however, this estimation can’t be generalized for all kinds of

bridges that depends on the country number of bridges for each type, the general climate conditions and population.

I.1.3. Failure Mechanism

Bridges have historically presented significant vulnerabilities during major seismic, wind and over loading traffic events, they present fundamental infrastructure to evacuate the affected people and to transport the emergency equipment and materials when a natural or human events occurs. For this raison, their loss of function or failure will result the loss of lives and several economical consequences. The following summarizes the failure mechanisms of highway bridges, including the observation of span collapse, structure component damages, and other structural component damages.

I.1.3.1. Unseating

During earthquakes, structure displacement is a major cause of highway bridge span damage and failure. Excessive displacements in the longitudinal direction can fail the bridge via unseating of the superstructure as shown in Fig.I.1.

Fig. I.1 Example of Unseating Failure in the 1999 Chi-Chi Earthquake in Taiwan
(Viewed on https://mceer.buffalo.edu)

Moreover, deck pounding or unseating failure can occur during hurricane due to serge and wave loads because of the lack connection between the bridge components. That is particularly possible for simply supported highway bridges if seats or corbels located at the abutments or piers don't possess sufficient length. The entire superstructure span can become unseated, resulting in sudden bridge collapse (Ataei , N . *et al.* 2012).

Moreover, the low stiffness, light weight and long spans of bridges make the lateral and torsional stiffness of these bridges low in comparison with regular non-cable bridges. Bridges built in vast areas such as rivers, coasts, and valleys are exposed to wind loads. The speed of the wind through a bridge varies frequently; in some moments it decreases and in some moments it increases.

Due to the above mentioned conditions, a lot of collapses and performance failures have happened since the bridge invention. Tacoma Narrows Bridge (Wiki Failures) and Silver Bridge over Ohio River are two examples of cable bridge failures which led to complete collapse of structures. In Fig.I.2 the Tacoma Narrows Bridge is shown at the moment of collapse, it can be observed the total failure of the super structure despite the columns and substructure strength.

Fig. I.2: Tacoma Narrows Bridge after Collapse Due to Wind Fluttering
(Viewed on https://en.wikipedia.org)

I.1.3.2. Column Flexural Failure

The two main reasons for column failure are the insufficient deformation capacity which results in flexure-shear and flexure failure and the lack of shear resistance which results in shear failure, Fig.I.3 is an example of column flexural failure which comes from the deficient reinforcement design for the unexpected seismic shaking, characterized by inadequate strength or inadequate ductility.

Flexural failure usually occurs when the longitudinal confinement is not sufficient, which leads to concrete crush as strains exceed the capacity and the column is not tough to sustain the imposed flexural deformations without failure.

Fig. I.3 Column Flexural Failure Due to Insufficient Ductility in the 1995 Kobe Earthquake
(Viewed on http://www.eng.buffalo.edu)

I.1.3.3. Column Shear Failure

The column shear failure is characterized by the failure of the transverse shear reinforcement. Shear failure resulting from seismic shaking is more prominent in old highway bridges due to insufficient shear reinforcement resulting in brittle and sudden failure. Such failures can occur at relatively low structural displacements,

at which stage the longitudinal reinforcement may have not yet yielded. Examples of shear failure can be found in several of the historical earthquakes as illustrated in Fig.I.4. Failure of a column can result in loss of vertical load carrying capacity which is often the primary cause of bridge collapse.

Fig. I.4 Shear Failure of Columns in Hanshin Expressway
(Viewed on http://www.fhwa.dot.gov)

I.1.3.4. Joint Failure

Joint failure can occur for various reasons, but experience shows that failures falls into several distinct categories. This list includes, but is not limited to: shipping and handling damage, improper installation/insufficient protection, during/after installation, improper anchoring, guiding, and supporting of the system, anchor failure in service, corrosion, system over-pressure, excessive bellows deflection, torsion, bellows erosion, and particulate matter in bellows convolutions restricting proper movement.

Joints may be exposed to critically damaging actions when the joints lie outside of the superstructure as shown in Fig.I.5. Although joint failures occurred in previous earthquakes, significant attention was not paid to joints until several spectacular failures were observed following the 1989 Loma Prieta earthquake.

Fig. I.5 Joint Damage to the Embarcadero Viaduct in San Francisco
(Viewed on http://www.fhwa.dot.gov)

1.1.3.5. Damages in Foundation

Reports of foundation failures during hard phenomena like wind and earthquakes are relatively rare, with the notable exception of situations in which liquefaction occurred. It is not clear whether failures are indeed that rare or whether many foundation failures are undetected because they remain underground. There are many reasons why older foundations might be vulnerable. Piles might have little confinement reinforcement, yet be subjected to large deformation demands. Older spread and pile-supported footings rarely have top flexural reinforcement or any shear reinforcement.

When considering the bridge structure alone, the actual behaviour of the bridge under dynamic loads may significantly differ from that from the analysis since the response of a bridge depends not only on the bridge itself, but also on the characteristics of the dynamic loads to which it is subjected.

The assumption of fixed support for a bridge upheld on soft soil ignores the interaction effects that result from the scattering of waves when reaching the foundation surface (kinematic interaction) and the flexibility and energy

dissipation of foundation-soil system (inertial interaction). These interaction effects lead to dynamic responses that may differ considerably in amplitude and frequency from what is obtained when a fixed support is assumed.

Foundation damage associated with liquefaction-induced lateral spreading has probably been the single greatest cause of extreme distress and collapse of bridges. The problem is especially critical for bridges with simple spans. The 1991 Costa Rica earthquake provides many examples of foundation damage. Fig.I.6 shows an abutment that rotated due to liquefaction and lateral spreading.

Fig. I.6 Abutment Failure during the 1991 Costa Rica Earthquake
(Viewed on http://www.u-cursos.cl)

The failure mechanism of pile is related to the force conditions of pile under dynamic loading, so the failure mechanism can be subcategorized to three types (Datta, T. K. 2010):

(1) The failure caused by additional dynamic stress that is induced by vibration. Such failure mode generally occurs when the ground motion level is high, the quality of pile is poor, and the soil layer is weak. Under such conditions, the reaction forces to piles from surrounding soil are relatively small, the deformation of piles are relatively large, and relatively big additional dynamic stresses are generated in pile shaft.

(2) The failure caused by additional static stress that is induced by soil lateral movement. Such failure mode usually occurs at bank-side site.

(3) The length of pile penetrating into steady soil layer is not enough or pile tip don't arrive at steady soil layer, so pile foundation is easy to lose bearing capacity due to liquefaction of sandy soil under dynamic loading.

I.2. Literature Review on Bridges Dynamics Analysis

Bridge vibration has been a concern to bridge designers and users for years. Much of the earlier studies of bridge vibration were begun after bridge failures due to vibration. Perhaps the most well known was Tacoma Narrows Bridge failure due to lateral vibrations from wind. Many of the problems however have only recently been addressed, through analytical and field studies.

Currently, bridge vibration studies include: suspension bridges, cable-stayed bridges, curved bridges, prestressed concrete bridges, and high speed transit structure bridges. Analytical studies and computer models are being used to handle such items as acceleration and deceleration of vehicles, surface roughness of the bridge deck, and multi-vehicle loading.

I.2.1. Field Tests

Much of the initial work in bridge vibration began with actual bridge testing. This enabled the researchers to identify the factors that most affected bridge vibrations. The initial tests involved simple span bridges only. This was followed by the study of multispan bridges and then by more complicated bridges, such as suspension bridges.

There were five simple span dynamic bridge field studies. (Kinnier, K.H. and Mckeel, W.T. 1965) looked at the influence of the bridge substructure on the dynamic behaviour. Their first study compared conventional and elastomeric influence bearings on a rolled-beam, composite bridge. In their second study, they

compared tall and short piers on a composite bridge by measuring strains and deflections caused by a 3-axle tractor-trailer. The earliest of the other three studies involved AASHO Road Tests. These involved 18 three beam bridges with 14 different vehicles. Both deflections and strains were measured.

The next study was by (Lashomb, S. M. *et al.*1985). They tested two steel stringer bridges and three plate-girder bridges with the load applied by a 2-axle, 10 ton dump truck. They measured deflections with a deflectometer and accelerometers. The remaining study was by (Biggs, J. M. 1964). He tested two single medium span stringer types through girder bridges, with the load applied by a 2-axle dump truck. The deflection was measured by deflectometers at mid-span, and strains and accelerations were measured on the axles of the truck.

Seven field studies were made involving both simple and continuous span bridges. (Billing, J.R. and Green, R. 1984) reviewed three series of dynamic tests done in Ontario, Canada in 1956 to 1957, 1969 to 1971, and 1980. In the first two series, deflection was measured, while in the last series, acceleration was measured. In the last two series, test vehicles were used. (Funkhouser, D. W. and Heins) tested 40 bridges with five different types of vehicles obtaining stress versus time records at several locations along the bridge.

(Green, R. 1997) summarized 52 bridge tests involving with both a test vehicle and normal traffic loading. He measured the deflections with a deflectograph. (Eyre, R. and Tilly, G. P. 1977) tested 23 bridges for damping characteristics by exciting 22 of them with reciprocating weights and one by dropped weights. (Schilling, C.G., Klippstein, K.H., Barsom, J.M. and Blake, G.T. 1978) studied fatigue in bridges by summarizing 15 field bridge tests subject to traffic loading.

Perhaps the most complete study was that by (Gaunt, J. T. and Sutton C. D. 1981). They tested 62 bridges under normal traffic and a test vehicle. Both accelerations and deflections were measured. Ten field studies were made specifically on continuous span bridges. (Green, R. 1977) studied two 3-span plate girder bridges with a tractor trailer combination. They measured strains for a

variety of loading cases. At about the same time as Edgerton and Beecroft‘s study, (Hayes, J. M. and Sbarounis, J. A. 1997) tested a 3-span, continuous, I-beam bridge by measuring strains due to vibrations caused by a test truck.

Another study in the same field was a test on an 8-span plate girder bridge and a 6-span rolled beam-bridge with 2-axle and 3-axle trucks and normal traffic where deflections were measured with a deflectometer. The next study was by (Gillespie, T. D. 1992) who tested four continuous span bridges. The loading was a van truck and a tractor trailer combination, and response was measured by strain gages.

In the last years dynamic testing and dynamic analyses has become a very useful tool on the health monitoring of the bridges all over the world. The strength and integrity of bridges will decrease during the serviceability stage due to the degradation mechanisms induced by traffic, wind, temperature, corrosion and environmental deterioration.

In order to detect the abnormal changes through non-destructive testing (NDT) technology or periodical evaluation (Montgomery, D. C. 2008), a fundamental but critical step is to obtain dynamic responses at some critical bridge locations. The mostly concerned dynamic responses of a multi-load bridge may include global response (displacement, velocity, and acceleration) and local response (acceleration and stress), which are mainly induced by traditional live load (such as highway, railway and wind loading) or accidental live load (such as ship impact and earthquake). Structural intrinsic characteristics could be extracted from these dynamic responses (or vibration signals) to develop all sorts of vibration-based damage detection techniques.

A well-known family of them is based on structural dynamic characteristics (such as frequencies, mode shapes, damping ratios, and strain mode shapes) and their derivatives. Some damage identification approaches were proposed based on the dynamic responses of bridge structures under moving vehicle loads. The dynamic responses of highway bridges also could be used for structural

assessment, for example, fatigue assessment at the critical locations over the service history of the bridge and assessment of extreme events such as complex traffic congestion coupled with moderate or even strong wind.

I.2.2. Bridge Structural Modelling and Analysis

Design of reinforced concrete bridges is normally done on the basis of a structural analysis. The purpose of the analysis is to find a distribution of sectional forces which fulfils equilibrium and is suitable for design. In the past structural analyses were often done with simplified models, for example two-dimensional (2D) equivalent beam or frame models. Such models are not able to describe the distribution of forces in transversal directions. Therefore a design according to a 2D equivalent model will not be according to the true linear elastic distribution, even though the design might fulfill requirements in ultimate limit state (ULS) after sufficient plastic redistribution (Mattias, Grahn. 2012).

With the recent introduction of (EUROCODE 2, 2005), (ASHTO, 2003) and the SWEDISH Transport Administrations the demands on structural analysis has been updated. A model for structural analysis has to be able to describe the response of the structure in its entirety. In practice this implies that 2D equivalent models are not sufficient and a 3D analysis describing the forces in multiple directions is needed.

I.2.2.1 Structural Modelling

Structural modelling is a tool to establish three mathematical models, including a structural model consisting of three basic components: structural members, joints (nodes, connecting edges or surfaces), and boundary conditions (supports and foundations); a material model and a load model. For designing a new structure, connection details and support conditions shall be made as close to the computational models as possible. For an existing structure evaluation, structures shall be modelled as close to the actual as-built structural conditions as possible.

The correct choice of modelling and analysis methods depends on the importance of the structure, the purpose of structural analysis and the required level of response accuracy.

Different types of elements may be used in bridge models to obtain characteristic responses of a structure system. Elements can be categorized based on their principal structural actions including: truss element, beam element, frame element, plate element, shell, plane element, solid and the NlLink element. Selecting the proper boundary condition has an important role in structural analysis. Effective modelling of support conditions at bearings and expansion joints requires a careful consideration of continuity of each translational and rotational component of displacement. For a static analysis, it is common to use a simpler assumption of supports (i.e. fixed, pinned, roller) without considering the soil/foundation system stiffness. However for dynamic analysis, representing the soil/foundation stiffness is essential. In most cases choosing a [6×6] stiffness matrix is adequate. There are two types of loads in a bridge design:

- **Permanent Loads:** Loads and forces that are assumed to be either constant upon completion of construction or varying only over a long time interval (AASHTO 3.2). Such loads include the self weight of structure elements, wearing surface, curbs, parapets and railings, utilities, locked-in force, secondary forces from post-tensioning, force effect due to shrinkage and due to creep, and pressure from earth retainments (CA 3.3.2).
- **Transient Loads:** Loads and forces that can vary over a short time interval relative to the lifetime of the structure (AASHTO 3.2). Such loads include gravity loads due to vehicular, railway and pedestrian traffic, lateral loads due to wind and water, ice flows, force effect due to temperature gradient and uniform temperature, and force effect due to settlement and earthquakes (CA 3.3.2).

The formulation of a mathematical model using discrete mathematical elements and their connections and interactions to capture the prototype behaviour is called Discretization (Barker, R. M. and Puckett, J. A. 2013). For this purpose:

Joints/Nodes are used to discretize elements and primary locations in structure at which displacements are of interest, elements are connected to each other at joints, masses, inertia, and loads are applied to elements and then transferred to joints, a typical model discretization for a bridge bent is shown on fig.I.7.

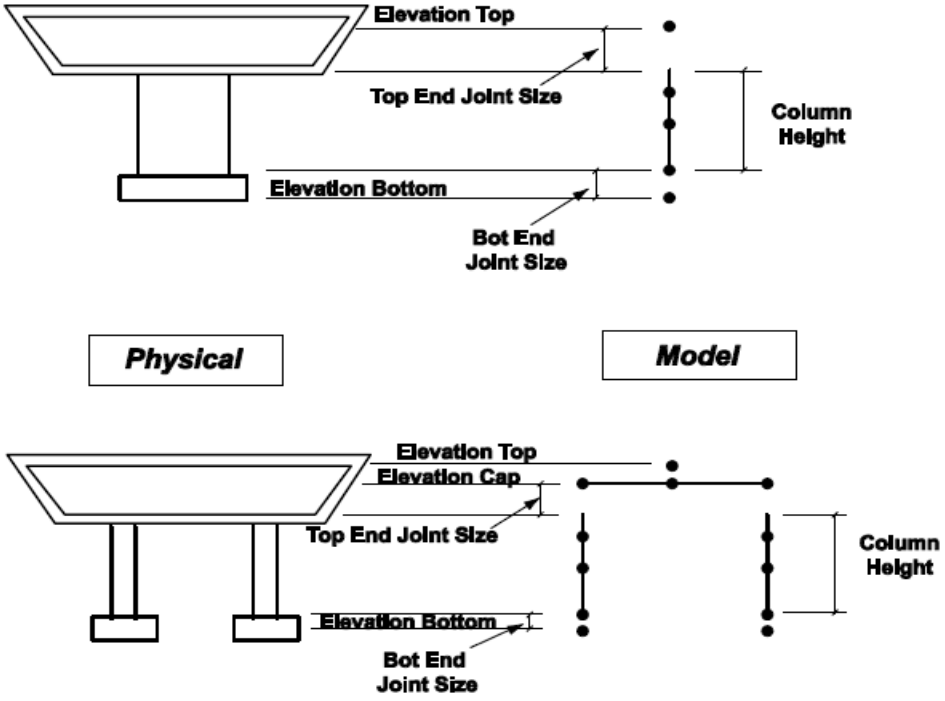

Fig. I.7 Model Discretization for Monolithic Connection
(Structural Modelling and Analysis 2015)

Based on the Structural Modelling Guidelines, the bridge construction can be modelled by the following three steps:

- **Lumped-Parameter Models (LPMs):** The bridge mass, stiffness, and damping components are usually combined and lumped at discrete locations. It requires significant experience to formulate equivalent force-deformation with only a few elements to represent structure response. For a cast-in-place prestressed (CIP/PS) concrete box girder superstructure, a beam element located at the centre of gravity of the box girder can be used. For non-box girder structures, a detailed model will be needed to evaluate the responses of each separate girder.

- **Structural Component Models (SCMs):** Based on idealized structural subsystems/elements to resemble geometry of the structure, structure response is given as an element force-deformations relationship. Gross moment of inertia is typically used for non-seismic analysis of concrete column modelling. Effective moment of inertia can be used when analyzing large deformation under loads, such as prestressing and thermal effects. Effective moment of inertia is the range between gross and cracked moment of inertia.

- **Finite Element Models (FEMs):** A bridge structure is discretized with finite-size elements. Element characteristics are derived from the constituent structural materials (AASHTO 4.2). Fig. I.8 shows the levels of modelling for seismic analysis of bridge structures.

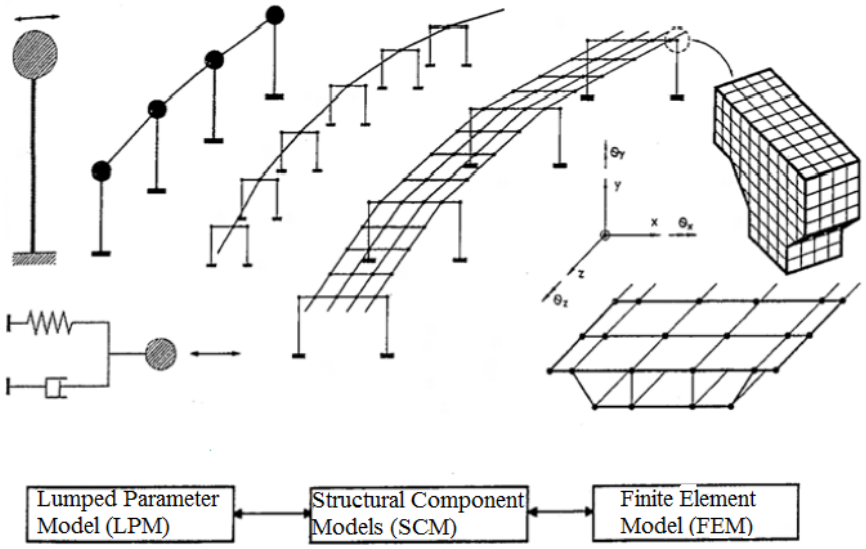

Fig. I.8 Levels of Modelling for Seismic Analysis of Bridge
(Priestley, et al 1996)

I.2.2.2 Structural Analysis and Analytical Solutions

Structural analysis is a process to analyze a structural system to predict its responses and behaviours by using physical laws and mathematical equations. The main objective of structural analysis is to determine internal forces, stresses and deformations of structures under various load effects.

Analytical equations to describe bridge vibration behaviour were initially developed by (Inglis,C.E.1913) for railroad bridges and (Timoshenko, S. and Young, D.H. 1940) for suspension bridges in the early 1900‘s. In the 1950‘s and early 1960‘s actual bridge tests, particularly of simple single span bridges, were undertaken to study bridge vibrations and to understand the parameters involved. Also during this time, model testing in the laboratory and simplified beam and moving force analytical models were used to study bridge vibrations.

As computers became more available in the 1960‘s and 1970‘s, much of the analytical work was done in developing computer models to describe both bridge vibrations and vehicles with sprung and unsprung mass models. During the same period, actual field tests of bridges began on more complicated bridges such as continuous bridges.

Typically, during the analytical phase of any bridge design, finite-element-based structural analysis programs are used to evaluate the structural integrity of the bridge system. Most structural analysis programs employ sound, well-established finite-element methodologies and algorithms to solve the analytical problem. Others employ such methods as moment distribution, column analogy, virtual work, finite difference, and finite strip, to name a few. It is of utmost importance for the users of these programs to understand the theories, assumptions, and limitations of numerical modelling using the finite-element method, as well as the limitations on the accuracy of the computer systems used to execute these programs. Many textbooks are available to study the theories and application of finite-element methodologies to practical engineering problems. It is strongly recommended that examination of these textbooks be made prior to using finite-element-based computer programs for any project work. For instance, when choosing the types of elements to use from the finite-element library, the user must consider some important factors such as the basic set of assumptions used in the element formulation, the types of behaviour that each element type captures, and the limitations on the physical behaviour of the system. Other important issues to consider include numerical solution techniques used in matrix

operations, computer numerical precision limitations, and solution methods used in a given analysis.

There are many solution algorithms that employ direct or iterative methods, and sparse solver technology for solving the same basic problems; however, selecting these solution methods efficiently requires the user to understand the best conditions in which to apply each method and the basis or assumptions involved with each method. Understanding the solution parameters such as tolerances for iterative methods and how they can affect the accuracy of a solution are also important, especially during the nonlinear analysis process.

Dynamic analysis is increasingly being required by many design codes today, especially in regions of high seismicity. Response spectrum analysis is frequently used and easily performed with today's analysis tools; however, a basic understanding of structural dynamics is crucial for obtaining the proper results efficiently and interpreting analysis responses. Basic linear structural dynamics theory can be found in many textbooks. While many analysis tools on the market today can perform very sophisticated analyses in a timely manner, the user too must be more savvy and knowledgeable to control the overall analysis effort and optimize the performance of such tools.

Conclusion

In general it could be said that verification and interpretation of 3D bridge structure behavior can be difficult under multiple presence of dynamic loads. The combination of dead and live loads with the bridge model presents a very complex problem to solve; a big number of parameters have to be considered.

Studies shown above were based mainly on either static amplificated equivalence, field test with strict parameters and an existing bridge construction or numerical analyses applied on a simplified bridge structure and one type of dynamic loading.

Since every bridge structure presents a dynamic model because of its own properties (length, type, elevation, climatic conditions, service type) it is not advised to consider a model and apply its results on the others, moreover an existing construction and in construction one don't behave in the same way.

In short, since modelling in 3D is in principle requirement for structural analysis today, it is beneficent to analyze the dynamic behaviour of a bridge under dynamic loads with a multiple presence and apply a model for each geometric kind of bridge construction.

Chapter II
Random Vibrations

Introduction

Every structure in civil engineering constitutes a continuous system when subjected to a time varying load, this system undergoes a vibratory behaviour. Vibrations are an engineering concern in this area because they may cause a catastrophic failure (complete collapse) of the structure because of excessive stresses and amplitudes (resulting mainly from resonance) or because of material fatigue over a period of time.

Vibrations of continuous systems is a particularly interesting subject where it is important to realize theoretically how do strings, rods, beams, plates, shells and other continuous bodies vibrate, with which shapes and at what frequencies, how they respond when subjected to dynamic exciting forces and pressures , all these information must be well studied to achieve the structure security.

Vehicle loads, earthquakes and wind are highly unpredictable events and time varying forces; their time of occurrence, frequency value, magnitude and duration are all variables which can't be known in advance that's why they are considered as source of random vibration and the best way of their characterization is the probability methods.

Random vibrations, which in recent years has found extensive applications in structural dynamics, machine vibrations, earthquake engineering, as well as in non-destructive testing and identification. We note that the concepts of random variables and random (or stochastic) processes, the latter being functions of both space and time in their most general form.

For instance, wind, water wave and earthquake-induced ground motions are loadings of random nature. Specifically, the former two types of loads can be viewed as comprising a rapidly fluctuating part superimposed on a slowly varying mean value. They can be classified as stationary random loads in the sense that there is a certain periodicity (and hence some predictability) in the fluctuating part. Earthquake loads are fully random and classified as non-stationary, a term that will be explained later on. Finally, there is some mild

stochasticity inherent in traffic induced loads, simply because the movement of vehicles cannot be fully controlled.

This section is a theoretical research background on vibrations but puts most emphasis on bridges vibration sources and mathematical structure analyses, where the dynamic loads applied on bridges were considered as random excitation.

II.1. Basic Terminology of Structural Vibration

The term vibration describes repetitive motion that can be measured and observed in a structure. Unwanted vibration can cause fatigue or degrade the performance of the structure. Therefore it is desirable to eliminate or reduce the effects of vibration.

In other cases, vibration is unavoidable or even desirable. In this case, the goal may be to understand the effect on the structure, or to control or modify the vibration, or to isolate it from the structure and minimize structural response.

Vibration analysis is divided into sub-categories such as free vs. forced vibration, sinusoidal vs. random vibration (Ryan, T. P. 2000), and linear vs. rotation-induced vibration.

Free vibration: Is the natural response of a structure to some impact or displacement. The response is completely determined by the properties of the structure, and its vibration can be understood by examining the structure's mechanical properties. For example, when you pluck a string of a guitar, it vibrates at the tuned frequency and generates the desired sound. The frequency of the tone is a function of the tension in the string and is not related to the plucking technique.

Forced vibration: Is the response of a structure to a repetitive forcing function that causes the structure to vibrate at the frequency of the excitation. For example, the rear view mirror on a car will always vibrate at the frequency associated with

the engine's RPMs. In forced vibration, there is a relationship between the amplitude of the forcing function and the corresponding vibration level. The relationship is dictated by the properties of the structure.

Sinusoidal vibration: Is a special class of vibration, the structure is excited by a forcing function that is a pure tone with a single frequency. Sinusoidal vibration is not very common in nature, but it provides an excellent engineering tool that enables us to understand complex vibrations by breaking them down into simple, one-tone vibrations. The motion of any point on the structure can be described as a sinusoidal function of time.

Random vibration: Is very common in nature, the vibration you feel when driving a car result from a complex combination of the rough road surface, engine vibration, wind buffeting the car's exterior, etc. Instead of trying to quantify each of these effects, they are commonly described by using statistical parameters. Random vibration quantifies the average vibration level over time across a frequency spectrum (Wirsching, P. H., Paez, T. L. and Ortiz, K. 2006).

II.2. Random Processes

II.2.1. Theory and Definition

Random vibration is somewhat of a misnomer. If the generally accepted meaning of the term "random" were applicable, it would not be possible to analyze a system subjected to "random" vibration. Furthermore, if this term were considered in the context of having no specific pattern (i.e., haphazard), it would not be possible to define a vibration environment, for the environment would vary in a totally unpredictable manner (Newland, D.1993).

Fortunately, this is not the case. The majority of random processes fall in a special category termed stationary. This means that the parameters by which random vibration is characterized do not change significantly when analyzed statistically over a given period of time - the RMS amplitude is constant with

time. For instance, the vibration generated by a particular event, say, a missile launch, will be statistically similar whether the event is measured today or six months from today (Robson, J. D.1964), By implication, this also means that the vibration would be statistically similar for all missiles of the same design. It is possible to subdivide a process into a number of sub-processes, each of which could be considered to be stationary. For example, a missile environment could consist of several stationary processes, such as: captive carry, buffet, launch and free flight. Each of these sub-processes has unique amplitude, frequency and time characteristics, requiring separate analyses and considerations.

The assumption of a stationary process is essential in both a technical and legal sense. As previously stated, it would not be possible for a designer to analyze a system, nor for a user to test a system prior to installation in the field, if the vibration excitation were not stationary. Consequently, it would not be possible to develop a legally binding specification. In subsequent conversations, it is assumed that the random excitation is a stationary process.

Any vibration is described by the time history of motion, where the amplitude of the motion is expressed in terms of displacement, velocity or acceleration.

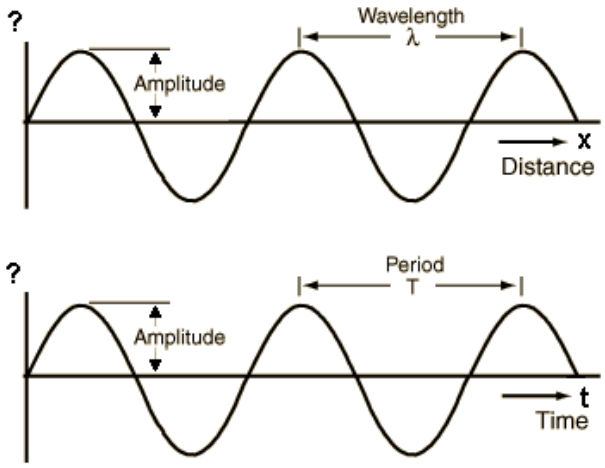

Fig.II.1 Amplitude-Time History of Sinusoidal Vibration
(Viewed on http://www.sengpielaudio.com)

Sinusoidal vibration is the simplest motion, and can be fully described by straightforward mathematical equations. The Fig.II.1 shows the amplitude time plot of a sinusoidal vibration and indicates that sinusoidal vibration is cyclic and repetitive. In other words, if frequency and amplitude (or time and amplitude) are defined the motion can be predicted at any point in time.

A random vibration is one whose absolute value is not predictable at any point in time. As opposed to sinusoidal vibration, there is no well defined periodicity, the amplitude at any point in time is not related to that at any other point in time, Fig.II.2 shows the amplitude time history of a random vibration where the lack of periodicity is apparent.

A major difference between sinusoidal vibration and random vibration lies in the fact that for the latter, numerous frequencies may be excited at the same time (Hasselman, T. K. and Hart, G. C., 1972). Thus structural resonances of different components can be excited simultaneously, the interaction of which could be vastly different from sinusoidal vibration, wherein each resonance would be excited separately.

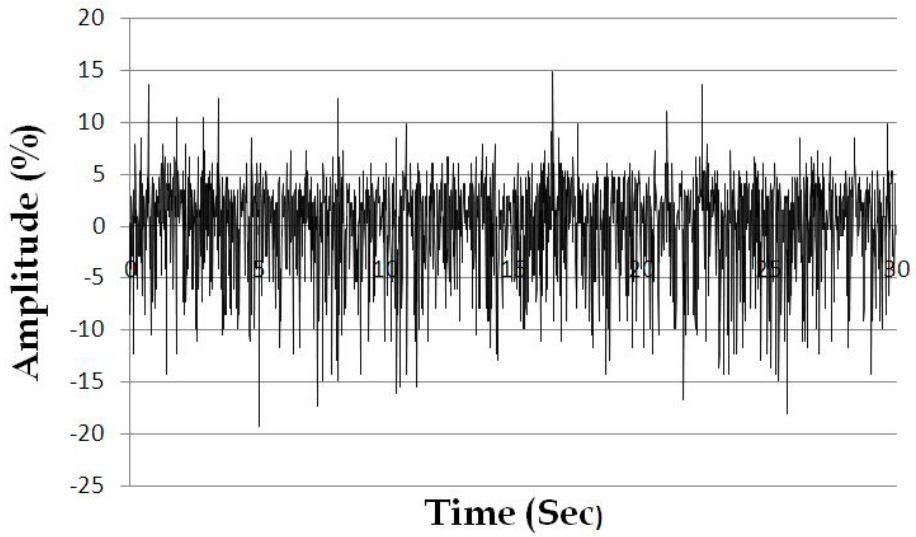

Fig.II.2 Amplitude-Time History of Random Vibration
(Viewed on http://www.intechopen.com)

The most obvious characteristic of random vibration is that it is non-periodic. The knowledge of the past history of random motion is adequate to predict the probability of occurrence of various acceleration and displacement magnitudes, but it is not sufficient to predict the precise magnitude at a specific instant (Dave Steinberg, D. 1988).

Although the instantaneous amplitude of a random vibration cannot be expressed mathematically as an exact function of time, it is possible to determine the probability of occurrence of particular amplitude on a statistical basis.

To characterize a stationary process, an ensemble of possible time histories must be obtained, wherein the amplitude is measured over the frequency range of excitation. Thus, the three parameters of interest are: frequency, time and amplitude. This information would provide the ability to analyze a random process in a statistical sense.

The characterization of random vibration typically results in a frequency spectrum of Power Spectral Density (PSD) or Acceleration Spectral Density (ASD), which designates the mean square value of some magnitude passed by a filter, divided by the bandwidth of the filter. Thus, Power Spectral Density defines the distribution of power over the frequency range of excitation.

If the outcome of a (conceptual) experiment is to assign a real value to variable *x*, then *x* is known as a random variable. Furthermore, if *x* assumes only a finite number of values, it is called a discrete random variable. Finally, if *x* assumes a continuous range of values, it is called a continuous random variable.

II.2.2. Random Forcing Function and Response

Consider a turbulent airflow passing over an aircraft wing. The turbulent airflow is a forcing function. Furthermore, the turbulent pressure at a particular location on the wing varies in a random manner with time (Nigam, N.1983).

For simplicity, consider the aircraft wing to be a single-degree-of-freedom system. The wing would vibrate in a sinusoidal manner if it were disturbed from its rest position and then allowed to vibrate freely. The turbulent airflow, however, forces the wing to undergo a random vibration response.

II.2.3. Random Base Excitation

Consider earthquake motion. The ground vibrates in random manner during the transient duration. Buildings, bridges, and other structures must be designed to withstand this excitation. An automobile travelling down a rough road is also subjected to random base excitation. The excitation may become periodic, however, if the road is a "washboard road."

One common characteristic of these examples is that the motion varies randomly with time. Thus, the amplitude cannot be expressed in terms of a "deterministic" mathematical function.

II.2.4. Random Time Functions

A random function is a function chosen randomly from a family of possible functions. Each realisation of a random function would result in a different function. Thus the concept of a random function is one example of a random element and hence is a generalization of the simpler idea of a random variable. Consider a random process that generates an infinite ensemble (or collection) of sample functions (or records) *x(t).* An example of this would be all possible acceleration records at a given locality, or wind pressure readings in tall buildings in a city. We then proceed to define probabilities for such ensemble. For example, at any time *t,* a first order distribution function and a first order probability density function (PDF) may be defined across the ensemble (Siebert, W. M.1958) (i.e. in the horizontal direction of Fig.II.3 as a limiting process in the form:

$$P(X,t)dX = P(X - dX < x(t) \leq X) \tag{II.1}$$

Where:

P(X,t): probability density function

X: Random variable

X(t):time variable function

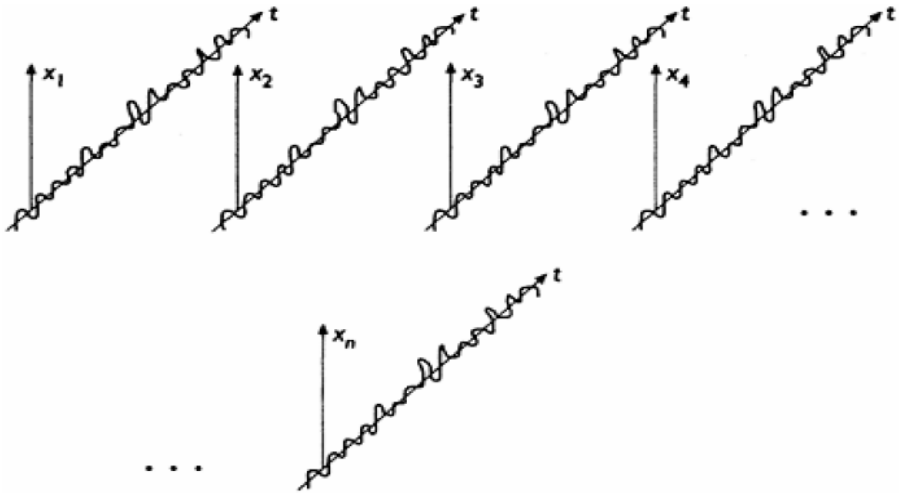

Fig.II.3 Ensemble of Records x(t).
(Vibrations and Waves 2009)

II.3. Spectral Analysis

The Fourier Transform (FT) of the autocorrelation function for a stationary process is the Power Spectral Density Function (PSDF) *Sx(ω),* that is:

$$Sx(\omega) = \frac{1}{2\pi} \int_{-\infty}^{\infty} R_x(\tau) \exp(-i\omega\tau) d\tau \qquad \text{(II.2)}$$

Also, the inverse Fourier transformation gives:

$$R_x(\tau) = \int_{-\infty}^{\infty} S_x(\omega) \exp(+i\omega\tau) d\omega \qquad \text{(II.3)}$$

In the above, ω is the frequency, $i2=-1$ and the factor $1/2\pi$may be associated with either member of the above pair or may be evenly split between them. Since $Rx(\tau)$ is a real and even function, Fourier cosine transforms may be used in lieu of the exponential transform shown above. The PSDF is also known as the mean square spectral density because:

$$R_x(0) = \int_{-\infty}^{\infty} S_x(\omega)d\omega = E(x^2) \tag{II.4}$$

This implies that $Sx(\omega)d\omega$ can be interpreted as the power or mean square density contained in an infinitesimal band of complex exponentials (sinusoids and co-sinusoids) into which the random function is resolved. The PSDF is a positive, real valued function and is even in ω. Since physical meaning can only be assigned to positive frequencies, an experimentally obtained spectrum is plotted by halving the measured $Sx(\omega)$ at each frequency and plotting the result for both positive and negative ω. A spectrum $Sxy(\omega)$ for the cross-correlation function $Rxy(\tau)$ can also be defined for the stationary case as in equations (II.2) and (II.3). As expected, the PSDF of an periodic process and the FT of a sample function $x(t)$ of the random process are related. When $x(t)$ is a non-periodic function, its FT $X_T(\omega)$ is given as:

$$X_T(\omega) = \int_0^T x(t)\exp(-\omega t)dt \tag{II.5}$$

Where $x(t)$ is assumed to be zero before $t=0$ and after $t=T$. An energy density spectrum for $x(t)$ is:

$$\phi_x(\omega, T) = \left|X_T(\omega)\right|^2 / 2\pi \tag{II.6}$$

And the power density spectrum is:

$$S_x(\omega, T) = \phi_x(\omega, T)T = \left|X_T(\omega)\right|^2 / 2\pi \tag{II.7}$$

The power density spectrum is now a random variable dependent on both *x(t)* and *T*. Although it can be shown that:

$$\lim_{T\to\infty} E[S_x(\omega, T)] = S_x(\omega) \tag{II.8}$$

The manner in which the power density spectrum approaches the PSDF needs to be investigated in each case. For a normal (or Gaussian) process, it is known that the variance of *Sx(ω, T)* does not approach zero as $T\rightarrow \infty$, and hence measurements of *Sx(ω, T)* provide questionable estimates for the PSDF.

II.4. Pseudo Excitation Method for Bridges Random Vibration Analysis

In the design of long-span bridges, the spatial effects of earthquakes, including the wave passage effect, the incoherence effect, and the local site effect, must be taken into account (Kiureghian, A.D. and Neuenhofer, A. 1992), (Ernesto, H. Z. and Vanmarcke, E. H. 1994). The random vibration method can fully account for the statistical nature as well as the spatial effects of earthquakes, and so has been widely regarded as a very promising method. Unfortunately the very low computational efficiency has become a bottle-neck for its practical use.

In the past 20 years, a very efficient method, known as the pseudo-excitation method (PEM), has been developed by researchers to cope with the above computational difficulty (Lin, J.H., Zhang, W.S. and Williams, F.W. 1994). This method is used for solving high-degree of freedom stochastic differential equation with multiple excitations developed by (Zhang *et al.* 2010) it can easily compute the 3D random seismic responses of long-span bridges using finite element models with many thousands of degrees of freedom (DOF) on a small personal computer, in which the dynamic loads effect is accounted for accurately.

This method has been applied to the design of some important long-span bridges in the world especially in China where the design codes were modified implementing this method in bridges dynamic analysis and design. Based on extensive research by many scholars and engineers, the Chinese official document

"Guidelines for Seismic Design of Highway Bridges" (JTG/T B01-01-2008) has formally recommended the pseudo-excitation method as a basic tool for seismic analysis of long-span bridges, which will further push forward the progress of design and construction for long-span bridges. PEM has also been introduced by whole chapters respectively in the "Vibration and Shock Handbook 2005" and "Bridge Engineering Handbook 2013".

II.4.1. A Bridge Subjected to Single Stationary Random Excitations

Consider a linear system subjected to a zero-mean stationary random excitation with a given power spectral density (PSD) $S_{xx}(\omega)$. Suppose that for two arbitrarily selected responses y(t) and z(t) , the auto-PSD $S_{yy}(\omega)$ and cross-PSD $S_{yz}(\omega)$ are desired. If $H_y(\omega)$ and $H_z(\omega)$ are the corresponding frequency response functions, and if x(t) is replaced by a sinusoidal excitation

$$\tilde{x} = \sqrt{S_{xx}(\omega)}\exp(i\omega t) \tag{II.9}$$

The responses of y(t) and z(t) would be:

$$\tilde{y} = \sqrt{S_{xx}(\omega)}H_y(\omega)\exp(i\omega t) \tag{II.10}$$

And

$$\tilde{z} = \sqrt{S_{xx}(\omega)}H_z(\omega)\exp(i\omega t) \tag{II.11}$$

It can be readily verified that (Lin, J.H., Zhao, Y. Y. and Zhang, Y.H. 2001):

$$\begin{aligned}\tilde{y} * \tilde{y} &= \sqrt{S_{xx}(\omega)}H_y^*(\omega)\exp(-i\omega t).\sqrt{S_{xx}(\omega)}H_y(\omega)\exp(i\omega t)\\ &= \left|H_y(\omega)\right|^2 S_{xx}(\omega) = S_{yy}(\omega)\end{aligned} \tag{II.12}$$

$$\begin{aligned}\tilde{y} * \tilde{z} &= \sqrt{S_{xx}(\omega)}H_y^*(\omega)\exp(-i\omega t).\sqrt{S_{xx}(\omega)}H_z(\omega)\exp(i\omega t)\\ &= H_y^*(\omega)S_{xx}(\omega)H_z(\omega) = S_{yz}(\omega)\end{aligned} \tag{II.13}$$

If y(t) and z(t) are two arbitrarily selected random response vectors of the structure with: $\tilde{y} = a_y exp(i\omega t)$ and $\tilde{z} = a_z exp(i\omega t)$ are the corresponding harmonic response vectors due to the pseudo excitation (II.9), it can also be proved that the PSD matrices of y(t) and z(t) are:

$$S_{yy}(\omega) = \tilde{y}^* \tilde{y}^T = a_y^* a_y^T \tag{II.14}$$

$$S_{yz}(\omega) = \tilde{y}^* \tilde{z}^T = a_y^* a_z^T \tag{II.15}$$

This means that the auto- and cross-PSD functions of two arbitrarily selected random responses can be computed using the corresponding pseudo harmonic responses.

Now, consider a structure subjected to a single seismic random acceleration excitation. Its equation of motion is:

$$M\ddot{y} + C\dot{y} + Ky = -ME\ddot{x}_g(t) \tag{II.16}$$

In which: M, C and K are its mass, damping and stiffness matrices; y is its displacement vector; the ground acceleration $\ddot{x}_g(t)$ is a stationary random process with a known PSD $S_{xg}(t)$ and E is a given as a constant vector indicating the distribution of inertia forces. Let the pseudo ground acceleration be:

$$\tilde{\ddot{x}}_g(t) = \sqrt{S_{xg}(\omega)} e^{i\omega t} \tag{II.17}$$

Substituting Eq. (II.17) into Eq. (II.16) gives the pseudo equations of motion:

$$M\ddot{y} + C\dot{y} + Ky = -ME\sqrt{S_{xg}(\omega)} e^{i\omega t} \tag{II.18}$$

Using the first q normalized modes for mode-superposition leads to the following equation:

$$\tilde{y}(t) = a_y(\omega) e^{i\omega t} = \sum_{j=1}^{q} \gamma_j H_j \phi_j \sqrt{S_{xg}(\omega)} e^{i\omega t} \tag{II.19}$$

In which ϕ_j , H_j and Υ_j are the j^{th} mass normalized mode, frequency response function and mode participation factor, respectively.

According to PEM:

$$S_{yy}(\omega) = \tilde{y}^* \tilde{y}^T = a_y^* a_y^T \tag{II.20}$$

Substituting Eq. (II.19) into Eq. (II.20) and expanding it gives the conventional complete quadratic combination (CQCA) algorithm:

$$S_{yy}(\omega) = \sum_{j=1}^{q} \sum_{k=1}^{q} \gamma_j \gamma_k \phi_j \phi_k^T H_j^*(\omega) H_k(\omega) S_{xg}(\omega) \tag{II.21}$$

This means that equations (II.20) and (II.21) are mathematically identical to each other. However, the computational effort required by equation (II.20) is approximately only $1/q^2$ of that required by equation (II.21). Hence, equation (II.20) is also known as the fast CQC algorithm.

II.4.2. A Bridge Subjected to Multiple Stationary Random Excitations

Consider a linear structure subjected to a number of stationary random excitations, which are denoted as an *m* dimensional stationary random process vector x(t) with known PSD matrix $S_{xx}(\omega)$. The equation of motion is:

$$M\ddot{y} + C\dot{y} + Ky = x(t) \tag{II.22}$$

The PSD matrix is Hermitian and so it can be decomposed, e.g. by using its eigenpairs ψ_j and d_j (j=1,2,…,r), into:

$$S_{xx}(\omega) = \sum_{j=1}^{r} d_j \psi_j^* \psi_j^T \qquad (r \le m) \tag{II.23}$$

In which r is the rank of $S_{xx}(\omega)$. Next, constitute r pseudo harmonic excitations:

$$\tilde{x}(t) = \sqrt{d_j}\,\psi_j \exp(i\omega t) \qquad (j = 1,2,\ldots,r) \tag{II.24}$$

By applying each of these pseudo harmonic excitations, two arbitrarily selected response vectors $y_j(t)$ and $z_j(t)$ of the structure, which can be displacements, internal forces or other linear responses, may be easily obtained and expressed as:

$$\tilde{y}_j(t) = a_{yj}(\omega)\exp(i\omega t) \tag{II.25}$$

$$\tilde{z}_j(t) = a_{zj}(\omega)\exp(i\omega t) \tag{II.26}$$

The corresponding PSD matrices can be computed by means of the following formulas:

$$S_{yy}(\omega) = \sum_{j=1}^{r} \tilde{y}_j^*(t)\tilde{y}_j^T(t) = \sum_{j=1}^{r} a_{yj}^*(\omega)a_{yj}^T(\omega) \tag{II.27}$$

$$S_{yz}(\omega) = \sum_{j=1}^{r} \tilde{y}_j^*(t)\tilde{z}_j^T(t) = \sum_{j=1}^{r} a_{yj}^*(\omega)a_{zj}^T(\omega) \tag{II.28}$$

The way used to decompose $S_{xx}(\omega)$ into the form of equation (II.23) is not unique. In fact, if there are too many random excitations. Clearly, when the bridge under consideration is subjected to the action of multiple seismic or wind-gust excitations, the PSD matrix of the excitations $S_{xx}(\omega)$ can be used to yield groups of harmonic responses will lead to the PSD a finite number of harmonic excitations. The resulting r groups of harmonic responses will lead to the PSD functions for such responses, which are exact numerical solutions.

II.4.3. Structures Subjected to Non-Stationary Random Excitations

Consider a linear system subjected to an evolutionary random excitation:

$$f(t) = g(t)x(t) \tag{II.29}$$

In which $g(t)$ is a slowly varying modulation function, while $x(t)$ is a zero-mean stationary random process with auto-PSD $S_{xx}(\omega)$. The deterministic functions $g(t)$ and $S_{xx}(\omega)$ are both assumed to be given.

In order to compute the PSD functions of various linear responses due to the action of *f(t)*, the pseudo excitation has the form:

$$\tilde{f}(\omega,t) = g(t)\sqrt{S_{xx}(\omega)}\exp(i\omega t) \tag{II.30}$$

Suppose that *y(t)* and *z(t)* are two arbitrarily selected response vectors, and *ỹ(ω,t)*, *z̃(ω,t)* are the corresponding transient responses due to the pseudo excitation *f(ω,t)* with the structure initially at rest. It has been proved that (Lin et al. 2005):

$$S_{yy}(\omega,t) = \tilde{y}^{*}(\omega,t)\tilde{y}^{T}(\omega,t) \tag{II.31}$$

$$S_{yz}(\omega,t) = \tilde{y}^{*}(\omega,t)\tilde{z}^{T}(\omega,t) \tag{II.32}$$

For cases with fully coherent excitations, partially coherent excitations, and non-uniformly modulated evolutionary random excitations, the corresponding pseudo-excitation algorithms are very similar to those for the stationary random excitation cases.

Conclusion

The history of the mathematical theory of random vibrations of mechanical systems come back to the previous century, starting with the work of (Einstein, A.1956), and continues until now days. The theory is essential to the representation and interpretation of realistic inputs and responses of structures and that what was presented briefly.

The topic of Introduction to Random Vibrations is the behavior of structural and mechanical systems when they are subjected to unpredictable, or random, vibrations. These vibrations may arise from natural phenomena such as earthquakes or wind, or from human-controlled causes such as the stresses placed on aircraft at takeoff and landing. Study and mastery of this topic enables

engineers to design and maintain structures capable of withstanding random vibrations, thereby protecting human life.

Introduction to Random Vibrations will lead readers in a user-friendly fashion to a thorough understanding of vibrations of linear and nonlinear systems that undergo stochastic-random-excitation.

Chapter III

Bridge-Vehicle Interaction

Introduction

In recent decades, with the rapid development of highway communication around the world, the increasing number of bridges, the emergence of new bridge's structure, the increasing bridge span and a significant increase in vehicle speed, the research of dynamic interaction between vehicles and the bridge is more and more intensive. The study of vehicle-bridge coupling vibration focuses on two aspects generally: accurate modelling of coupled vehicle-bridge system and efficient methods and algorithms for simulating the dynamic response.

When the vehicles run across the bridge, the pocket weight of the vehicles, irregularities of the bridge and the acceleration and braking of the vehicle can lead to excessive vibrations. The vibration will be transferred to the bridge by tires, which can make the bridge vibrate forcefully. The bridge will vibrate in vertical, transverse and longitudinal direction, which could lead to damage in the bridge structure. This problem with interaction and mutual effects is related to the coupled vibrations between the vehicle and the bridge.

Running vehicles on the bridge at high speed can lead to damage to the bridge structure. At the same time, the vibration of the bridge can affect the stability, the comfortableness and the safety of the running vehicles and that makes the problem more complicated is structural analyses.

A major goal of this chapter is to create a simplified model of a vehicle-bridge system relevant to the real system and to use it in order to study the influence of appropriate parameters to vehicle-bridge vibrations and interacting forces.

III.1. Research Works Analysis

In recent years, dynamic analysis of coupled vehicle-bridge systems has received much attention. The road surface roughness is well known to be a random process. It is very difficult to perform a vibration analysis concerning

such random vibration (Lou and Zeng 2005, Xia 2000, Lei and Noda 2002, Zhai 1996). Furthermore, very little research concerning optimal analysis with the consideration of random response appears in the literature. There are two difficulties for the optimal analysis (Yamazaki et al. 1988, Bouazara and Richard 2001, Cassis and Schmit 1976, Kapoor and Kumarasamy 1981, Naude and Snyman 2003): One is that the conventional method for random vibration analysis require much computational effort, the other is that, generally, the objective function for optimal analysis is highly nonlinear and the calculation procedure for sensitive analysis is very complicated.

Many research works were performed in this area including the effect of road roughness, vehicle lines loading, vehicle models and speeds in addition to the bridge structural type. In this section a brief overview on bridge-vehicle interaction studies over the past decades is presented, it puts more emphasis on cable bridges which is the structural kind of the bridge studied in this work.

III.1.1. Cable Stayed Bridge Model

In early research in this area, simplified bridge models were employed to study vehicle-bridge interactions. For example, a cable-stayed bridge was simulated as a beam resting on an elastic foundation by (Meisenholder,S.G. and Weidlinger,P.1974) for the dynamic analysis of cable-stayed guide ways subject to track-levitated vehicles moving at high speeds. (Mao,Q.H. 1989) investigated the impact factor of a cable-stayed bridge, which was assumed to be formed of continuous elastic beams supported by intermediate elastic supports.

More recently, with the development of finite element (FE) technology, it has become common practice to use a computer software package to establish a finite element model (FEM) of a cable-supported bridge. This technology establishes an accurate bridge model that takes into account the geometric non-linear behaviour of a cable-supported bridge. To make the bridge model close to the realistic bridge in terms of its dynamic properties, the modal frequencies and shapes determined

by dynamic tests are used for further model validation or updating. Many FEMs of cable-supported bridges have been established for the analysis of train-bridge interactions.

The first generation of Bridge model was a spinal beam model (Xu *et al*., 1997) in which the hybrid steel deck was represented by a single beam with equivalent cross-sectional properties, two bridge towers made of reinforced concrete that were modelled by three-dimensional Timoshenko beam elements, and cables and suspenders that were modelled by cable elements to account for geometric nonlinearity due to cable tension.

The model was validated by comparing it with measurements of the first 18 modal frequency and shapes of the actual bridge. Using this model, (Guo *et al.* 2007) predicted the dynamic displacement and acceleration responses of coupled train and bridge systems in cross winds, and verified the results by measuring the responses in different cases. However, they modelled the bridge deck as a simplified spine beam of equivalent sectional properties, and were thus unable to capture the local stress and strain behaviour of the bridge.

A second generation bridge model was established to overcome this weakness; the modelling work is based on the previous model developed by (Liu et al., 2009). In this model, beam elements were used to model the bridge deck to closely replicate the geometric details of the complicated deck in reality. The bridge model was also updated using the first 18 measured natural frequencies and mode shapes. Based on this model, (Xu *et al.* 2010) computed the stress and acceleration responses of local critical components under running trains and verified them against measured responses.

III.1.2. Modelling of Road Vehicles

To analyze the dynamic interaction between a bridge and running road vehicles, a model of road vehicles must be established. A sophisticated road vehicle model is required to make the simulation as realistic as possible. A road

vehicle is modelled as a combination of several rigid bodies, each of which is connected by a set of springs and dashpots which model the elastic and damping effects of the tires and suspension systems, respectively (Karoumi, R. 1998). There are various configurations of road vehicles, such as a tractor and trailer with different axle spacing.

Road vehicle models that contain several DOFs have been devised for vehicle-bridge interaction analysis. For example, (Guo *et al*. 2001) modelled a 17-DOF four-axle heavy tractor-trailer vehicle, as shown in Fig.III.1, to investigate the interaction between vehicles and a cable-stayed bridge.

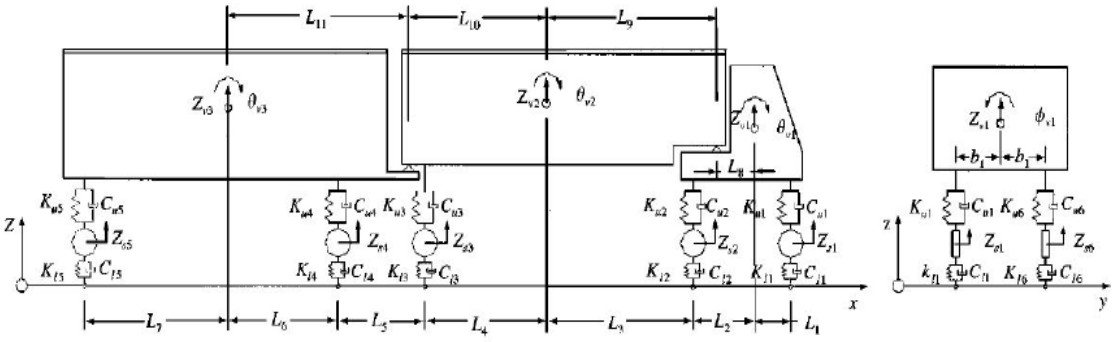

Fig.III.1 Dynamic Model of a Tractor-Trailer
(Guo and Xu, 2001)

A total of three DOFs were assigned to rigid bodies representing either the tractor or the trailer to account for vertical, rolling, and pitching motions. Only one DOF was assigned to the rigid body representing the axle set moving in the vertical direction.

III.1.3. Simulation of Road Vehicle Flow

On long-span bridges there is a high probability of the simultaneous presence of multiple road vehicles, including heavy trucks. This may lead to larger-amplitude stress responses and greater fatigue damage of the local bridge components than would be the case with only one road vehicle.

The simulation of road vehicle flow is thus important in the analysis of the dynamic interaction between road vehicles and bridges. Rather simple patterns of road vehicle flow have been assumed in most vehicle-bridge coupled dynamic analyses (Guo and Xu, 2001; Xu and Guo, 2003; Cai and Chen, 2004; Li, Q. *et al*. 2010; Chen et al., 2007) in which either one or several vehicles are distributed on the bridge in an assumed (usually uniform) pattern.

Obviously, such assumptions do not represent actual road traffic conditions, recently, (Chen and Wu 2010) improved on this approach and applied the cellular automaton (CA) traffic simulation model to simulate traffic flow on a bridge and an approaching roadway with four lanes. Using this model, they simulated a complicated road vehicle flow on long-span bridges in terms of vehicle number, vehicle type combination, and driver operation characteristics, such as lane changing, acceleration, or deceleration.

III.1.4. Modelling of Road Surface Roughness

Road surface roughness is an important factor that greatly affects vehicle-bridge interactions. (Paultre *et al.* 1992) pointed out that road surface or pavement roughness can significantly affect the impact response of a bridge. The roughness or surface profile depends primarily on the workmanship involved in the construction of the pavement or roadway and how it is maintained, which, although random in nature, may contain some inherent frequencies (Yang, Y.B., Wu, Y.S.2001).

In most cases, surface roughness, which is three-dimensional in reality, is often approximated by a two dimensional profile. To account for its random nature, the road profile can be modelled as a stationary Gaussian random process and derived using a certain power spectral density function. Other methods similar to this have been widely adopted by researchers studying vehicle-induced bridge vibration (Honda *et al.*, 1982; Inbanathan and Wieland, 1987; Coussy *et al*., 1989; Hwang and Nowak, 1991; Wang and Huang, 1992; Chatterjee *et al*., 1994; Chang and

Lee, 1994; Henchi *et al*., 1998; Pan and Li, 2002). (Dodds, C.J., Robson, J.D.1973) developed power spectral density functions that were later were modified and used by (Wang, T.L., Huang, D.1992) and (Huang, D., *et al*.1993). This approach was also adopted by (Guo, W.H. *et al*. 2001) and (Xu, Y.L. et al. 2003) in their dynamic analyses of coupled vehicle-bridge and wind-vehicle-bridge systems.

III.1.5. The Problem Solution Methods

Studies of the dynamic effects on bridges subjected to moving loads have been carried out ever since the first railway bridges were built in the early 19th century. Since that time vehicle speed and vehicle mass to the bridge mass ratio have been increased, resulting in much greater dynamic effects (Paz, M. and Leigh, W. 2004).

In recent years, the interest in traffic induced vibrations has been increasing due to the introduction of high-speed vehicles, like the TGV train in France and the Shinkansen train in Japan with speeds exceeding 300 km/h. The increasing dynamic effects are not only imposing severe conditions upon bridge design but also upon vehicle design, in order to give an acceptable level of comfort for the passengers.

The dynamic analysis of vehicle-bridge coupled system requires two sets of equations of motion for the bridge and vehicles, respectively. These describe the interaction or contact forces at the contact points of the two subsystems. Because the contact points move from time to time, the system matrices are generally time dependent, and must be updated and factorized at each time step. The various solution methods can be generalized into two groups according to whether or not an iterative procedure is needed at each time step.

The first group of methods solves the equations of motion of a coupled vehicle-bridge system at each time step without iteration. This approach has been widely used in coupled vehicle-bridge analysis (Olsson, 1985; Yang *et al*., 1999;

Yang and Wu, 2001; Au *et al*., 2001; Sun and Dhanasekar, 2002, Henchi *et al*., 1998; Xia *et al*., 2000; Xia *et al.*, 2003; Xu *et al*., 2003; Biondi *et al*., 2005; Humar, 1995; Lou and Zeng, 2004).

These methods have good computational stability, and are convenient for dealing with vehicle-bridge interaction problems when the vehicle model is relatively simple. The main disadvantage is that the equations of motion of the coupled system are time dependent, and thus the characteristic matrices must be modified at each time step. In addition, the equations of motion of the coupled vehicle-bridge system become very difficult to determine.

The second group of methods solves the equations for the vehicles and bridge separately, and requires an iterative process to obtain convergence for the displacements of the vehicles and bridge at all contact points. Many studies have applied this type of method to investigate vehicle-bridge interactions (Coussy and Vanhoove,1989; Hwang and Nowak,1991; Yang and Fonder 1996; Zhai and Cai 1997; and Zhai and Cai 2003).

The advantage of these methods is that the dynamic property matrices in the two sets of equations of motion remain constant, which is convenient for the consideration of nonlinear vehicle-bridge interactions and nonlinear vehicle models (Li *et al.*, 2010). However, in engineering applications, the iterative convergence is a critical problem with this type of method.

The low convergence rate and occasional divergence of the solution have also been noted (Wu and Yang, 2003). (Li *et al*. 2010) investigated the performance of these iterative schemes using the Wilson-θ method, Newmark-β method, and an explicit integration method proposed by (Zhai, 2007), and found that the latter gave a much higher convergence rate than the former two methods, a mathematical and structural software programme is needed because of the infinite number of variables and iterations operations.

III.2. Moving Force Identification

Various methods were applied on different bridge-vehicle systems and developed to identify the interaction force between bridge and vehicle based on vibration theory and system identification technique and they can mainly be divided into two categories:

- Methods based on finite element method (FEM).
- Methods based on modal superposition technique with a continuous bridge model.

In the last kind, the modal superposition technique is firstly employed to decouple the equation of motion of the bridge and force model to a set of ordinary differential equations. Then the relationship between the moving forces and bridge responses in each mode can be formulated. Finally, the inverse problem can be solved by least-squares estimation with regularization or other optimization methods among which we use in this work are the Method of Moments and the Time Domain Method for a comparative study (OBrien, E.J.*et al*.2014).

III.2.1Vehicle Load Models

The structural form of vehicles is generally complex. From the point of view of vibration, a vehicle may be seen as complex multi-variant system consisting of "mass, stiffness and damping". Then different simplified analysis models are formed. Three kinds of simplified models are commonly used: the moving mass model, the moving force model and the spring mass model. In the last kind three models were used by researchers which are two degrees of freedom vehicle model with single axle, double-axle-2D model of vehicle with four degrees of freedom and three-dimensional model with seven degrees of freedom (Zhang,W.2012).

As illustrated in Fig.III.2, the vehicle models used in this study include a moving force model and moving mass model for the axle vehicle force

identification and the last one was used to model the subsystem of the vehicle in the interaction coupled system bridge-vehicle.

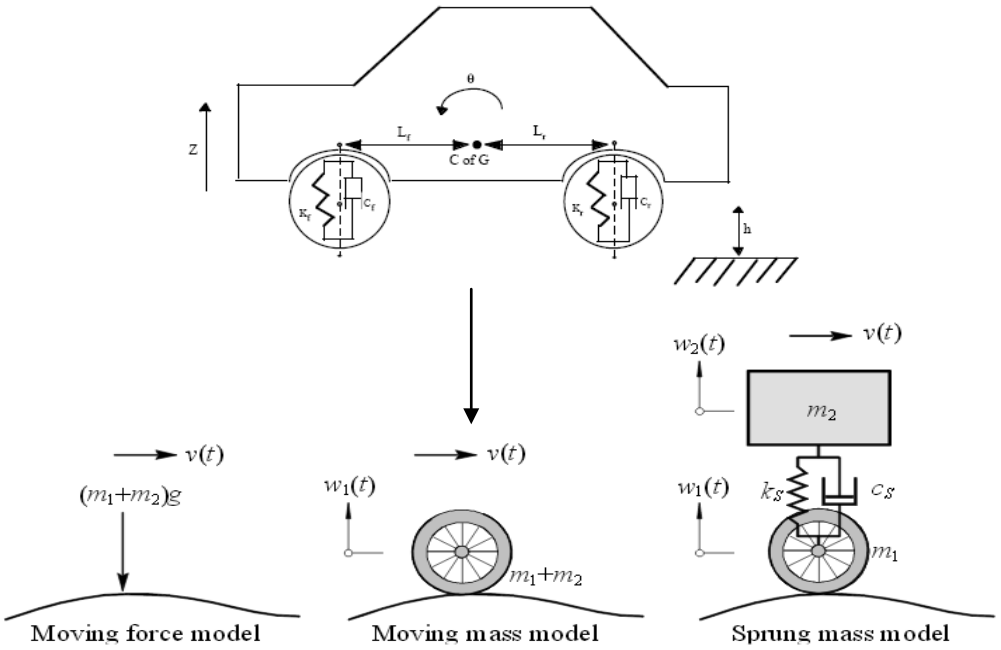

Fig.III.2 Vehicle Model

(Viewed on http://www.mathworks.com)

The moving force model (constant force magnitude) is sufficient if the inertia forces of the vehicle are much smaller than the dead weight of the vehicle. For a vehicle moving along a straight path at a constant speed, these inertia effects are mainly caused by bridge deformations (bridge-vehicle interaction) and bridge surface irregularities. Hence factors that are believed to contribute in creating vehicle inertia effects include: high vehicle speed, flexible bridge structure, large vehicle mass, small bridge mass, stiff vehicle suspension system and large surface irregularities.

The sprung mass model is acceptable, when the bridge span is considerably larger than the vehicle axle base as the case is for cable supported bridges. The use of simplified models may be more effective in identifying correlation between the governing bridge-vehicle interaction parameters and the bridge response.

III.2.1.1. Moving Force Model

The constant force F moves towards the right with a constant speed on the simple supported bridge as shown in Fig.III.3, here the quality of the moving load is ignored. When the time is equal to 0, F is located in the left supporting place, and when the time is equal to T, F moves to the right supporting place, according to the vibration analysis, the expression of vibration equation of the bridge is as follows:

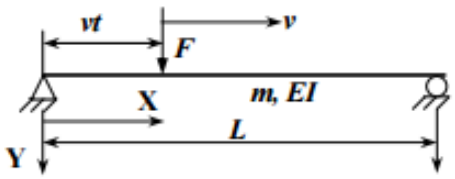

Fig.III.3 The Constant Force Through the Simple Supported Bridge with Constant Speed

(Latin American Journal of Solids and Structures 2013)

The equation of motion of the bridge modeled as a simple beam of Bernouli subjected to a constant load is follows:

$$EI\frac{\partial^4 y}{\partial x^4}+m\frac{\partial^2 y}{\partial x^2}=F(x,t) \tag{III.1}$$

Where EI stands for the bending stiffness of the bridge and m is the quality of unit length. Assume that the dynamic displacement of the forced vibrations y(x,t) can be expressed as series form of vibration mode:

$$y(x,t\ )=\sum_{N=1}^{N}A_n(t)\phi_n(x) \tag{III.2}$$

Where:

$y(x, t)$: is the dynamic displacement

$A_n(t)$: Function of time

$\Phi_n(x)$: Mode shapes

The forced vibration equation can be gotten by putting the formula (III.1) into the formula (III.2) and the orthogonality of vibration mode. Using the standardization of vibration mode, the simplified vibration equation of bridge under the moving constant force with a constant speed is:

$$\ddot{A}_n + \omega_n^2 A_n = \frac{2F}{ml}\sin\frac{n\pi vt}{l}(n = 1,2,...,N) \tag{III.3}$$

Vibration mode of the simple supported beam bridge is expressed for equation (III.1), so the expression of the dynamic response is shown as equation (III.4).

$$\phi_n(x) = \sin(\frac{n\pi x}{l})$$
$$y(x,t\ ) = \frac{2F}{ml}\sum_{N=1}^{N}\frac{1}{\omega_n^2 - \Omega_n^2}\sin\Omega_n t - \frac{\Omega_n}{\omega_n}\sin\omega_n t)\sin\frac{n\pi x}{l} \tag{III.4}$$

Where ω_n is each order natural frequency of the simple supported beam and $\Omega_n = m\pi v/l$ is the generalized flexible dynamic frequency of the moving constant force.

III.2.1.2. Moving Mass Model

In this study a harmonic force presenting the load model which passes through the simple supported beam at a constant speed is considered, the dynamic response expression of the studied mechanism is as follows:

$$y(x,t\ ) = \frac{F}{ml}\sum_{N=1}^{N}\left\{\frac{1}{\omega_n^2 - (\Omega_p - \Omega_n)^2}\left[\sin(\Omega_n + \Omega_p)t - \frac{\Omega_n + \Omega_p}{\omega_n}\sin\omega_n t)\right] - \frac{1}{\omega_n^2 - (\Omega_p - \Omega_n)^2}\left[\sin(\Omega_p - \Omega_n)t - \frac{\Omega_p - \Omega_n}{\omega_n}\sin\omega_n t)\right]\right\}\sin\frac{n\pi x}{l} \tag{III.5}$$

Where ω_n is each order natural frequency of the simple beam, Ω_n is each order generalized frequency related with the moving speed, and Ω_p is disturbance frequency of the harmonic load. When only the resonance of fundamental

vibration mode is considered, resonance will occur at $\Omega_p = \omega_1$, and the maximum dynamic response will appear in the time that harmonic force leaves bridge spans , that is $t=l/v$, at this time dynamic response is expressed as follows:

$$y(x,t) = \frac{2F_l}{\omega_l m\pi v}\sin\frac{\pi x}{l}\sin\omega_l\frac{l}{v} \tag{III.6}$$

Maximum mid-span deflection will occur in $\sin(\omega l / v)=1$. At this point the dynamic magnification factor is:

$$\mu = \frac{\omega_l}{\Omega_l} = 2\sin\frac{T_c}{T_l} \tag{III.7}$$

Where: T_c is the required time of the harmonic force through the whole beam.

From equation (III.1) we can see, for moving harmonic force, resonance occurs in $\Omega_p=\omega_1$, the dynamic magnification factor will depend on the speed, the slower the speed is, the more time is through the beam and the greater the vibration response is.

III.2.2. Method of Moments for Moving Force Identification

This method was proposed by (Yu, L. and Chan, T.H.T. 2007) in which the moving vehicle loads were described as a combination of whole basis functions, such as the orthogonal Legendre or Fourier series, and the force identification can be transformed into a parameter identification problem.

The dynamic vehicle load $f(t)$ can be expressed as follows in terms of a series of basis function $\psi_0(t)$, $\psi_1(t)$, $\psi_2(t)$, …, $\psi_n(t)$ (Harrington , 1968).

$$f(t) = \sum_k \alpha_k \psi_k(t) \tag{III.8}$$

Or in matrix form:

$$f(t) = \psi.\alpha \tag{III.9}$$

Where: $\psi_k(t)=P_k(t)$

Or: $\psi_k(t)=sin(k\pi ct/L)$ (Jorgensen, 2004).

The bending moment of a beam is expressed after the use of a test function ω_j as:

$$m(x,t_j)=\sum_{k=0}^{m}\alpha_k.l_k \qquad (j=0,1,...,N) \tag{III.10}$$

$$l_{jk}=\sum_{n=1}^{\infty}\frac{2EI\pi^2}{\rho L^3}\frac{n^2}{\omega_n^{'}}\sin\frac{n\pi x}{L}\times\int_0^{tj}e^{-\xi_n\omega_n(t_j-\tau)}\sin\omega_n^{'}(t_j-\tau)\sin\frac{n\pi c\tau}{L}\psi_k(\tau)d\tau \tag{III.11}$$

Equations (III.9) and (III.10) can be rewritten in discrete terms and rearranged into a set of equations

$$\underset{(N-1)\times 1}{M}=\underset{(N-1)\times(m+1)}{L}\cdot\underset{(m+1)\times 1}{\alpha} \tag{III.12}$$

$$\underset{(N-1)\times(m+1)}{L}=\underset{(N-1)\times(N_B-1)}{B}\cdot\underset{(N_B-1)\times(m+1)}{\psi} \tag{III.13}$$

Where:

Ψ: is the matrix of basic functions

M: the time-series vector of the measured bending moment responses

α: the coefficient vector

- If N-1=m+1, the coefficient α can be obtained directly by solving Equation (III.8).

-If N-1>m+1 *or* N-1<m+1, the least-squares method can be used to find the coefficient α.

Substituting α into Equation (III.4), the time history of the moving loads can be obtained finally.

In order to confirm the accuracy of the developed numerical model, a simply supported beam at two opposite edges and subjected to two moving vehicle loads is simulated and illustrated.

III.2.2.1. Simulation Data

The information below gives details of the material properties and the moving force:

Time-varying loads:

$f1(t) = 58\,800\times[1+0.1\sin(10\pi t)+0.05\sin(40\pi t)]$ N

$f2(t) = 137\,200\times[1-0.1\sin(10\pi t)+0.05\sin(50\pi t)]$ N

ls = 8 m, EI =1.27914×1011N·m2, ρ =12 000 kg/m, L=40m, f1 =3.2 Hz, f2=12.8 Hz, f3 =28.8 Hz, c=40m/s.

Only the three first modes of the beam are included in the calculation because the analysis frequency is in the range 0 to 40 Hz

Random noise is added to the calculated responses to simulate the polluted measurements as the one in Ref (Yu, L. 2002). The Fourier basis functions are only adopted for the Method of Moments (MOM) in the following simulation. The MOM is used to identify both the two axle constant and time-varying loads from bending moment and/or acceleration responses at 1/4, 1/2, and 3/4 spans in twelve combination cases. A comparison on the identified moving forces due to the two solutions for MOM is illustrated too as shown in Fig.III.4 later.

III.2.2.2. Simulation Results

Table III.1 shows the comparison on the EP (Error percentage) values of two axle constant loads identified by MOM under the 5% noise level as well as including the effect of two different solutions, i.e. the SVD (Singular Value Decomposition) and regularization solutions.

Compared the SVD results with the regularization results, it can be found from Table1 that the EP (Error Percentage) values for all cases, except for the case of 1/4a, 1/2a and 3/4a, are significantly reduced if the regularization solution are

adopted. For this method, the EP values are also significantly improved when the bending moment responses are only used to identify the two moving loads. However, when only the acceleration responses, or the combination of acceleration and bending moment responses are used to identify the two moving loads, the RQPE (Real Quantity of Percentage Error) values are close to each other whether the SVD or the regularization solution is adopted.

Table III.1. Comparison of EP of Two Axle Constant Loads under 5% Noise Using the Regularization and the SVD Solutions for Different Sensor Locations

Method of Moments (MOM)			
Axle 1		Axle 2	
SVD	Reg	SVD	Reg
1,06	0,76	0,25	0,05
0,79	0,39	0,37	0,04
0,18	0,18	0,24	0,24
0,10	0,10	0,21	0,21
0,26	0,26	0,15	0,15
0,13	0,13	0,11	0,11
0,04	0,04	0,18	0,18
0,17	0,17	0,20	0,20
0,25	0,25	0,20	0,20
0,41	0,41	0,18	0,18
0,23	0,23	0,13	0,13
0,14	0,14	0,22	0,22

As mentioned in Fig.III.4, the regularization results are in agreement with the SVD results except for the moment at the beginning and the end of time histories of moving forces as well as the moment at the accessing and exiting of vehicle. It shows that the fluctuation of identified moving forces can be effectively bounded at the moment mentioned above if the Regularization solution is adopted to solve

the system equation for MOM. The identified results by the Regularization solution are obviously improved. They are clearly better than the results by the SVD solution and more reasonable in practice.

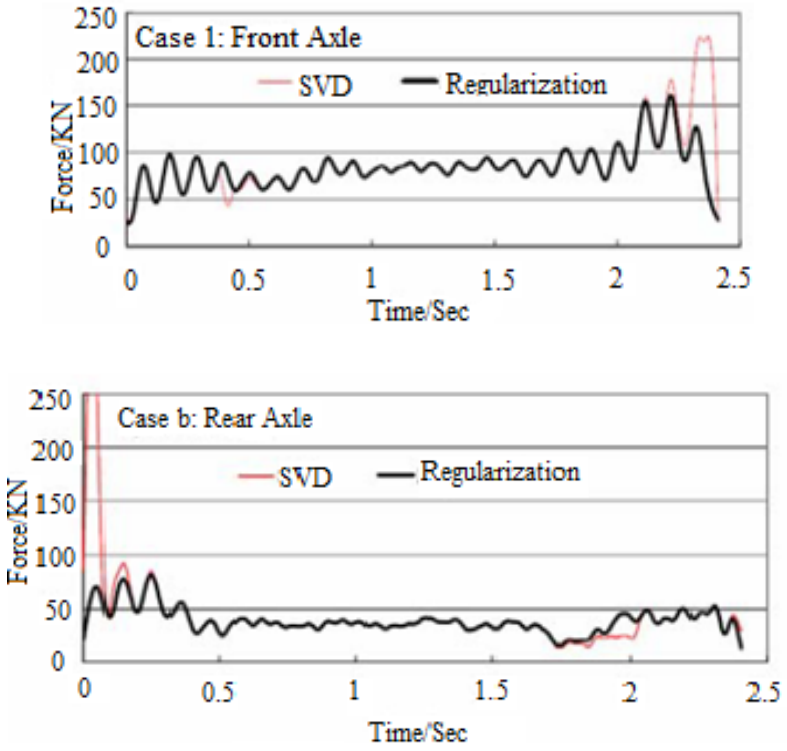

Fig.III.4 Effect of Two Solutions on Moving Forces for MOMA (Matlab Program Model)

III.2.3. FEM Modern Hypothesis

Owing to the introduction and extensive application of the computer and the finite element method, since the 1970s, the main features of modern theory on vibration analysis of vehicles are: considering vehicle model that can be closer to the truth and idealizing bridge for the finite element or finite item model with more quality. The main theories include multi-axial vehicle model, the applications of finite item method and modal analytical method. This section is a simulation using SAP2000 V16 structural software of a bridge subjected to a moving vehicle. It aims from one side at studying the effect of moving vehicles

speed on the structure response and from another side at recognizing the effect of the moving load model for the bridge dynamic analysis.

III.2.3.1 FEM Simulation Data

The bridge was modelled as a simple supported beam meshed into 10 segments; its characteristics are described in detail below in table III.2. Vehicle loading is assumed to be a series of 10 moving forces of 3500 KN, with different speeds values to be 180, 120 and 80 km/h to analyze the speed effect on the bridge response (see Appendix 1). The non linear model analysis was used to perform the dynamic response of the beam.

Table III.2. Bridge Model Characteristics

Elastic modulus (N/m^2)	Beam length (m)	Area of section (m^2)	Width (m)	Height (m)
$2x10^{11}$	32	1	1	1

III.2.3.2 FEM Simulation Results

Twelve modes of vibrations were selected for analysis when moving load post processing is used for analyzing the results. Displacement of the mid-span node in the transverse direction is chosen as Y axis, and modes of vibration were chosen as horizontal axis, thus displacement-time relationship curves of the node in the mid-span can be drawn as shown in Figs III.4a, b and c, when the car passes through the bridge with a speed of 180km/h, 120km/h and 80km/h. The deformation of the simple supported beam is also shown in Fig.III.5 when the displacement of the mid-span node reaches the maximum value. The results were compared to those obtained in the research work of (Ji,J *et al.,* 2012) where the bridge was modeled as a beam having the same characteristics as the ones of this study model and the vehicle was considered as a moving force.

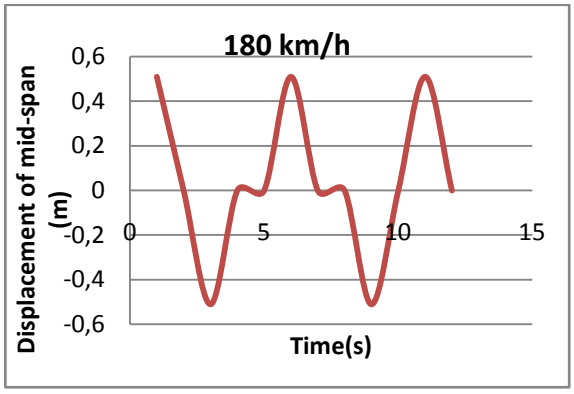

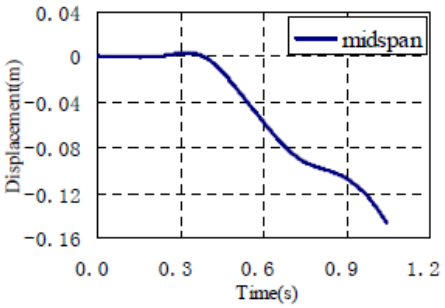

Framework model Ji model

(a) Vehicle running with 180km/h

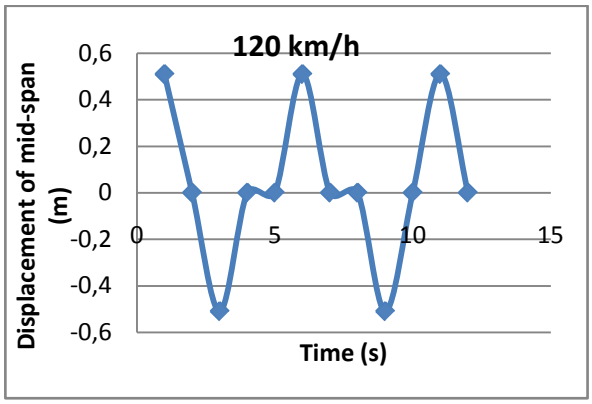

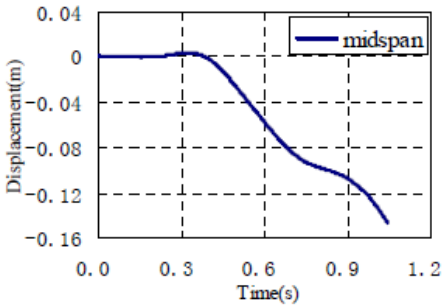

Framework model Ji model

(b) Vehicle running with 120km/h

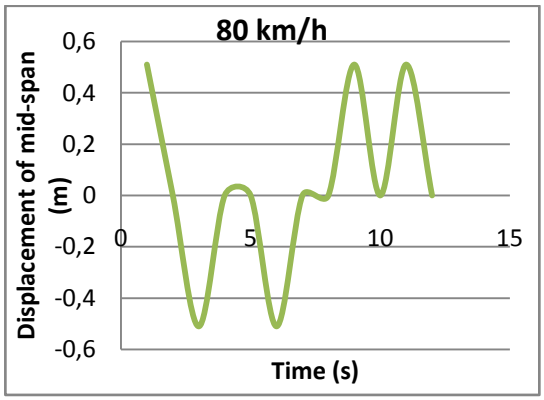

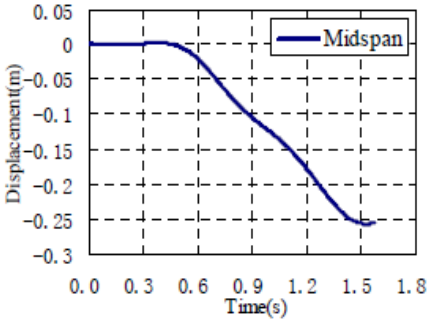

Framework model Ji model

(c) Vehicle running with 80km/h

Fig.III.5 Mid-span Displacements Under Moving Loads

(Sap2000 V16 Model)

Fig.III.6 Deformed Shape of the Bridge Model
(Sap2000 V16 Model, Ji,J et al., 2012)

The peak values of each moving load speed are summarized in table III.3 with the relative time of vibration, the results show that the displacement of the mid-span of the bridge model is the same for the vehicle speeds 180 and 120 km/h which means that the two high speeds have the same effect on the bridge response whereas for the speed 80 km/h, the mid-span node moves differently with a lower value, we can observe too that the first mode always contains the max deformation.

It can be seen too from the figures, when the constant force of (Ji,J et al., 2012) model moves at a uniform speed of 180km/h, 120km/h and 80km/h, the maximum dynamic deflection at the mid-span of simple supported beam is,-0.147m, -0.257m and -0.320m respectively. It shows that the maximum dynamic deflection at the mid-span of beam is gradually reduced with the increasing of the speed. Whereas in the proposed model of this study, the increasing in speed produces the increasing of deflection at mid-span still a certain value which is 120km/m in this model where the structure is stabilized and vibrates with the same mode.

Table III.3. Max and Min Displacement Values with the Corresponding Modes

	Framework model		Ji model	
Speed (Km/h)	Time (s)	Max Value of Displacement (m)	Time (s)	Max Value of Displacement (m)
180	1,05	0,516	1,05	-0,147
120	1	0,516	1,05	-0,257
80	0,9	0,510	1,5	-0,320

III.3. Bridge-Vehicle Coupled System Frame Work

Dynamic analysis of vehicle-bridge coupled system requires two sets of equations of motion for the bridge and vehicles, respectively. These describe the interaction or contact forces at the contact points of the two subsystems. Because the contact points move from time to time, the system matrices are generally time dependent and must be updated and factorized at each time step. The various solution methods can be generalized into two groups according to whether or not an iterative procedure is needed at each time step (Chen, Z. W. 2010).

In this study, the long cable bridge was chosen to be studied because of its high sensibility to moving vehicles, and dynamic loads. The vehicle-bridge interaction model consists of the vehicle subsystem and the bridge subsystem, which are linked by the assumed forces interaction.

The vehicle and the bridge are presented by two separate finite element models that are established using a commercial software package. The nonlinear forces of the springs and the forces of the road vehicles are treated as pseudo forces in the vehicle subsystems. The subsystems are coupled through the contacts between the bridge and road vehicles. To allow the complex computation of these forces, the coupled equations of motion of the bridge and road vehicle subsystems are expressed as follows.

III.3.1. The Vehicle Equation of Motion

The equation of motion for a vehicle can be expressed as follows:

$$[M_v]\{\ddot{x}_v\}+[C_v]\{\dot{x}_v\}+[K_v]\{x_v\}=\{F_v\} \quad \text{(III.14)}$$

Where: $[M_v]$, $[C_v]$ and $[K_v]$ are the mass, damping, and stiffness matrices of the vehicle, respectively; $\{\ddot{x}_v\}, \{\dot{x}_v\}$ and $\{x_v\}$ are the acceleration, the speed and the displacement vectors of the vehicle respectively and $\{F_b\}$ is the vector of the wheel-road contact forces acting on the vehicle.

III.3.2. The Bridge Equation of Motion

The equation of motion of the bridge can be written as follows:

$$[M_b]\{\ddot{x}_b\}+[C_b]\{\dot{x}_b\}+[K_b]\{x_b\}=\{F_b\} \quad \text{(III.15)}$$

Where: $[M_b]$, $[C_b]$ and $[K_b]$ are the mass, damping, and stiffness matrices of the bridge, respectively; $\{\ddot{x}_b\}, \{\dot{x}_b\}$ and $\{x_b\}$ are the acceleration, the speed and the displacement vectors of the vehicle respectively and $\{F_v\}$ is the vector of the wheel road contact forces acting on the bridge.

III.3.3. The Road Surface Condition

Road surface condition is a very important factor that affects the dynamic responses of both the bridge and vehicles. Deterioration of bridge road surfaces can occur at both the bridge deck and joints due to factors like aging, varying environmental conditions, corrosion, increased gross vehicle weight, etc (Karaki,G.2011). Fig.III.7 shows two examples of degraded bridge road surface in the pavement and joint.

Fig.III.7 Deteriorated bridge approach joint over Doc and Tom Creek (Viewed on http://www.fhwa.dot.gov)

A road surface profile is usually assumed to be a zero-mean stationary Gaussian random process and can be generated through an inverse Fourier transformation based on a power spectral density (PSD) function (Dodds and Robson 1973) such as:

$$r(x) = \sum_{k=1}^{N} \sqrt{2\varphi(n_k)\Delta n}\cos(2\pi n_k \mathrm{X} + \theta_k) \tag{III.16}$$

Where θ_k is the random phase angle uniformly distributed from 0 to 2π, φ is the PSD function (m^3/cycle/m) for the road surface elevation; and n_k is the wave number (cycle/m). In the present study, the following PSD function (Huang and Wang 1992) was used:

$$\varphi(n) = \varphi(n_0)\left(\frac{n}{n_0}\right)^{-2} \qquad (n_1 < n < n_2) \tag{III.17}$$

Where n is the spatial frequency (cycle/m); n_0 is the discontinuity frequency of 1/2π (cycle/m); $\varphi(n_0)$ is the roughness coefficient (m^3/cycle) whose value is chosen depending on the road condition; and n_1 and n_2 are the lower and upper cut-off frequencies, respectively. The International Organization for Standardization (ISO 1995) has proposed a road roughness classification index from A (very good) to H (very poor) according to different values of $\varphi(n_0)$ (ASHTO. 2003).

III.3.4. Assembling the Vehicle-Bridge Coupled System

Vehicles travelling on a bridge are connected to the bridge via contact points as shown in the VB (Vehicle Bridge) coupled system in Fig.III.8. Using the displacement relationship and the interaction force relationship at the contact points, the vehicle-bridge coupled system can be established by combining the equations of motion of both the bridge and vehicle, as shown below:

$$\begin{cases} M_b \ddot{x}_b + C_b \dot{x}_b + K_b x_b = F_b \\ M_v \ddot{x}_v + C_v \dot{x}_v + K_v x_v = F_v \end{cases} \tag{III.18}$$

The interaction forces acting on the bridge F_b and on the vehicles F_v are actually action and reaction forces existing at the contact points. In terms of finite element modelling, these interaction forces may not apply right at any node.

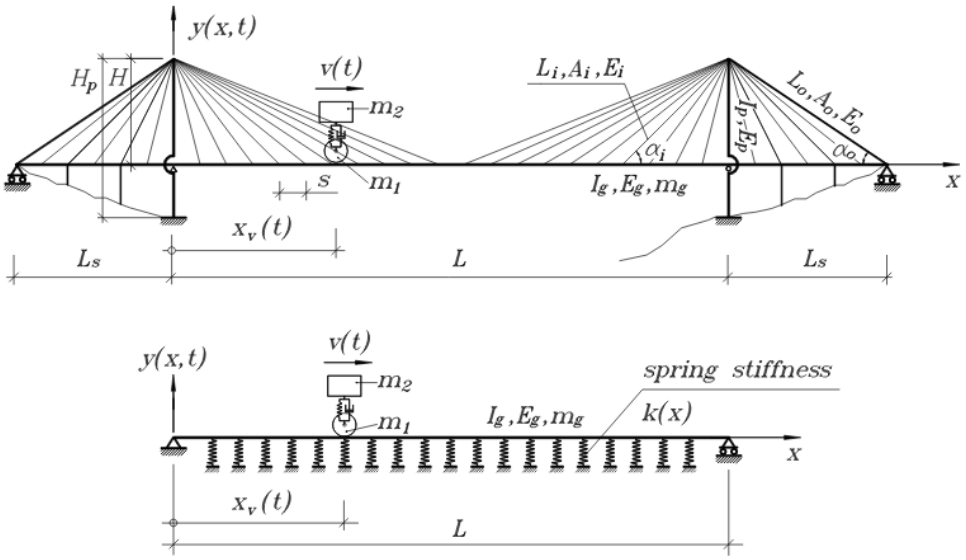

Fig.III.8 Cable Stayed Bridge FE Model with Sprung Mass Vehicle Loading

(Viewed on: Karoumi, R. 1998)

Therefore, the interaction forces need to be transformed into equivalent nodal forces $\{F_b^{eq}\}$ in the finite element analysis. This can be done using the virtual

work principle, which states that the work done by the equivalent nodal forces and the actual force should be equal, which can be expressed as:

$$\{x_{b-nodal}\}^T \{F^{eq}\} = x_{contzct}.F \tag{III.19}$$

Where $\{x_{b-nodal}\}$ is the displacement vector for all the nodes of the element in contact; $d_{contact}$ is the displacement of the element at the contact point; F^{eq} is the equivalent force vector applied at all the nodes of the element in contact; and F is the real force acting at the contact point.

Since $x_{contact}$ can be expressed using the displacement at each node of the element as below:

$$x_{contact} = [N_e]\{x_{b-nodal}\} \tag{III.20}$$

Where $[N_e]$ is the shape function of the element in contact. From previous last equations we can easily obtain the following relationship between the equivalent nodal forces and the interaction force acting on the element in contact:

$$\{F^{eq}\} = [N_e]^T.F \tag{III.21}$$

As discussed earlier, F_b are the interaction forces acting on the bridge and F_v are the reaction forces of that acting on the vehicles. Therefore, the following relationship holds:

$$\{F_b\} = -\{F_v\} \tag{III.22}$$

From the relations cited previously we can easly obtain:

$$\begin{aligned}&[M_b]\{\ddot{x}_b\} + [C_b]\{\dot{x}_b\} + [K_b]\{x_b\} \\ &= [K_{b-v}]\{x_v\} - [K_{b-vb}]\{x_v\} - \{F_{b-r}\} + [C_{b-v}]\{\dot{x}_v\} - [K_{b-cb}]\{x_b\} \\ &- [C_{b-b}]\{\dot{x}_b\} - \{F_{b-cr}\}\end{aligned} \tag{III.23}$$

III.3.5 Vehicle-Bridge Coupled System Modelling

In order to validate the analytical study described in the previous section of the coupled system vehicle-bridge, a three dimensional model was established using structural software SAP2000 V 16 and mathematical software Matlab to simulate the vehicle excitation applied on the system.

A highway cable stayed bridge was chosen for the bridge model because of its high sensibility to dynamic loads, the bridge information are described in table III.4, the vehicle loads were applied as a power spectral density of time history function obtained from data station records called *Vibration data* and which were plotted using Matlab software to convert results from frequency time variation to a power spectral density as shown in Appendix 2.

Table III.4. Bridge Model Description

Length (m)	Width (m)	Modulus of Elasticity (Gpa)	Pylon Height (m)	Cable Diameter (m)
200	6	19	50	0,6

III.3.6 Simulation Results

Table III.5 summarizes the total response modal information of the bridge-vehicle coupled system where it can be observed that the period of vibration of the first mode is about 0,55 sec which represents a very small period and reflect the effect of the vehicle loading on a bridge response.

The PSD of the vehicle loading is represented in Fig.III.9, the curves were obtained using the command “show plot data”, the max frequency is clearly at the time 4,5 sec.

Table III.5. Modal Properties of Output Model Results

TABLE: Modal Periods And Frequencies						
OutputCase	**StepType**	**StepNum**	**Period**	**Frequency**	**CircFreq**	**Eigenvalue**
Text	Text	Unitless	Sec	Cyc/sec	rad/sec	rad2/sec2
MODAL	Mode	1	0,553128	1,8079	11,359	129,04
MODAL	Mode	2	0,553128	1,8079	11,359	129,04
MODAL	Mode	3	0,219809	4,5494	28,585	817,09
MODAL	Mode	4	0,219807	4,5494	28,585	817,1
MODAL	Mode	5	0,193141	5,1776	32,532	1058,3
MODAL	Mode	6	0,193141	5,1776	32,532	1058,3
MODAL	Mode	7	0,098949	10,106	63,499	4032,1
MODAL	Mode	8	0,098949	10,106	63,499	4032,1
MODAL	Mode	9	0,066254	15,093	94,835	8993,6
MODAL	Mode	10	0,066254	15,093	94,835	8993,7
MODAL	Mode	11	0,061752	16,194	101,75	10353
MODAL	Mode	12	0,061752	16,194	101,75	10353

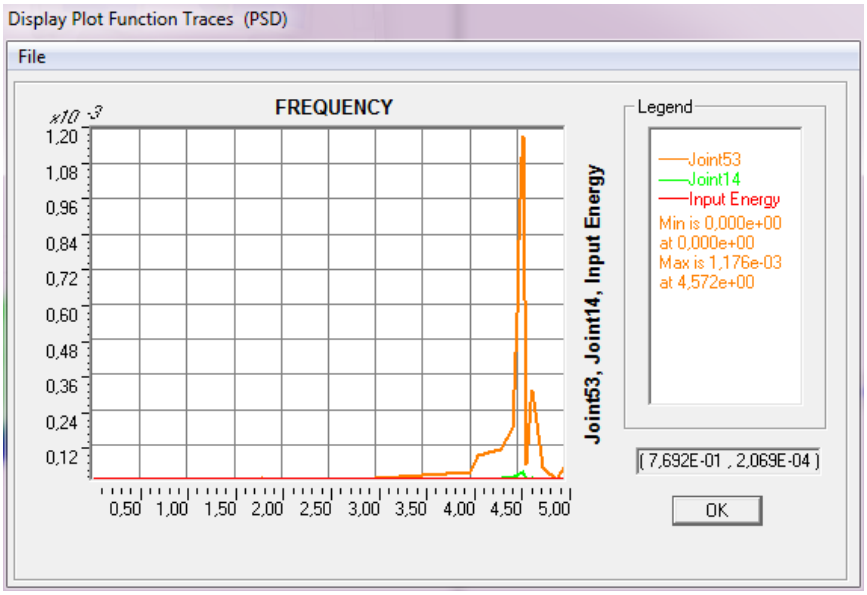

Fig.III.9 Plot Function Traces (PSD)

(SAP2000 V16 Model)

The deformed shape of the bridge structural elements is presented in Fig.III.10 and the axle forces in Fig.III.11 in which the max of deformation and axle force are located at the mid-span so it can be concluded that it is considered as the most week section in the deck.

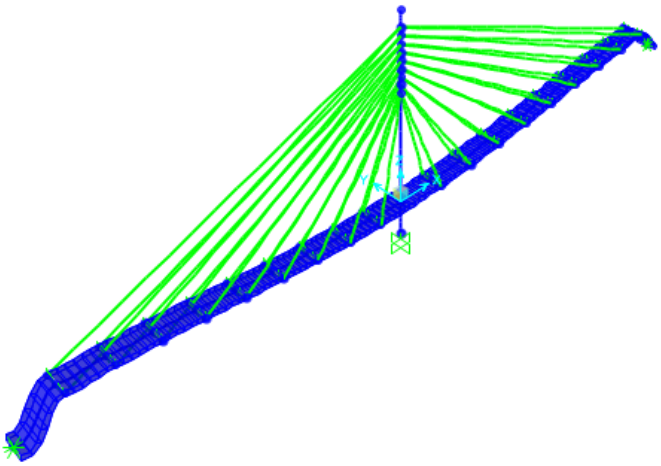

Fig.III. 10 B-V Model Deformed Shape under PSD Vehicle Loading

(SAP2000 V16 Model)

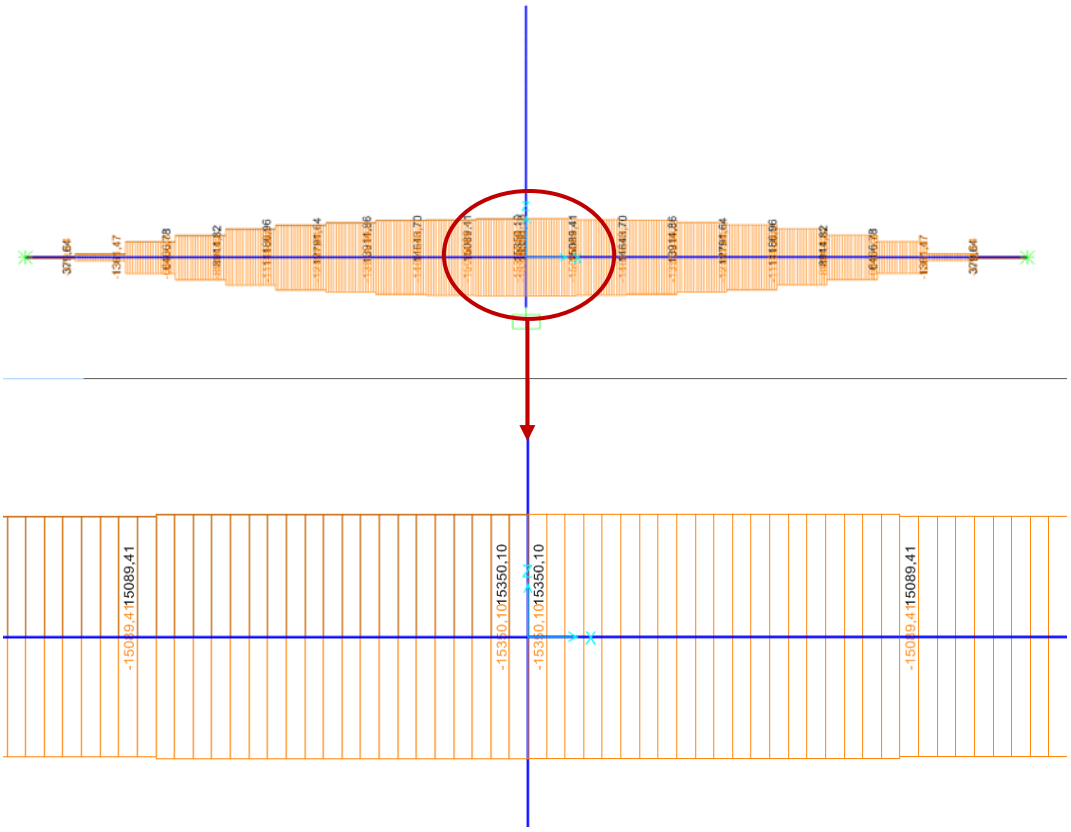

Fig.III.11 Axle force values diagram

(SAP2000 V16 Model)

The max value of the axle force applied on the structure and which represents the moving load is 15350,10 KN and located at mid span, this value is clearly higher than the one obtained by a simplified model where the load is considered as a moving force like the results of (Ji,J et al., 2012) research work in which the max value of the applied force was 3484 KN, that confirms the under estimate of this kind of loads in dynamic analysis of bridges.

Conclusion

To conclude with, a bridge structure subjected to variable scenarios of vehicles is a very complex problem because of the variety of dominating parameters such as the vehicle kind, speed and number in addition to the bridge type and configuration.

The study of the coupled system bridge-vehicle presented here shows the importance of the way how to apply the vehicle loading into the bridge for dynamic analysis. Results show that the moving force model is more effective than the moving mass model, moreover, in the moving mass model, the choice of the solution function has a considerable effect on results, it was obvious that regularization solution is more adopted to solve the system equation for MOM (Method of Moments) compared to the SVD (Singular Value Decomposition) solution.

The vehicle speed has also an important consequence on the bridge response; it has been confirmed by results obtained in the 2D beam model under various moving load speeds that the vehicles running over 120km/h have a significant increasing in mid span displacement in the vertical direction.

The proposed model herein using a PSD (Power Spectral Density) to simulate vehicle loads has significant results as compared to the moving mass model. Values of mid-span deflection, the system vibration period and normal forces are quite bigger than the ones obtained by the moving mass model which confirms that the PSD is more realistic model of vehicle loads on bridge structure. Finally,

it was demonstrated too that the mid-span is the most affected area of a bridge structure when subjected to moving vehicle loads.

Chapter IV
Wind-Bridge-Vehicle Interaction

Introduction

Wind is the flow of air movement caused by differences in pressure. When structures immerse in the wind, the interactions between the wind and the structures might change the pressure distribution of structural surface or induce the structures to vibrate in a single or multiple frequencies. In addition, the location of bridges might be exposed to strong winds from wind storms, for instance, tropical cyclones (named as hurricanes in North America or typhoons in Asia-Pacific), thunderstorm, tornados, and downbursts (Chen, S.R., Wu, J.2010). Compared with earthquakes, wind loading produces roughly equal amounts of damage over a long period (Holmes,H. 2001).

With the development of modern materials and construction techniques, the span length of bridges has reached to thousands of meters, such as suspension and cable-stayed bridges. Structural engineers and researchers have conducted various scientific investigations on bridge aerodynamics (Davenport,R. 1962, Scanlan and Tomko 1971, Simiu and Scanlan 1996, Bucher and Lin 1988). Three approaches are currently used in the investigation of bridge aerodynamics: the wind tunnel experiment approach, the analytical approach and the computational fluid dynamics approach (Chen,Y, 2004). As the backbones of the transportation lines in coastal areas and being vulnerable to wind loads, long-span bridges must be designed to withstand the drag forces induced by the mean wind, maintain dynamic stability under extreme wind conditions, and avoid serious fatigue failure under large wind induced vibrations due to aero-elastic effects. In order to investigate wind effects on structures analytically, wind induced vibrations were categorized as buffeting, flutter, galloping and vortex induced vibrations. The wind forces on bridges could be stated as the summation of static, self-excited, and buffeting force. Buffeting and vortex forces are similar, while the former is random vibrations and the latter is periodic vibrations. Under the dynamic effects from these two kinds of wind induced vibrations, fatigue damage would accumulate and may lead to an eventual collapse of bridges.

IV.1. Wind Dynamic Loads Classes

When a flexible structure is immersed in a given flow field, the bridge will be subject to mean and fluctuating wind forces. To simulate these forces a linear approximation of the time-averaged static and time-varying wind force components must be formulated (Davenport, 1962; Scanlan, 1978). The dynamic wind loads can be generally classified as: self-excited, buffeting and vortex-shedding induced.

IV.1.1. Self Excited Forces

For a given structure immersed in wind, the motion of the structure perturbs the flow around it such that the modified flow pattern produces additional aerodynamic damping and stiffness loads that are called *self-excited* wind loads. The *self-excited* wind loads will either transfer energy from wind to the structural motion or help in dissipating the kinetic energy of the structure.

Above a certain wind speed, the energy increment exceeds the energy dissipation from wind such that the kinetic energy of the structure keeps increasing which makes the structure dynamically unstable. This critical wind speed at which the structure becomes unstable is called flutter speed.

The additional energy injected into the oscillating structure by the aerodynamic forces increases the magnitude of vibration, sometimes to catastrophic levels (Ding *et al.*2000). The self-excited forces on a bridge deck are attributable to the interactions between wind and the motion of the bridge. When the energy of motion extracted from the flow exceeds the energy dissipated by the system through mechanical damping, the magnitude of vibration can reach catastrophic levels (Shum, 2004).

IV.1.2. Buffeting Wind

Buffeting action is a random vibration caused by turbulent wind that excites certain modes of vibration across a bridge depending on the spectral distribution of the pressure vectors (Ding *et al*. 2000).

Although the buffeting response may not lead to catastrophic failure, it can lead to structural fatigue and affect the safety of passing vehicles (Boonyapinyo *et al.* 1999). Hence, buffeting analysis has received much attention in recent years in research into the structural safety of bridges under turbulent wind action (Chen et al., 2000a, 2000b; Ding et al., 2000; Chen and Kareem, 2001; Chen and Cai, 2003; Xu and Guo, 2003; Xu et al., 2003; Guo et al.,2007).

The fluctuating wind loads can be calculated based on a statistical description of the turbulence characteristics of the undisturbed flow approaching the structure. Using admittance function formulation proposed by (Davenport,1962), the turbulence characteristics can be converted from the wind properties into wind loads on the structure. The frequency-domain admittance function formulation can be also transformed to time-domain indicial function formulation which can be used in time-domain structural analysis.

IV.1.3. Vortex Wind

Shedding of alternating vortices from the top and bottom surfaces of a solid body immersed in wind could be observed in its wake. The shed vortices are accompanied by periodically changing pressure distributions around the bluff body which can induce periodic aerodynamic loads on the body, termed as *vortex-shedding* induced loads.

Vortex shedding is perhaps one of the most studied phenomena of fluid mechanics, especially its interaction with circular cylinders; see for example (Goswami *et al*. 2005). When a vortex is formed on one side of a body, it

immediately increases flow velocity on the opposite side, which results, according to Bernouilli theory, in a pressure reduction.

Under certain conditions such as a case of a cylinder, the vorticity in the shear layers of the body becomes periodic forming alternating vortices downstream. The periodic vortex street causes a fluctuating force on the body. If it is flexible or supported flexibly, an interaction takes place between downstream flow and body displacements. These periodic vortices are called Von Karman Vortex Street, named after Von Karman who studies the phenomenon around 1910. The fundamentals of this phenomenon can be found in classical literature such as (Simiu & Scanlan) and (Dyrbye & Hansen).

IV.2. Research Background on Bridge-Vehicle Response to Wind Loads

The bridge vibration is a multi-frequency vibration at low wind speeds. However, when the wind speed approaches the flutter wind speed, the multi-frequency vibration merges into a single-frequency dominated flutter vibration.

When trains and road vehicles are running on long-span bridges under crosswinds, complicated dynamic interactions occur among the trains, road vehicles, cable-supported bridge, and wind. The buffeting response of the bridge due to crosswind is superimposed on the dynamic response of the bridge due to railway and road vehicles. The large vibration of the bridge will in turn considerably affect the safety and ride comfort of the drivers of the road vehicles. Thus, the dynamic responses of a coupled vehicle-bridge system under crosswinds are of great concern to both engineers and researchers.

However, the interaction between wind and vehicles must also be taken into account in a coupled wind-vehicle-bridge analysis. Many studies have investigated wind-vehicle interactions in the past few decades. (Balzer) developed a theory to estimate the aerodynamic forces on a moving vehicle using Taylor's hypothesis of "frozen turbulence." For engineering applications, (Cooper) proposed the power spectral density (PSD), square-root coherence function,

phase-lag function, and aerodynamic admittance function to model the unsteady side forces on a moving vehicle and laid down the foundations for investigating the effects of wind on a moving vehicle in the frequency domain. Baker developed a theoretical model that describes the dynamics of vehicles in crosswinds in the time domain, which was later extended to include driver behaviour. (Baker) further investigated both the steady and unsteady aerodynamic forces acting on a variety of vehicles and carried out extensive studies of the interaction between aerodynamic forces and moving vehicles. These approaches have all been applied in coupled vehicle-bridge analysis. For example, (Xu et al.) simulated the aerodynamic wind forces acting on running road vehicles using the quasi-steady approach and (Xu and Ding) derived and simulated the steady and unsteady aerodynamic forces acting on a moving railway vehicle in crosswinds in the time domain.

Based on these separate studies on the various types of dynamic interactions among wind, vehicles (trains or road vehicles), and long-span bridges, several researchers in the last decade have examined the wind-vehicle-bridge coupled system as a whole. For instance, studies have been carried out on coupled road vehicle and cable-stayed bridge systems and on coupled train and cable-supported bridge systems in crosswinds. In the recent years, several new advances have been made both in numerical simulation technologies and in wind tunnel measurements. (Chen et al.) proposed a wind-vehicle-bridge framework which enables considering the dynamic effects induced by simultaneous actions of railway, highway and wind loading, and it was applied to analyze dynamic stress of long suspension bridges. (Li et al.) extended the wind-vehicle-bridge couple analysis to the case of two trains meeting on a long-span suspension bridge. (Chen and Wu) proposed a semi deterministic analytical model which is able to consider dynamic interactions between the bridge, wind, and stochastic “real” traffic. Based on the wind tunnel tests, (Dorigatti et al.) measured crosswind loads on high sided vehicles over long-span bridges, taking three different vehicles (van, double deck bus, and lorry) and two different bridge deck configurations into

consideration. (Zhu et al.) investigated aerodynamic coefficients of road vehicles by adopting different road vehicles types, wind directions and vehicle positions. (Li et al) studied the effects of sudden changes of wind loads as the train passing through a bridge tower or two trains passing each other by using the wind tunnel test rig with moving train models. (Han et al.) developed an experimental setup for measuring the aerodynamic characteristics of vehicles and the bridge in wind tunnel and then investigated the influences of parameters adopted in the tests.

IV.3. Framework

The wind loads acting on the vehicle-bridge system includes both steady and unsteady aerodynamic forces in the time domain that can takes into account the effects of moving speed and the spatial correlation of the vehicles with wind forces on the bridge.

To simplify the wind-vehicle-bridge dynamic analysis, the following assumptions are considered in the modelling of the vehicle-bridge system in this study:

- 3D slab deck, beams and column elements are used to model the bridge deck and tower of the cable-stayed bridge studied herein as mentioned in the previous chapter.
- The road vehicles running on the bridge are assumed to travel at a constant speed, and the vehicle is regarded as a rigid car body supported by spring-damper units.
- The interactions of the vehicle–bridge system are regarded as no separation and side slipping of the wheels of running vehicles.
- The vehicle accidents running on bridge deck, such as overturning and lateral sliding, would be excluded in the present investigations.

The wind, the vehicle and the bridge subsystems of the WVB (Wind Vehicle Bridge) system are linked by wind-vehicle interaction, bridge-vehicle interaction

and wind-bridge interaction. The interactions are the connections between the subsystems, as shown in Fig.IV.1.

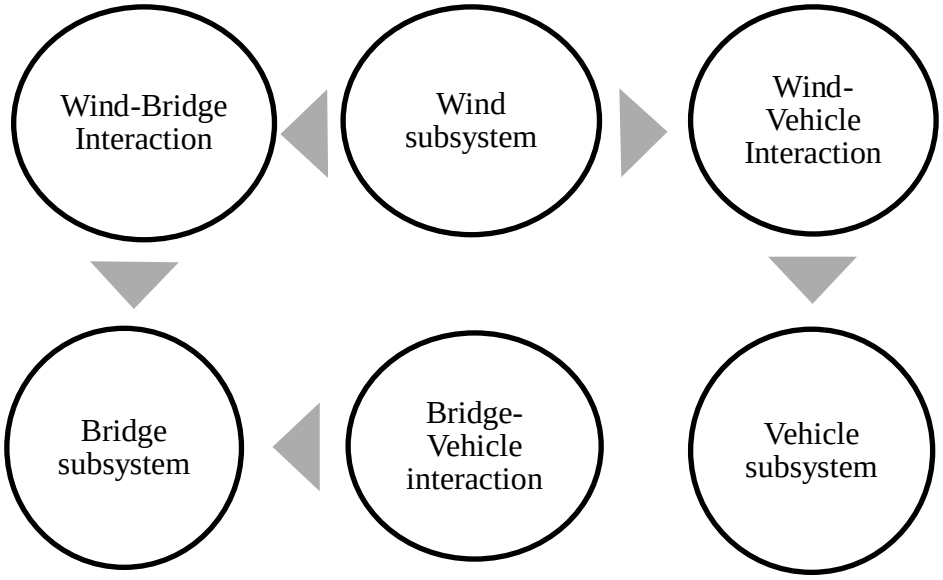

Fig.IV.1 The Interaction Relation of WVB System

IV.3.1. Problem Formulation

A two span cable-stayed bridge presented in chapter III is simulated by finite element modelling. The three major components of the bridge modelled by finite elements are:

- The bridge deck is modelled as a number of beam-column elements incorporating all the axial and inertial properties.
- Each of the towers is modelled by a number of beam-column elements with the axial and flexibility.
- Each stay cable is represented as a two-node bar or truss element of which the axial stiffness is related to the axial tension.

The axial bar element considering the sagging effect caused by self-weight is used to represent the curved cable, for which the equivalent modulus Eeq is given by Ernst as follows:

$$E_{eq} = \frac{E_S}{1 + \left[\frac{(w_c L_h)^2 (T_i + T_f) E_s A_c}{24 (T_i T_f)^2} \right]} \tag{IV.1}$$

Where E_s is the elastic modulus, L_h the horizontal projected length, w_c the weight per unit length, A_c the cross-sectional area, and T_i the initial cable tension resulting from the dead loads of the bridge and T_f the final cable tension caused by the real acting loads including vehicular loads and wind actions. The equation of motion of the whole bridge and vehicle under wind actions are written as:

$$\begin{aligned} &[M_b]\{\ddot{x}_b\} + [C_b]\{\dot{x}_b\} + [K_b]\{x_b\} = \{P_{b-w}\} - \{F_c\} \\ &[M_c]\{\ddot{x}_c\} + [C_c]\{\dot{x}_c\} + [K_c]\{x_c\} = \{P_{c-w}\} + \{P_c\} + \{f_c\} \end{aligned} \tag{IV.2}$$

Where $[M]$, $[C_b]$, $[K_b]$ denote the mass, damping, and stiffness matrices, $\{x_b\}$ the displacements of the beam element, $\{P_{b\text{-}w}\}$ nodal aerodynamic forces acting on the beam element, and $\{f_c\}$ the contact forces existing between the vehicle system and the beam element. Also, $[M_c]$, $[C_c]$, $[K_c]$ denote the mass, damping, and stiffness matrices of the sprung mass, $\{x_c\}$ the vertical deflections of the wheel and sprung masses, and $\{P_{c\text{-}w}\}$ aerodynamic forces acting on the moving vehicles. Here, the aerodynamic force vectors of $\{P_{b\text{-}w}\}$ and $\{P_{c\text{-}w}\}$ will be described in detail in the following section.

IV.3.2. Simulation of Wind Loads

Wind-induced vibrations of moving vehicles on cable-stayed bridges are of concerns in this chapter. In this section, the wind loads acting on the vehicle-bridge system will be presented. The aerodynamic coefficient curves for the lift force and moment on the deck section are related to the angle of attack (Simiu and Scanlan 1996). The wind loads acting on the vehicle-bridge system are generated in the time domain by digital simulation techniques that can account for the spatial correlation of stochastic wind velocity field. Then an incremental iteration-based computational framework will be presented for dynamic analysis of the wind-vehicle-bridge system.

IV.3.2.1. Wind Loadings on the Bridge Deck

Fig.IV.2 shows lateral wind load acting on the bridge deck with a mean velocity V and incident angle α_0. As indicated, the effective angle α of attack along the oncoming wind flow can be expressed as $\alpha(x,t) = \alpha_0 + \theta(x,t)$.

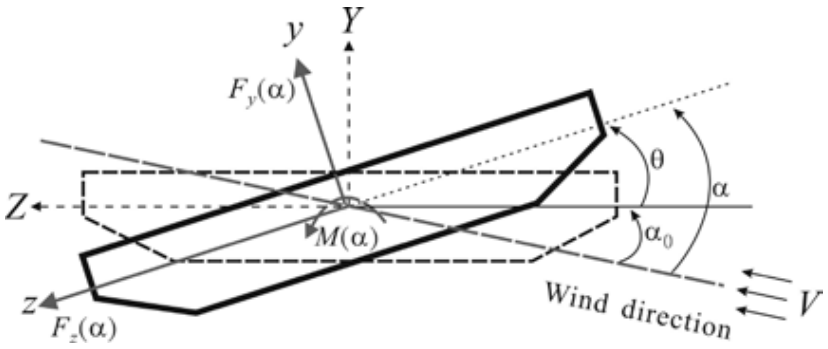

Fig.IV.2 Wind Loads Acting on the Bridge Deck Section

(Viewed on : Eurocode 1 : Actions on structures - Part 1-4: General actions - Wind actions)

Since only the vertical and torsional vibrations of the beam are concerned, the lateral vibration of the beam caused by the aerodynamic drag force will be ignored. The *aerodynamic lift force* and *pitching moment* acting on the bridge deck can be expressed in terms of α as follows:

$$F_y(\alpha) = \frac{\rho V^2 B}{2} C_y(\alpha), F_z(\alpha) = \frac{\rho V^2 D}{2} C_z(\alpha)$$
$$M(\alpha) = \frac{\rho V^2 B^2}{2} C_M(\alpha)$$
$$V = V_0 + w \qquad \text{(IV.3)}$$

Where V_0 is the velocity of mean wind, v_w is velocity of fluctuating wind, ρ is the air density, B is the bridge deck width, D is the bridge deck depth, C_z is aerodynamic lift coefficient, C_y is the aerodynamic lateral coefficient, and C_M is the aerodynamic moment coefficient. In this study, the aerodynamic coefficients of drag (C_y), lift (C_z) and moment (C_M) of the bridge are given as: $C_D = 1.18$, $C_L = 0.21$, and $C_M = 0.12$ (Xu 2003), respectively.

IV.3.2.2. Simulation of Quasi-Steady Aerodynamic Forces on Moving Vehicle

Fig.IV.3 shows the wind load model acting on a running vehicle with a mean velocity *U* and turbulent velocity *w*.

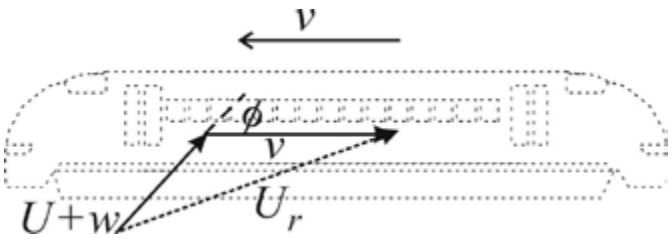

Fig.IV.3 Relative Wind Velocity and Natural Wind Velocity to a Moving Vehicle

(Viewed on : Eurocode 1 : Actions on structures - Part 1-4: General actions - Wind actions)

The *aerodynamic forces* and *moments* acting at the mass centre of the moving vehicle are expressed as:

$$F_s = \frac{\rho A_s U_r^{\,2}}{2} C_{cS}(\varphi), M_y = \frac{\rho A_s d_e U_r^{\,2}}{2} C_{cY}(\varphi)$$
$$F_L = \frac{\rho A_T U_r^{\,2}}{2} C_{cL}(\varphi), M_p = \frac{\rho A_T h_v U_r^{\,2}}{2} C_{cM}(\varphi)$$
$$U_r = \sqrt{[v + U\cos\phi]^2 + [U + w)\sin\phi]^2}$$
$$\tan\phi = \frac{(U + w)\sin\phi}{v + U\cos\phi} \qquad \text{(IV.4)}$$

where ρ is the air density (ρ = 1.2kg/m3), A_S is the side surface area of the vehicle; A_T is the top surface area of the vehicle; *de* is the reference eccentricity of aerodynamic yawing moment about the mass centre, h_v is the reference height of vehicle's mass center C_{cS} is aerodynamic coefficient of vehicle's side; C_{cL} is aerodynamic lift coefficient, C_{cP} is aerodynamic ralling moment coefficient; (φ=arctan(*U* / *v*)) is yaw angle, U_r is the relative wind velocity around the vehicle moving at speed *v* and *w* represent the turbulent wind speed component.

IV.3.3. Response Analysis Procedure

To perform the interaction analysis of a vehicle travelling over guide way under oncoming wind flows in the time domain, the following simplified spectral representation of turbulent wind (Xu et al. 2003) is employed to generate the time history of turbulent airflow velocity $w_j(t)$ in mean wind flow direction (lateral) at the jth point on the suspended beam as:

$$w_j(t) = \sqrt{2(\Delta\omega)} \sum_{n=1}^{j} \left[\sum_{i=1}^{N_f} \sqrt{S_w(\omega_{ni}) G_{jn}(\omega_{ni})} \cos(\omega_{ni} + \psi_{ni}) \right] \tag{IV.5}$$

Where $j=1,2,...,N_s$, N_f is the total number of frequency intervals represented by a sufficiently large number, N_s is the total number of points along the guide way to simulate, S_w (ω) is the spectral density of turbulence in along-wind direction (Kaimal's longitudinal wind spectrum), ψ_{ni} is a random variable uniformly distributed between 0 and 2π, $\Delta\omega = \omega_{up} / N_f$ is the frequency increment, ω_{up} is the upper cut-off frequency with the condition that the value of $S_w(\omega)$ is less than a preset small number ε when $\omega > \omega_{up}$ and the related wind spectrums used in equation (IV.5) are given by:

Horizontal wind spectrum:

$$S_H(\omega) = \frac{200 \times \overline{U}^2}{\left[1 + 50 \frac{\omega}{2\pi} \left(\frac{z}{V_0}\right)\right]^{5/3}} \left(\frac{z}{V_0}\right) \tag{IV.6}$$

Lateral wind spectrum:

$$S_L(\omega) = \frac{15 \times \overline{U}^2}{\left[1 + 9{,}5 \frac{\omega}{2\pi} \left(\frac{z}{V_0}\right)\right]^{5/3}} \left(\frac{z}{V_0}\right) \tag{IV.7}$$

Vertical wind spectrum:

$$S_V(\omega) = \frac{3{,}36 \times \overline{U}^2}{\left[1 + 910\frac{\omega}{2\pi}\left(\frac{z}{V_0}\right)\right]^{5/3}}\left(\frac{z}{V_0}\right) \tag{IV.8}$$

With the steady wind speed of:

$$\overline{U} = \frac{KV_0}{\ln\left(\frac{z}{z_0}\right)} \tag{IV.9}$$

$$G_{jn}(\omega) = \begin{cases} 0 & 1 \le j \le N_S \\ C^{|j-n|} & n = 1, n \le j \le N_S \\ C^{|j-n|}\sqrt{1-C^2} & 2 \le n \le j \le N_S \end{cases} \tag{IV.10}$$

With :

$$C = \exp\left(\frac{-\lambda\omega \times l_{jn}}{2\pi V_0}\right) \tag{IV.11}$$

Here, V_0 means the velocity of wind at height z, $\bar{U}$ stands for the shear velocity of airflow related to von Karman's constant K = 0.4 and the ground roughness z_0, λ is an exponential decay factor taken between 7 and 10, l_{jn} is the distance between the simulated points j and n and $C^{j\text{-}n}$ is the coherence function between points j and n (Xu et al. 2003). In this chapter, the following wind parameters are used: z = 30m, z_0 = 0.012 for open site and λ = 7.

The wind time history used in this work was obtained from Kenneth Thomsen, Riso National Laboratory updated on 3 January 24, 2006, plotted using the Matlab software as illustrated in Appendix 3. Fig.IV.4 shows the time history of fluctuating wind velocities generated by equation (IV.6) in the lateral direction called Kaimal's wind spectrum data.

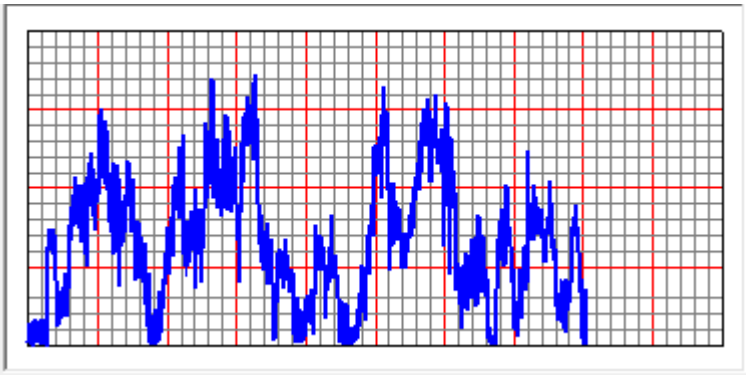

Fig.IV.4 Wind Time History Graph in Lateral Direction

(Viewed on: http://www.vibrationdata.com/data.htm)

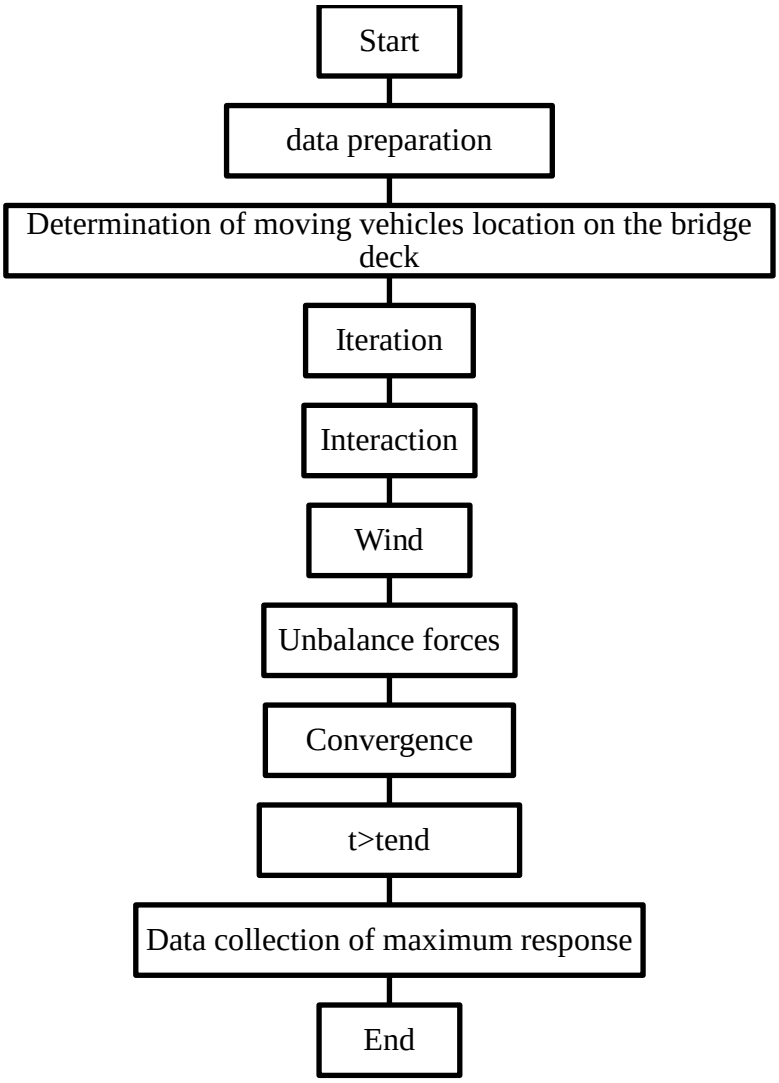

Fig.IV.5: Analysis Procedure of Nonlinear Incremental Iterative Method

To investigate the dynamic response of the vehicle-bridge system under wind actions, Fig.IV.5 shows the analysis procedure of the wind-vehicle-bridge system based on incremental-iterative approaches. Here, the nonlinear aerodynamic curves are simulated by a sequence of piecewise connected linear segments for time history response analysis of the VBI system under the action of wind loads and that what was applied using SAP2000 software using the command “Non linear Direct Integration”.

IV.3.4. Numerical Simulation Results

The bridge model was a cable stayed bridge where the deck is supported by a roller at the connection with the pylon. The pylon is made of concrete with elastic modulus E_c=35GPa and density ρ_c = 2.4t/m3, and the steel bridge deck and stay cable with E_s = 210GPa

In the following numerical illustrations, a traffic flow was considered, the vehicles running on the bridge at one line with two directional ways as mentioned in Appendix 4, the time history of lateral wind (described previously) was applied on the coupled model vehicle-bridge, the plot function was extracted from SAP2000 output data as shown in fFig.IV.6.

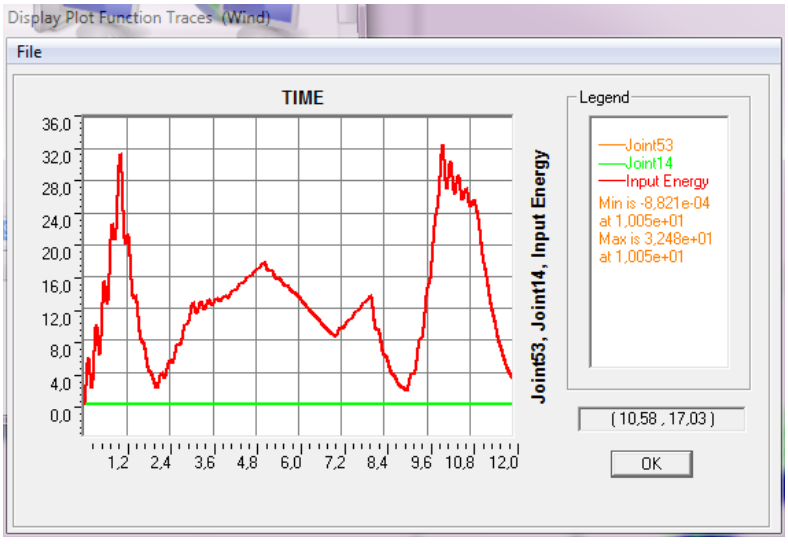

Fig.IV.6: Plot Function of Wind Time History

Fig.IV.7shows the deformed shape of the bridge-vehicle model under lateral wind and table IV.1 shows the midpoint displacement response of the bridge. As indicated, the higher displacement of the mid span under wind is in the lateral direction in addition to a rotation in the three directions. For the moving loading it can be observed that the max of displacement is in the transverse direction which confirms the effect of the two kinds of loading on the bridge response

As the road car moves on the bridge with lower speeds, it may spend more time passing through the long-span bridge. Thus it experiences more small fluctuating excitations transferring from the vibrating bridge deck induced by wind actions.

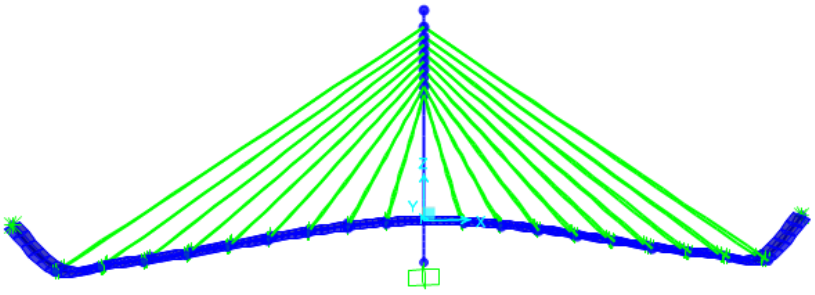

Fig.IV.7: Bridge Deformed Shape under Wind Loading

Table IV.1 Max and Min Displacements of Mid-Span

Joint	**Output Case**	**Step Type**	**U1**	**U2**	**U3**	**R1**	**R2**	**R3**
Text	Text	Text	m	m	m	Radians	Radians	Radians
12	Wind	Max	0	2,24 E-12	0	0	0	0
12	Wind	Min	9,419 E-15	0	-1,6 E-12	-4,499 E-13	-1,887 E-15	-3,457 E-18
12	MOVING	Max	2,262 E-12	0	0	0	4,739 E-13	0
12	MOVING	Min	-2,262 E-12	0	-8,69 E-16	0	-4,739 E-13	0

Fig.IV.8 shows the displacements of the mid span of the bridge in the three directions (X, Y and Z) in which it is clearly observed that the transverse direction contains the max displacement with a very big value compared to the others directions.

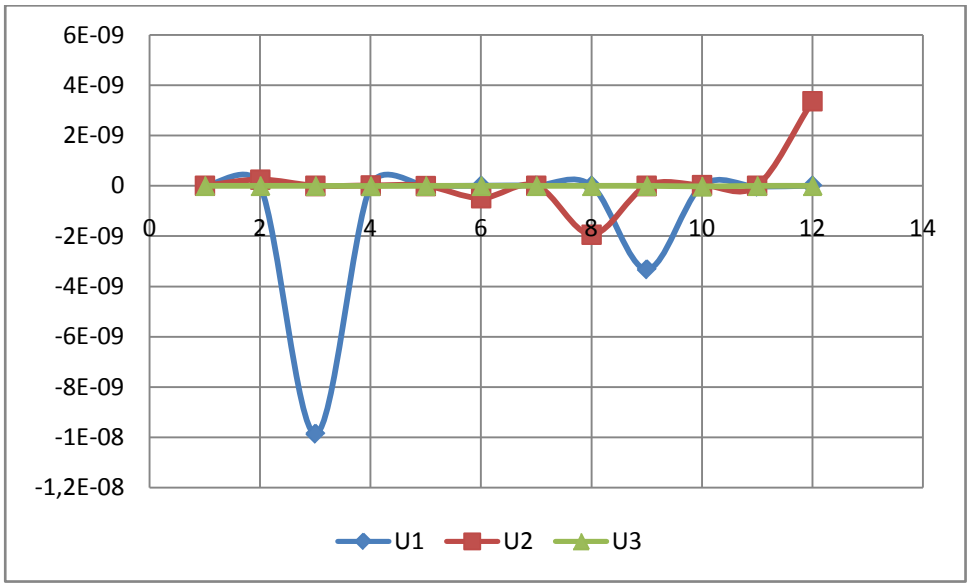

Fig.IV.8 Time History Response of Vertical Midpoint Deflection of the Bridge

Conclusion

In this chapter, a review on wind forces types and effect on bridge was given first. Secondly, Kaimal's wind forces model was established and applied for the coupled system analysis. Finally a computational framework based on FE modelling for wind-vehicle–bridge system was established and solved using an incremental iterative approach where the kaimals lateral spectrum was applied as a time history function for the wind forces and moving force model for the vehicle loading.

The numerical simulation results shows that the effect of two directional vehicles running on the bridge deck is crucial to the VBI system in the transverse direction at mid span under wind actions with a displacement of 2,24E-12m and

under moving forces with a displacement of 2,26E-12m in the longitudinal direction.

Approximately, wind excitation applied on the bridge model in the transverse direction and vehicle forces in the longitudinal direction have the same effect on the bridge responses. That is justified by the moderate wind applied effort, which has the same vibrational effect as the running vehicle, whereas in the case of strong winds the results will unquestionably differ but doesn't represent the general case applied in design calculation.

Chapter V
Bridge Seismic Vibration Mitigation

Introduction

During the time you are reading this sentence there is a 3% probability that there is a magnitude 5.0 or above earthquake occurring somewhere in the world. Most of these events pass unnoticed except by sophisticated sensory equipment. However, when a large earthquake strikes a populated area the results can be catastrophic with widespread damage to buildings, transportation networks and essential service.

Bridges have historically presented significant vulnerabilities during major seismic events, they present fundamental infrastructure to evacuate the affected people and to transport the emergency equipment and materials when a major earthquake occurs. For this raison, their loss of function or failure will result the loss of lives and several economical consequences. One of the most essential reasons of highway bridges failure by earthquakes is seismic shaking, which was well recognized after the 1971 San Fernando earthquake by (Wang,2014). As a result of seismic shaking, highway bridges suffer severe damages to structural components.

Following each major seismic event, structural designs and codes are modified to reflect lessons learnt. There is a strong correlation throughout the world between the occurrence of major earthquakes and advances in seismic design of bridges. In the conventional method of seismic design the structures are designed to dissipate the energy induced by the design earthquake through inelastic deformations as mentioned (Datta,2010).The areas of energy dissipation by inelastic deformations are called plastic hinges as detailed in (Shatarat,2012) work. They are typically located at the base of the foundation units above ground level and are detailed for ductile behavior; they are placed in points accessible for repair. However, severe damage to bridges still occurs resulting in costly repair or demolition and rebuilding.

Reducing the dynamic response of structures can be achieved by structural strengthening, increased ductility or additional damping. It is impractical in

both cost and structural element size to build all structures with sufficient strength to withstand large seismic events. In contrast, high ductility results in severe damage during larger earthquakes. Hence, any solutions have significant cost or damage outcomes and thus any seismic upgrade or solution implementation is a compromise.

Seismic isolation systems by aseismic bearings are used during the last two decades to improve the seismic performance of bridges and reduce the damages degree by absorbing a significant quantity of the energy induced by earthquake and transmitted to the structure (Benjumea and Chio, 2012).

These bearings protect the substructure by restricting the transmission of horizontal acceleration and dissipating the seismic energy through damping as illustrated by (Moehle and Eberhard,2000). Considerable efforts have been made in the past two decades to develop improved seismic isolation design procedure for new bridges and retrofit guidelines for existing bridges (Mitoulis and Tegos 2010).

The suitability of a particular arrangement and type of isolation system will depend on many factors including the span, number of continuous spans, and seismicity of the region, frequencies of vibration of the relatively severe components of the earthquake, maintenance and replacement facilities (Hu,2008).

V.1. Isolation System Elements

There are two interrelated ideas behind developing a seismic isolation system: the first one is to make the structure much more flexible than it is, by altering the way it rests on the ground, hence shift it to the long period range of the response spectrum that is typically characterized by reduced accelerations and consequently reduced inertial forces as illustrated by (Preumont and Seto,2008); the second is to introduce some kind of ‘fuse’ between the structure and the ground, whereby the

amount of base shear to be transferred from the shaking ground to the structure is controlled by the strength of the fuse.

By making the structure more flexible, one might achieve lower seismic forces, but displacements tend to increase. It is therefore essential to also control the amount of horizontal displacement of the isolated structure and an efficient way to do this is by increasing its damping.

Currently used isolation systems are based on the concept of flexible supports placed between the superstructure and the substructure shown in Fig.V.1 which can either remain essentially elastic (linear isolation) or enter the inelastic range (non-linear isolation) upon exceeding a certain level of horizontal shear as mentioned (Kawashima and Shoji,1998).

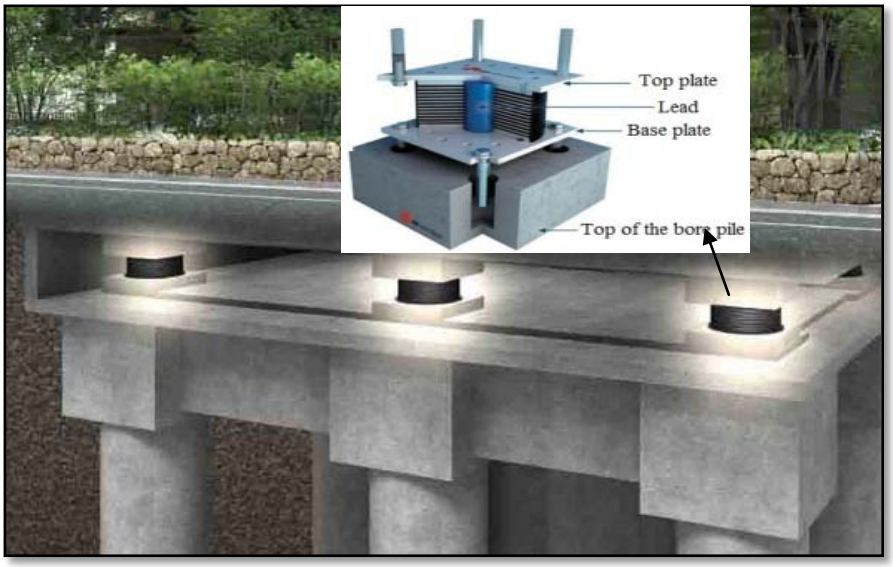

Fig.V.1 Bridge Isolation Mechanism

Common isolation systems in use today include elastomeric and sliding bearings with and without dampers or damping mechanisms. For example, elastomeric bearings may be fabricated from a high damping rubber compound or contain a lead core. Sliding bearings dissipate energy by friction, and may use a separate mechanism to provide a self-centering capability or employ a curved sliding surface that may be spherical, conical, or of varying curvature.

Combinations of elastomeric and sliding bearings are also used, together with roller-based systems, but less frequently. The rollers may be cylinders or balls sandwiched between flat or curved plates. Variations on this theme usually involve added damping mechanisms such as metallic and hydraulic dampers.

As illustrated in Fig.V.2, in (Hanson and Soong,2001) research work, the basic elements included in a seismic isolation system are:

- Horizontally flexible supporting devices (isolators) located either between the structure and its foundation or at a higher level in the structure; in buildings the flexible supports are commonly located at the superstructure-foundation interface, whereas in bridges they are located at the top of the piers and abutments.

- A supplemental damping device (or energy dissipator) for reducing the relative horizontal displacement between the superstructure and substructure (i.e. the portion of the structure below the isolators).

- Some means for controlling displacements at service levels of lateral loading (i.e. wind loading).

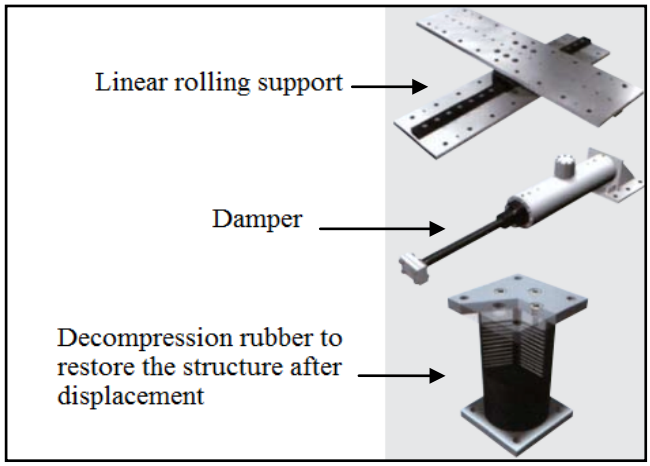

Fig.V.2 Basic Components of Seismic Isolation System

Using seismic isolation bearings to control earthquake induced vibration of bridges and buildings is considered to be a relatively matured technology and such devices have been installed in many structures world-wide in recent decades.

Today, there are many types of isolators including, among others, rubber (elastomeric) bearings, roller bearings, sliding plates, rocking structures, cable supports, sleeved piles, helical springs, and air cushions classified in three categories as mentioned (Charalampos,2011):

- *Hysteretic dampers*: wherein energy dissipation is taking place by yielding of metals such as lead and mild steel, which have hysteresis loops very close to elastoplastic. A popular isolator that incorporates a damping device is the lead-rubber bearing, which is an elastomeric bearing (layers of rubber reinforced with thin steel plates to increase the vertical stiffness) with a lead core which provides both damping (after yield) and resistance to service lateral loads.

- *Viscous dampers*: such as the oil dampers commonly used in the motor industry, but also newer devices such as shear panels containing high viscocity fluids that have recently been developed in Japan. These mechanical devices are separate from the isolators.

- *Frictional dampers*: based on the concept of friction between different materials, for instance stainless steel and PTFE (Teflon). Such systems have a number of advantages, but (unlike the previous ones) they need to be supplemented by a restoring force mechanism (i.e. a means for returning the isolated structure to its initial position after a strong earthquake). An efficient system in this category is the friction pendulum, wherein the sliding surface of the bearing is concave, hence the restoring force is provided by the horizontal component of the weight of the structure itself.

V.2. Aseismic Bearings Behaviour

The major purpose of the bearings for seismic isolation is to decrease the breaking energy of earthquakes that is applied to the structure. The energy dissipators may be simply classified as hysteretic or viscoelastic (Constantinou, Soong, and Dargush, 1998).

Hysteretic dissipators include the yielding of metals due to flexure, shear, torsion, or extrusion (metallic dampers) and sliding (friction dampers). They are all essentially displacement-dependent devices.

Viscoelastic systems include viscoelastic solids, fluid orificing (fluid dampers), and viscoelastic fluids. They are essentially velocity-dependent devices (viscous in nature) and many are also frequency dependent. Some other energy dissipators are modifications of the above set and may include elastic springs or pressurized cylinders to develop pre-load and re-centering capabilities.

Various kinds of devices have been used for this scope as detailled in the following sections.

V.2.1. Lead Rubber Bearing (LRB)

The elastomeric LRB which are generally used for base isolation of structures consist of two steel fixing plates located at the top and bottom of the bearing, several alternating layers of rubber and steel shims and a central lead core as shown in Fig.V.3 (a) (Skinner *et al.*1993). The elastomeric material provides the isolation component with lateral flexibility; the lead core provides energy dissipation (or damping), while the internal steel shims enhance the vertical load capacity whilst minimizing bulging. All elements contribute to the lateral stiffness. The steel shims, together with the top and bottom steel fixing plates, also confine plastic deformation of the central lead core. The rubber layers deform laterally during seismic excitation of the structure, allowing the structure to translate horizontally, and the bearing to absorb energy when the lead core yields (Kaab and Ounis 2011).

The nonlinear behavior of a LRB isolator can be effectively idealized in terms of a bilinear force-deflection curve, with constant values throughout multiple cycles of loading as shown on Fig.V.3 (b). The parameters of the bilinear approximation expressing the law of hysteretic behavior are the following (Kaab *et al.* 2013):

D_y: the yield displacement with:

$$D_y = Q/(K_1 - K_2) \tag{V.1}$$

D: The design displacement of lead rubber bearing LRB

E_H: Energy dissipated by cycle corresponding to the design displacement, equal to the total area of hysteresis loop, it is given by the following formula:

$$E_H = 4Q(D - K_y) \tag{V.2}$$

F_y: The yield force in a monotonous loading

Q: The force, corresponding to null displacement during a cyclic loading, represents also the characteristic strength and the yield force of lead bar for the LRB.

$$Q = F_y - K_2 D_y \tag{V.3}$$

F_{max}: The maximum shear force corresponding to the design displacement D

K_1: Elastic stiffness for a monotonous loading also equals to the stiffness of unloading in cyclic loading, with:

$$K_1 = F_y /- D_y \tag{V.4}$$

K_2: The post elastic stiffness, with:

$$K_2 = (F_{\max} - F_y)/(D - D_y) \tag{V.5}$$

K_{eff}: The effective stiffness of the LRB, it is given by the following formula:

$$K_{eff} = K_2 + \frac{Q}{D} \qquad D \geq D_y \tag{V.6}$$

B_{eff}: The effective damping factor of the seismic base isolation system, it is expressed as follows:

$$\beta_{eff} = \frac{4Q\ (D - D_y)}{2\pi K_{eff} D^2} \tag{V.7}$$

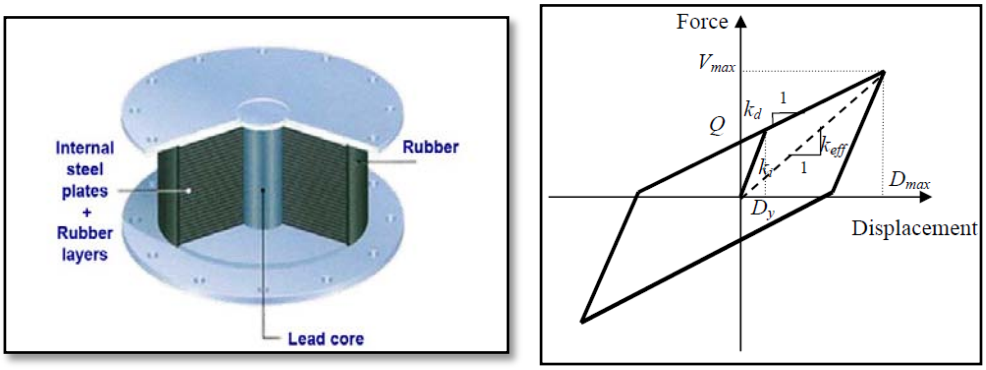

(a) Components (b) Idealized Hysteresis Loop

Fig.V.3 LRB Isolation Bearing

V.2.2.Friction Pendulum System (FPS)

A FPS is comprised of a stainless steel concave surface, an articulated sliding element and cover plate (Petti *et al.* 2013). The slider is finished with a self-lubricating composite liner (e.g. Teflon). During an earthquake, the articulated slider, within the bearing, travels along the concave surface causing the supported structure to move with gentle pendulum motions as illustrated in Fig.V.4.

Movement of the slider generates a dynamic frictional force that provides the required damping to absorb the earthquake energy. Friction at the interface is dependent on the contact between the Teflon-coated slider and the stainless steel surface, which increases with pressure. Values of the friction coefficient ranging between 3% to 10% are considered reasonable for a FPS to be effective.

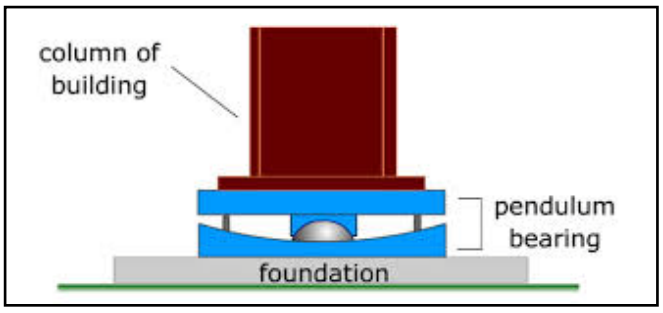

Fig.V.4 FPS Isolation Bearing

The isolator period is a function of the radius of curvature (R) of the concave surface. The natural period is independent of the mass of the supported structure, and is determined from the pendulum equation (Soon and Young1998):

$$T = 2\pi\sqrt{\frac{R}{g}} \tag{V.8}$$

Where g is the acceleration due to gravity

The horizontal stiffness (K_H) of the system, which provides the restoring capability, is provided by:

$$K_H = \frac{W}{R} \tag{V.9}$$

Where W is the weight of the structure

The movement of the slider generates a dynamic friction force that provides the required damping for absorbing earthquake energy. The base shear V, transmitted to the structure as the bearing slides to a distance (D), away from the neutral position, includes the restoring forces and the friction forces as can be seen on the following equation, where μ is the friction coefficient:

$$V = \mu W + \frac{W}{R}D \tag{V.10}$$

The characterized constant (Q) of the isolation system is the maximum frictional force, which is defined as:

$$Q = \mu W \tag{V.11}$$

The effective stiffness (k_{eff}) of the isolation system is a function of the estimated largest bearing displacement (D), for a given value of μ and R, and is determined by the following formula:

$$K_{eff} = \frac{V}{D} = \frac{\mu W}{D} + \frac{W}{R} \tag{V.12}$$

A typical hysteresis loop of a FPS can be idealized as shown in Fig.V.5. The dissipated energy (area inside the hysteretic loop) for one cycle of sliding, with amplitude (*A*), can be estimated as:

$$E_D = 4\mu\, WA \tag{V.13}$$

Thus the damping of the system can be estimated as:

$$\beta = \frac{E_D}{4\pi K_{eff} A^2} = \frac{2}{\pi}\frac{\mu}{A/R + \mu} \tag{V.14}$$

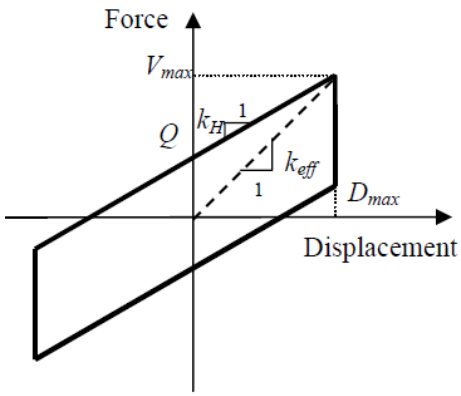

Fig.V.5 Hysteresis Loop of a FPS

V.3. Equation of Motion in Terms of Energy

(Kappos,2002), defined the equation of motion for an isolated structure in terms of displacements as given as in (V.15):

$$M\ddot{x}(t) + C\dot{x}(t) + Kx(t) = -Mr\ddot{x}_g(t) \tag{V.15}$$

Where M is the mass matrix, C is the matrix of the damping constant and K is the stiffness matrix. Integration with regard to the movement of (V.15) which represents the motion in terms of strength, gives us the equation of dynamic equilibrium in terms of energy given as follows:

$$\int_0^t [dx(t)]^T M \ddot{x}(t) + \int_0^t [dx(t)]^T C \dot{x}(t) + \int_0^t [dx(t)]^T Kx(t)$$
$$= -\int_0^t [dx(t)]^T Mr \ddot{x}_g(t) \qquad \text{(V.16)}$$
$$E_K(t) + E_D(t) + E_S(t) + E_H(t) = E_I(t)$$

With:

$E_I(t)$ = input energy of seism.

$E_K(t)$ = kinetic energy.

$E_D(t)$ = energy dissipated by structural damping.

$E_S(t)$ = stored potential energy.

$E_H(t)$ = energy dissipated by the hysteretic behavior of the damping of the isolation system.

V.4. Description of the Isolated Bridge and the Seismic Excitation

The In order to demonstrate the effectiveness of seismic isolation a cable stayed bridge with a long span and continuous deck made of reinforced concrete is considered. The properties of the bridge deck, pylon and cables are given with detail in chapter III.

The bridge is modeled mathematically as shown in Fig.V.6.a as a discrete model and as a finite elements model as shown in Fig.V.3.b. The fundamental time period of the pylons is about 0.1 sec and the corresponding time period of the non-isolated bridge works out to be 0.55 sec in both longitudinal and transverse directions. The damping in the deck and piers is taken as 5% of the critical in all modes of vibration. In addition, the number of elements considered in the bridge deck, pylon and cables are 21, 2 and 36, respectively.

The earthquake excitation was inset as a time history spectrum (Acceleration according to time) as shows Fig.V.7. The seismic excitation corresponds to Solomon earthquake in 2004 with a magnitude of 6.8 obtained from vibration data website.

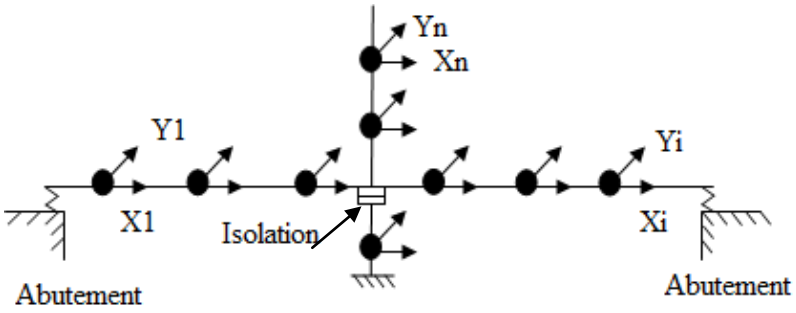

Fig.V.6.a Discrete Model of Isolated Bridge

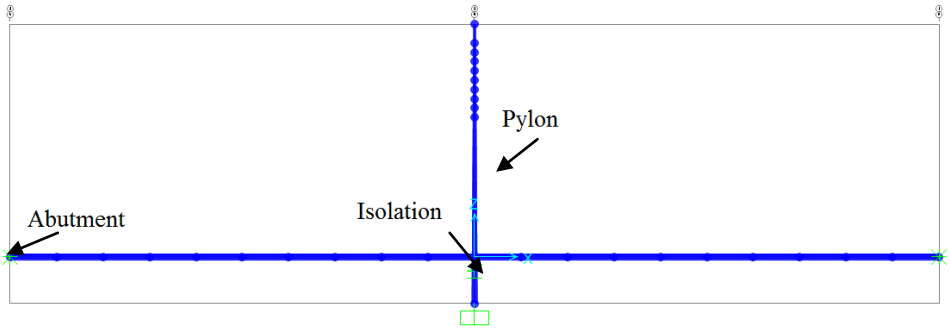

Fig.V.6.b 3D Modeling of Isolated Bridge

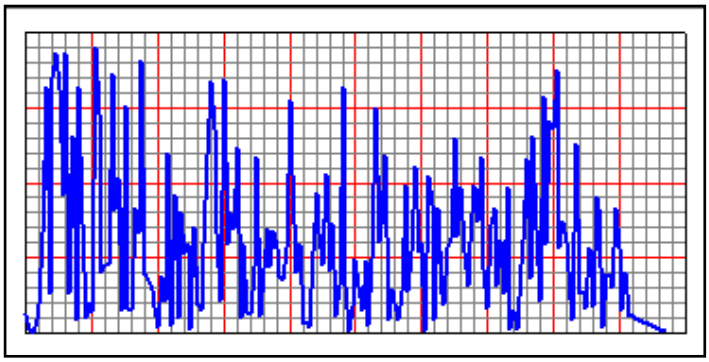

Fig.V.7 Solomon Earthquake Time History Function
(Obtained from SAP2000 model)

Response quantities of interest for the bridge system under consideration (in both longitudinal and transverse directions) are the base shear in the pylon and the relative displacement of the aseismic bearings at the top of pylon. The pylon base shear is directly proportional to the forces exerted in the bridge system due to

earthquake ground motion (Jumbo and Chiang 2008). On the other hand, the relative displacements of the isolation bearing are crucial from the design point of view of isolation system and separation joints at the abutment level.

SAP2000 structural analysis software is capable of Time History Analysis, including Multiple Base Excitation. SAP2000 facilitates the dynamic modeling of base isolators as link elements, which can be assigned various stiffness properties. By the help of this software the bridge model with different types of bearings was created in a numerical simulation to validate the mathematical model, two categories of isolation systems were used: the elastomeric bearings including the N-Z and the LRB and the frictional bearings including the FPS isolator which were modeled using N-link command detailed in Appendix 5; each device has its own properties as detailed in table V.1.

Table V.1 Physical and Mechanical Characteristics of Isolation Bearings

Bearing Model	Rotational Inertia (Kgm^2)	Mass (Kg)	Weight (KN)	Diameter (m)	Effective Stiffness K_{eff} (KN/m)	Effective Damping ζ (%)
LRB	1,82x10E10	84	845	0,8	2477	30
N-Z	2,4x10E9	90	908	0,8	1900	20
FPS	1,1x10E10	68	687	0,7	2000	10

V.5. Results and Discussion

V.5.1. Kobe Earthquake

In Figs. 38a, 38b and 38c, the time variation of the base shear in the pier and relative displacement of the bearings of the bridge isolated by the LRB, N-Z and FPS is shown. The LRB system is designed to provide isolation period of 2 sec (based on rigid deck and pier condition) and 10 percent damping ratio. The isolation period for the N-Z and the FPS system is taken as 2.5 sec. The yield strength of the N-Z system is taken as 5 percent of deck weight and the friction

coefficient of FPS system is considered as 0.05. The system is subjected to Kobe, 1995 earthquake ground motion in the longitudinal and transverse directions.

The base shear in the piers is significantly reduced (about 80 to 90%) for the isolated system as compared to the non isolated system in the both directions of the bridge. This indicates that the isolation systems are quite effective in reducing the earthquake response of the bridge system. The maximum peak displacement of the bearing is 32.87, 27.65 and 31.50 for LRB, N-Z and FPS system, respectively in the longitudinal direction of the bridge.

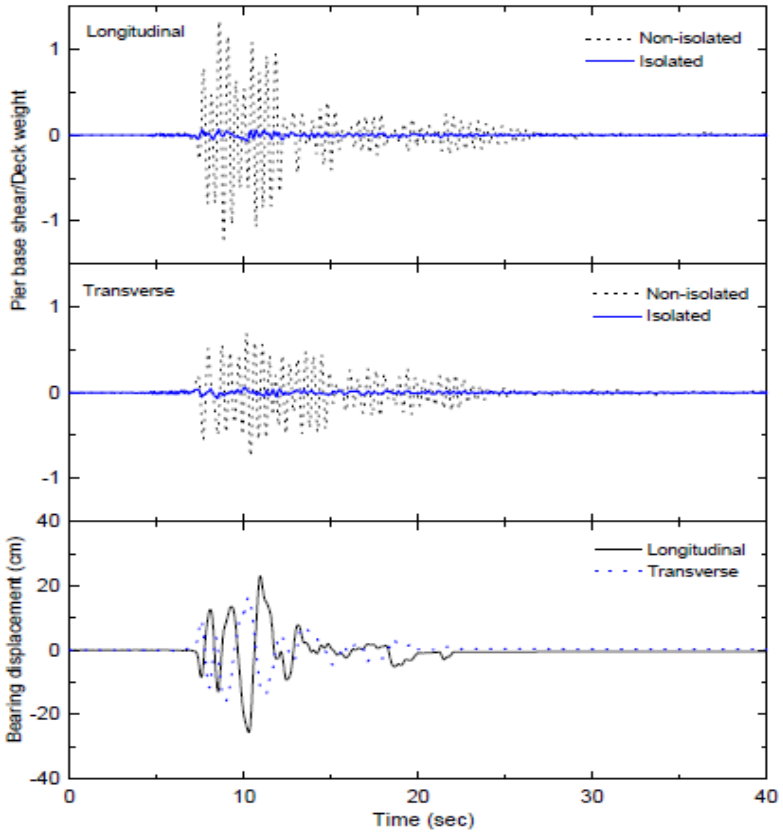

(a) LRB isolation system

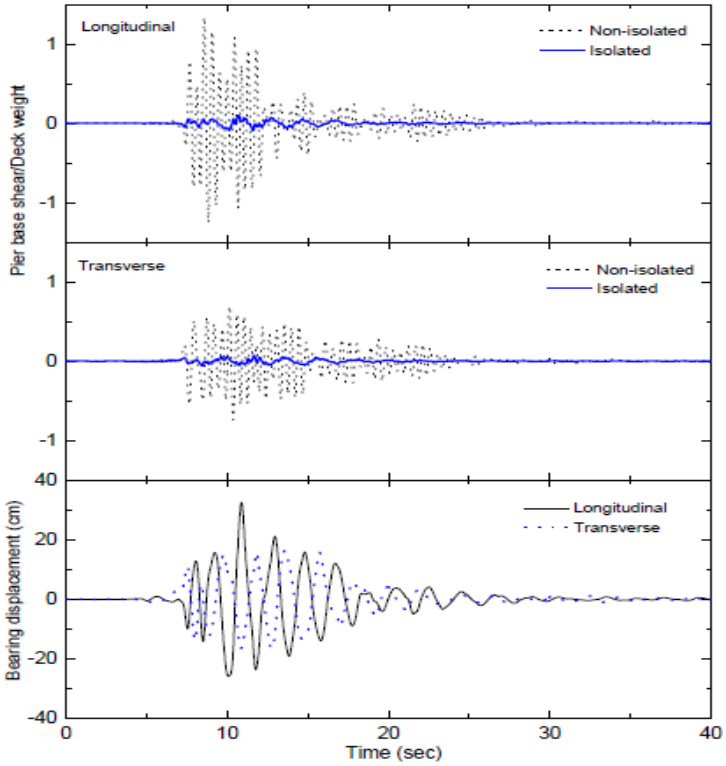

(b) FPS isolation system

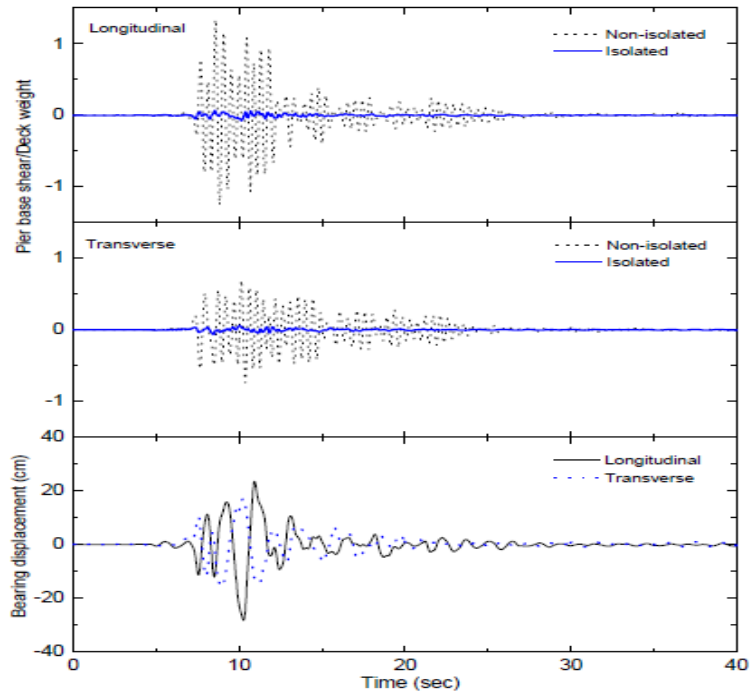

(c) N-Z isolation system

Fig.V.38 Time Variation of Base Shear and Bearing Displacement of the Isolated Bridge under Kobe 1995 Earthquake Motion

V.5.1. Solomon Earthquake

Twelve vibration modes were taken into account in the bridge response analysis, the comparison results is between the isolated and non isolated structures. As illustrated in table V.8 the presence of aseismic bearings has a considerable effect on the fundamental period of vibration of the structure for all kinds of bearings with a little difference between the period increasing values (66%) for sliding bearing and (23%) for the friction bearing kind which means that the LRB bearing type is more efficient for this structure.

Table V.2 Natural Vibration Period of the Isolated and Non Isolated Bridge Model

	Period of Vibration		
Vibration Mode	Non Isolated	Isolated with LRB	Isolated with FPS
1	0,553148	0,919365	0,681502
2	0,553138	0,553138	0,553138
3	0,220941	0,553127	0,553109
4	0,219809	0,220941	0,220941
5	0,193147	0,219809	0,219809
6	0,193143	0,193143	0,193143
7	0,098952	0,193142	0,193142
8	0,098951	0,098951	0,098951
9	0,06629	0,09895	0,09895
10	0,066257	0,06629	0,06629
11	0,061753	0,066257	0,066257
12	0,061752	0,061752	0,061752

Moreover and as shown in Fig.V.9a and Fig.V.9b, the displacement of the isolation bearing is significantly reduced in both longitudinal and transversal

directions especially in the interval [0,2-0,6s] for longitudinal direction and [0-0,2s] for transversal direction which makes obvious the main role of such bearings in bridge displacement restriction.

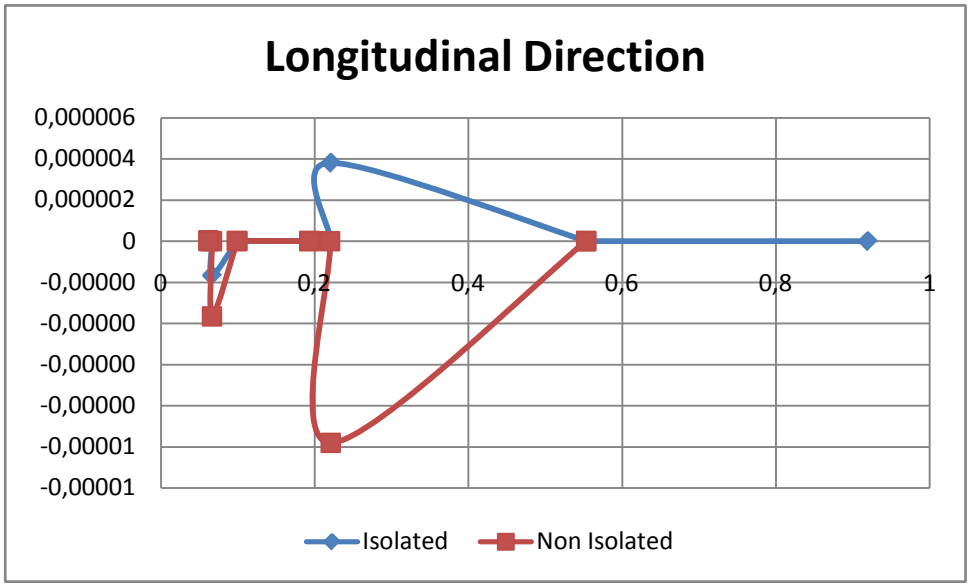

(a) Displacement in Longitudinal Direction

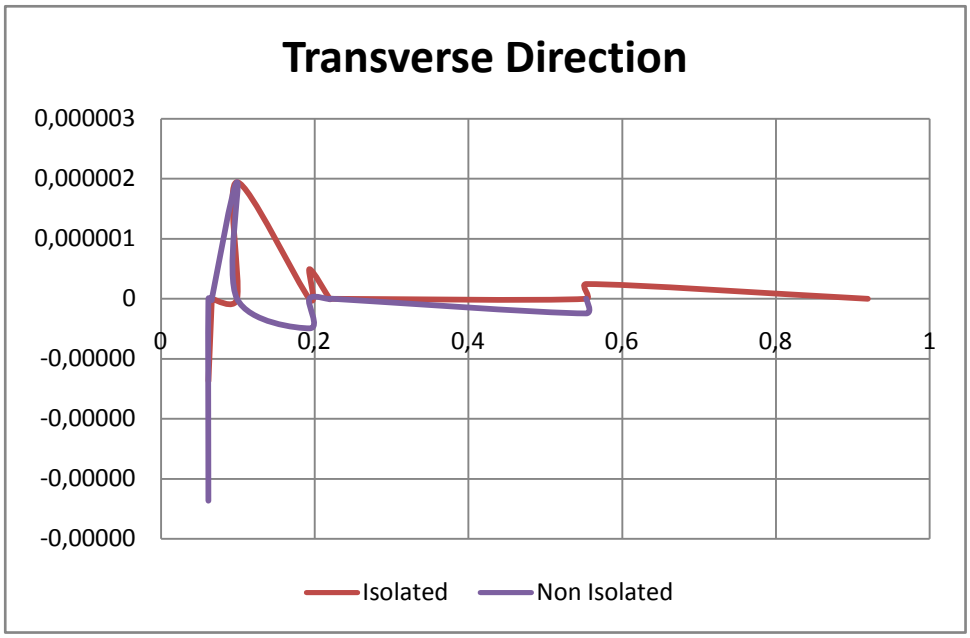

(b) Displacement in Transversal Direction

Fig.V.9 Bearing Displacement in longitudinal and Transversal Directions under Solomon Earthquake of Isolated and Non Isolated Models

Conclusion

This chapter sheds light on recent and economical technique for bridge protection against several damages and collapse due to earthquake forces and the effectiveness evaluation of the seismic isolation in bridges construction.

This comparative study on seismically isolated bridges against earthquake excitation puts most emphasis on the time variation of base shear and bearing displacement in order to understand the behavior of seismically isolated bridges with a comparison between isolated and non isolated bridges. The results show that the base shear in the pylons is significantly reduced for the isolated system as compared to the non isolated system in both directions of the bridge.

Bridge fundamental period is significantly increased using isolation devices with a higher rate in the case of LRB bearing as compared to the FPS; which indicates that the use of aseismic systems is effective in reducing the earthquake response of the bridge.

General Conclusion

In this dissertation, dynamic response performance of existing and in construction bridges under multiple dynamic loads from vehicles winds and earthquake were analyzed. Each component of the studied system was considered as a subsystem where it was modelled as a three dimensional model and then equations of motion were established and combined after. A simulation was applied using structural software to validate the analytical formulation of this complex problem.

Three kinds of dynamic loads were taken into account in this research work; traffic, wind and earthquake applied on a cable supported bridge because of his very high sensitivity to such loads. The way of application of these loads is very important; the structure response is mainly depending on the input excitation.

Vehicle loads were determined first by a moving force and a moving mass then applied on a simply supported beam, modelling the bridge, with different velocities and traffic lines, results obtained show that the moving force is more obvious to model a vehicle load running a bridge, in addition the force velocity has a very important effect on results when it exceeds 80 km/h. As vibrations induced by vehicles are random loads in reality (they vary in space and time) a power spectral density representing this random process was considered and compared to the two previous models. The achieved results of the numerical simulation were more realistic and relevant so we can deduce that the power spectral density is the most attractive way to model vehicle loads applied on a bridge structure.

Long span bridges are very responsive to wind loads especially in the presence of another source of vibration like vehicles, for this purpose a study of the coupled system vehicle-bridge-wind was established to perform the effect of wind loads on the bridge-vehicle system. The wind was applied as a time history of moderate wind in lateral direction when vehicles were modelled as moving forces in two

bidirectional lines. All the bridge structural components were affected by the combined loads (wind and vehicle), the obtained results demonstrate that a moderate wind has a considerable effect when it strikes the bridge in the lateral direction, whereas in the case of the vehicle load, the longitudinal direction is the more effected area. So we can say that the presence of vehicles and a strong wind in the same time has several consequences on long bridges and can cause failure of structural components when the total stress exceeds the bridge resistance. As a result, it has been recognized that vehicle and wind forces have a considerable effect on the bridge response for both long and short time of loads application, especially when subjected to a high wind speed and crowded flux of traffic because of the long duration of loading scenarios.

Seismic loads represent the most critical applied forces in the case of strong earthquakes despite its short duration. As a retrofit way to decrease the transmitted vibrations to the bridge structure, a recent technique is required in some design codes which is based on the use of special bearings having the capacity of absorbing a part of the transmitted energy to the structure. A comparative study was applied on the studied structure under a strong earthquake with and without the use of aseismic bearings.

The comparative study between isolated and non isolated bridges with aseismic bearings was performed using three kinds of bearings to be the LRB, N-Z and FPS. The research work results show the effectiveness of the use of such bearings in the structure period of vibration lengthening so to offer a supplemented time to the structure to respond to the seismic excitation. It was noted that the LRB bearing had a more interesting effect than the FPS in the period increasing with a rate of 30% of difference.

The displacement was tested at the level of bearings in the two models (isolated and non isolated) and a remarkable displacement increasing was found when aseismic bearings are introduced which is clearly justified by these devices aptitude to absorb energy so reduce transmitted vibrations to the bridge structure

which can significantly reduce the probability of damage or failure of such structures when subjected not only to earthquakes but to other sources of vibrations such as traffic, human induced vibration, wind and other unknown and non identified sources.

So many kinds of isolation devices are used now days, the difference between them corresponds to the cost, the bridge type, location and configuration. Moreover such devices require a damping mechanism to return the structure to its initial position after displacements.

A new research work opens horizon on the study of isolated bridges under other dynamic loads sources as human induced vibration, wind and vehicle with road profile irregularities. In the later exchanged induced vibrations between the vehicle and the road profile will amplificate the vibration excitation which is a very interesting topic in as future research work.

Finally, random of nature still exists so it is impossible to achieve the total security.

Bibliography

ASHTO. 2003, *"Guide Manual for Condition Evaluation and Load and Resistance Factor Rating (LRFR) of Highway Bridges"*, USA

ASCE. 1982, Committee on fatigue and fracture reliability of the committee on structural safety and reliability of the structural division, fatigue reliability 1–4. *Journal of Structural Engineering*, 108, pp.3–88

Ataei, N., McCarthy, E. and Padgett, J. E. 2012, "*Application of Shape Memory Alloys (SMAs) for prevention of bridge deck unseating during hurricane wave and surge loading*", Bridge Maintenance Safety and Management journal, Proceedings of the Sixth International IABMAS Conference, Stresa, Lake Maggiore, Italy, 8-12 July 2012, pp.1945–1952

Au, F.T.K., Wang, J.J., Cheung, Y.K.2001, "Impact Study of Cable-Stayed Bridge under Railway Traffic Using Various Models, *Journal of Sound and Vibration*, Vol240(3), pp.447–465

Barker, R. M. and Puckett, J. A. 2013, *Design of Highway Bridges: A LRFD Approach,* 3rd Edition, John Wiley & Sons, Inc., New York, NY

Biggs, J. M. 1964, *Introduction to Structural Dynamics*, McGraw-Hill Companies, Austin, TX, U.S.A

Billing, J.R. and Green, R. 1984, "Design Provisions for Dynamic Loading of Highway Bridges", *Transportation Research Record*, No. 950, pp. 94-103

Biondi, B., Muscolino, G., Sofi, A.2005, "A Substructure Approach for the Dynamic Analysis of Train-Track-Bridge System", *Computers and Structures*, Vol 83(28–30), pp.2271–2281

Bouazara, M., Richard, M. J., 2001, "An Optimization Method Designed to Improve 3-D Vehicle Comfort and Road Holding Capability Through the Use of Active and Semi-Active Suspensions", *European Journal of Mechanics*, 20(3), pp. 509-520

BS. 7608: 1993.code of practice for fatigue design and assessment of steel structures, British Standard Institute

Cai, C.S. and Chen, S.R. 2004, "Framework of Vehicle-Bridge-Wind Dynamic Analysis", *Journal of Wind Engineering and Industrial Aerodynamics*, 92(7-8), pp.579-607

Cassis, J. H., Schmit, L. A., 1976, "Optimal Structural Designs with Dynamic Constraints", *ASCE Journalof the Structural Division*, 102(1), pp. 2053-2071

Chen, S.R., Wu, J.2010, "Dynamic Performance Simulation of Long-Span Bridge under Combined Loads of Stochastic Traffic and Wind", *Journal of Bridge Engineering*, Vol 15(3), pp.219–230

Chatterjee, P.K., Datta, T.K., Surana, C.S.1994, "Vibration Suspension Bridges under Vehicular Movement", *Journal of Structural Engineering*, Vol 120(3), pp.681–703

Chang, D., Lee, H.1994, "Impact Factors for Simple-Span Highway Girder Bridges", *Journal of Structural Engineering*, Vol 120(3), pp.704–715

Chen, S.R., Cai, C.S. 2007, "Equivalent Wheel Load Approach for Slender Cable-Stayed Bridge Fatigue Assessment under Traffic and Wind: Feasibility Study", *Journal of Bridge Engineering*, Vol12(6), pp.755–764

Chen, S.R. and Wu, J. 2010, "Dynamic Performance Simulation of Long-Span Bridge under Combined Loads of Stochastic Traffic and Wind", *Journal of Bridge Engineering*, ASCE, 15(3), pp. 219-230

Chen, Z. W. 2010, Fatigue and Reliability Analyses of Multiload Suspension Bridges with WASHMS, D.Sc. Thesis, Hong Kong Polytechnic University

Coussy, O., Said, M., Van Hoove, J.P.1989, "The Influence of Random Surface Irregularities on the Dynamic Response of Bridges under Suspended Moving Loads", *Journal of Sound and Vibration*, Vol 130(2), pp.313–320

Davenport, A.G., King, J.P. and Larose, G.L. 1992, "Taut Strip Model Tests", Proceedings of the 1st International Symposium on Aerodynamics of Large Bridges, Copenhagen, Denmark, February

Datta, T. K. 2010, *Seismic Analysis of Structures*, Indian Institute of Technology Delhi, India

Dodds, C.J., Robson, J.D.1973, "The Description of Road Surface Roughness", *Journal of Sound Vibration*, Vol 31(2), pp.175–183

Einstein, A.1956, Investigations on the Theory of Brownian Movement, R. Furth, Ed., Dover Publications, Inc., New York, USA

Ernesto, H. Z. and Vanmarcke, E. H. 1994, "Seismic Random Vibration Analysis of Multi-Support Structural Systems", *Journal of Engineering Mechanics, ASCE*, Vol 12, pp. 1107-1128

EUROCODE 2. 2005, "Design of Concrete Structures, Concrete Bridges, Design and Detailing Rules",UK

Eyre, R. and Tilly, G. P. 1977, "Damping Measurements on Steel and Composite Bridges", *Transport and Road Research Laboratory Supplementary Report 275*, Symposium on Dynamic Behavior of Bridges, Crowthorne, England, May 19, pp. 22-39

Funkhouser, D. W. and Heins, C. P. 1972, Skew and Elevated Support Effects on Curved Bridges, Civ. Eng. Dept. Report No. 46, Univ. Maryland, College Park

Gaunt, J. T. and Sutton C. D. 1981, *Highway Bridge Vibration Studies*, Purdue University, West Lafayette, Ind, USA

Gillespie, T. D. 1992, "Fundamentals of Vehicle Dynamics," SAE Technical Paper, Washington, DC, USA

Goswami,P., Mandal, A., Upadhyaya ,H.C. and Hourdin, F. 2005, "*Advance Forecasting of Cyclone Track Over North Indian Ocean Using a Global Circulation Model*", Mausam,Vol 57(1), pp.111-118

Green, R. 1977, "Dynamic response of bridge superstructures Ontario observations", *Transport and Road Re-search Laboratory Supplementary Report 275*, Symposium on Dynamic Behavior of Bridges, Crowthorne, England,pp. 40 – 55

Green, R. 1997, "Reinforced Concrete Colum Design", *Trends in structural Mechanics*, pp. 281-288

Guo, W.H. and Xu, Y.L. 2001, "Fully Computerized Approach to Study Cable stayed-Bridge-Vehicle Interaction", *Journal of Sound and Vibration*, 248(4),pp. 745-761

Guo, W., Xia, H., Xu, Y.L. 2007, "Dynamic Response of a Long Span Suspension Bridge and Running Safety of a Train under Wind Action", *Frontiers of Architecture and Civil Engineering in China*, Vol1(1), pp71–79

Guo, W.W., Xu, Y.L., Xia, H., Chen, J., Zhang, W.S., and Shum, K.M. 2007, "Dynamic Response of Suspension Bridge to Typhoon and Trains. II: Numerical Results",*Journal of Structural Engineering*, ASCE, 133(1), pp. 12-21

Hasselman, T. K., Hart, G. C.1972, "Modal Analysis of Random Structural Systems," *Journal of the Engineering Mechanics Division, ASCE*, V. 98, No. EM3, pp. 561-790

Hayes, J. M. and Sbarounis, J. A. 1997, "Vibration Study of Three-Span Continuous I-Beam Bridge," HRB Bulletin 124, National Academy of Science. Washington

Henchi, K., Fafard, M., Talbot, M., Dhatt, G.1998, "An Efficient Algorithm for Dynamic Analysis of Bridges under Moving Vehicles using a Coupled Modal and Physical Components Approach", *Journal of Sound and Vibration*, Vol 212(4), pp.663–683

Holmes, J.D. 2001, *Wind Loading of Structures*, Spon Press, Abingdon, UK

Honda, H., Kajikawa, Y., Kobori, T. 1982, "Spectra of Road Surface Roughness of Bridges" *Journal of the Structural Division*, Vol 108, pp.1956–1966

Huang, D., Wang,T.L., Shahawy, M.1993, "Impact Studies of Multigirder Concrete Bridges, *Journal of Structural Engineering*, Vol 119(8), pp.2387–2402

Humar, J.L., Kashif, A.H.1995, "Dynamic Response Analysis of Slab-Type Bridges", *Journal of Structural Engineering*, Vol 121(1), pp.48–62

Hwang, E.S., Nowak, A.S. 1991, "Simulation of Dynamic Load for Bridges", *Journal of Structural Engineering*, Vol 117, pp.1413–1434

Inbanathan, M.J., Wieland, M.1987, "Bridge Vibrations Due to Vehicle Moving over Rough Surface", *Journal of Structural Engineering*, Vol 113(9), pp.1994–2008

Inglis, C. E. 1913, "Stresses in a Plate Due to the Presence of Cracks and Sharp Corners," *Spie Milestone Series*, Vol. 137, pp. 3-17

Ji,J., Zhang,W., Wenyan Zhao,W., Chaoqing Yuan,C., Yu,Y. 2012, "Analysis and Comparison on Dynamic Characteristics of the Bridge Subjected to Moving Load Based on ANSYS", *Journal of Convergence Information Technology(JCIT)*, Vol7, (8), pp.159-168

Jorgensen, E., Volakis, J.L., Meincke, P., and Breinbjerg, O. 2004, "Higher Order Hierarchical Legendre Basis Functions for Electromagnetic Modeling", *IEEE Transactions on Antennas and Propagation*, Vol 52 (11), pp.2985-2995

Karoumi, R. 1998, Response of Cable-Stayed and Suspension Bridges to Moving Loads, Doctoral Thesis, Royal Institute of Technology, Stockholm, Sweden

Kapoor, M. P., Kumarasamy, K., 1981, *Optimum Configuration of Transmission Towers in Dynamic Response Regime*, Proceedings of International Symposium on Optimum Structural Design, Tucson, Arizona

Kappos, A. J. 2002, *Dynamic Loading and Design of Structures*, Spon Press, New York, USA

Karaki, G.2011, Assessment of Coupled Models of Bridges Considering Time-Dependent Vehicular Loading, Bauhaus University, Weimar, Germany

Kinnier, K.H. and Mckeel, W.T. 1965, "Substructure Influence on Dynamic Stress Response of Superstructures in Composite Bridges", *Highway Research Record*, Vol 103,pp. 31-40

Kiureghian, A.D. and Neuenhofer, A. 1992, "Response Spectrum Method for Multi-support Seismic Excitations," *Earthquake Engineering and Structural Dynamics*, 21(8),pp.713-740

Lashomb, S. M. *et al.*1985, Study of Bridge Vibrations for Connecticut, F.R. Thesis, University of Connecticut

Lei, X., Noda, N. A., 2002, "Analyses of Dynamic Response of Vehicle and Track Coupling System with Random Irregularity of Track Vertical Profile", *Journal of Sound and Vibration*, 258(1), pp. 147-165

Li, Q., Xu, Y.L., Wu, D.J., Chen, Z.W. 2010, "Computer-Aided Nonlinear Vehicle-Bridge Interaction Analysis", *Journal of Vibration and* Control, Vol 16, pp.1791–1816

Lin, J.H., Zhang, W.S. and Williams, F.W. 1994, "Pseudo-Excitation Algorithm for Non Stationary Random Seismic Responses", *Engineering Structures*, Vol 16,pp. 270- 276

Lin, J.H., Zhao, Y. Y. and Zhang, Y.H. 2001, "Accurate and Highly Efficient Algorithms for Structural Stationary/ Non-Stationary Random Responses", *Computer Methods in Applied Mechanics and Engineering*, 191 (1-2), pp. 103-111

Lin, J. H. and Zhang, Y. H., 2005, "Seismic Random Vibration of Long-span Structures", C. de Silva (Ed.), Chapter 30 in *Vibration and Shock Handbook*. CRC Press: Boca Raton, Florida

Liu, T.T., Xu, Y.L., Zhang, W.S., Wong, K.Y., Zhou, H.J., and Chan, K.W.Y. 2009, "Buffeting-Induced Stresses in a Long Suspension Bridge: Structural Health Monitoring Orientated Stress Analysis", *Wind and Structures*, 12(6), pp. 479-504

Lou, P., Zeng, Q.Y.2004, "Formulation of Equations of Vertical Motion for Vehicle-Track-Bridge System", *Journal of the China Railway Society*, Vol 26(5), pp 71

Lou, P., Zeng, Q. Y., 2005, "Formulation of Equation of Motion of Finite Element Form for Vehicle-Track-Bridge Interaction System with Two Types of Vehicle Model", *International Journal for Numerical Methods in Engineering*, 62(3), pp. 435-474

Mao, Q.H., 1989, Research on the Highway Bridge Vibration Due to Moving Vehicles, PhD thesis, Tongji University, Shang Hai, China

MATTIAS, Grahn. 2012, Structural Analysis and Design of Concrete Bridges: Current Modeling Procedures and Impact on Design, Master Thesis, Chalmers University of Technology, Göteborg, Sweden

Meisenholder, S. G. and Weidlinger, P., 1974, "Dynamic Interaction Aspects of Cable-Stayed Guideways for High Speed Ground Transportation", *Journal of dynamic Systems, Measurement and Control*, ASMS, Vol74 -Aut-R,pp. 180-192

Ministry of Transport of The Peoples Republic of China, *Guidelines for Seismic Design of Highway Bridges*, JTG/T B01-01- 2008, Beijing, 2008 (in Chinese)

Montgomery, D. C. 2008, *Design and Analysis of Experiments*, John Wiley & Sons, Hoboken, NJ, USA

Naude, A.F., Snyman, J.A., 2003, "Optimization of Road Vehicle Passive Suspension Systems, Part 2, Qualification and Case Study", *Applied Mathematical Modelling*. 27(4), pp.263-274

Newland, D.1993, An *Introduction to Random Vibrations, Spectral and Wavelet Analysis*, Third Edition, Longman, New York, USA

Nigam, N.1983, *Introduction to Random Vibrations*, Cambridge, MIT Press, UK

OBrien, E.J., McGetrick, P. and González, A.,2014, " A Drive-by Inspection System via Vehicle Moving Force Identification", *Smart Structures and Systems*, Vol 13 (5), pp. 821-848

Olsson, M. 1985, "Finite Element, Modal Coordinate Analysis of Structures Subjected to Moving Loads", *Journal of Sound and Vibration*, Vol 99(1), pp.1–12

Pan, T.C., Li, J.,1992, "Dynamic Vehicle Element Method for Transient Response of Coupled Vehicle-Structure Systems", *Journal of Structural Engineering*, Vol 128(2), pp.214–223

Paultre, A.V., Chaallal, O., and Proulx, J. 1992, "Bridge Dynamics and Dynamic Amplification Factors – a Review of Analytical Experimental Findings", *Canadian Journal of Civil Engineering*, 19, pp. 260-278

Paz, M. and Leigh, W. 2004, *Structural Dynamics: Theory and Computation, Fifth Edition*, Kluwer Academic Publishers, Norwell, Massachusetts, USA

Robson, J. D.1964, *An Introduction to Random Vibration*, Edinburgh, University Press, Edinburgh

Ryan, T. P. 2000, *Modern Engineering Statistics: Solutions Manual to Accompany*, John Wiley & Sons, Hoboken, NJ, USA

Schilling, C.G., Klippstein, K.H., Barsom, J.M. and Blake, G.T. 1978, "Fatigue of Welded Steel Bridge Members Under Variable Amplitude Loadings", NCHRP ,188

Siebert, W. M.1958, "The Description of Random Processes," *Chapter 2 in Random Vibration*, S. Crandall, Ed

Steinberg, D. 1988, *Vibration Analysis for Electronic Equipment*, Wiley, University of California

Sun, Y.Q., Dhanasekar, M., 2002, "A Dynamic Model for the Vertical Interaction of the Rail Track and Wagon System", *International Journal of Solids and Structures*, Vol 39(5),pp.1337–1359

Timoshenko, S. and Young, D.H. 1940, *Engineering Mechanics, 2nd Edition*, McGraw-Hill Book Company, Ventura, CA, U.S.A

Wang, T.L., Huang, D.1992, "Cable-Stayed Bridge Vibration due to Road Surface Roughness", *Journal of Structural Engineering*, Vol 118(5), pp.1354–1374

Wesley, C. 2014, Bridge Failure Rates, Consequences and Predictive Trends, Doctorate Thesis, Utah State University, Logan, Utah, USA

Wirsching, P. H., Paez, T. L., Ortiz, K. 2006, *Random Vibrations, Theory and Practice,* , John Wiley and Sons, New York, USA

Wu, Y.S., Yang, Y.B.2003, "Steady-State Response and Riding Comfort of Trains Moving over a Series of Simply Supported Bridges", *Engineering Structures*, Vol 25(2), pp.251–265

Xia, H., Xu, Y.L., Chan, T.H.T.2000, "Dynamic Interaction of Long Suspension Bridges with Running Trains", *Journal of Sound and Vibration*, Vol 237(2), pp.263–280

Xia, H., Zhang, N., de Roeck, G.2003, "Dynamic Analysis of High Speed Railway Bridge under Articulated Trains", *Computers and Structures*, Vol 81(26-27), pp.2467–2478

Xu, Y.L., Ko, J.M. and Yu. Z. 1997, "Modal Analysis of Tower-Cable System of Tsing Ma Long Suspension Bridge", *Engineering Structures*, Vol 19,pp 857–867

Xu, Y.L., Ko, J.M. and Zhang, W.S., 1997, "Vibration Studies of Tsing Ma Suspension Bridge", *Journal of Bridge Engineering*, ASCE, 2(4), pp.149- 156

Xu, Y.L., Wang, L.Y.2003, "Analytical Study of Wind-Rain-Induced Cable Vibration: SDOF Model", *Journal of Wind Engineering and Industrial Aerodynamics*, Vol 91(1-2), pp.27–40

Xu, Y.L. & Guo, W.H. 2003, "Dynamic Analysis of Coupled Road Vehicle and Cable-Stayed Bridge Systems under Turbulent Wind", *Engineering Structures*, Vol. 25, 473-486

Xu, Y.L., Xia, H., Yan, Q.S.2003, "Dynamic Response of Suspension Bridge to High Wind and Running Train", *Journal of Bridge Engineering*, Vol 8(1), pp.46–55

Xu, Y.L., Li, Q., Wu, D.J. and Chen, Z.W. 2010, "Stress and Acceleration Response Analysis of Vehicle-Bridge Systems Using Mode Superposition Method", *Engineering Structures*, 32(5), pp.1356-1368

Yamazaki, F., Shinozuka, M., Dasgupta, G.; 1988, "Neumann Expansion for Stochastic Finite Element Analysis", *Journal of Engineering Mechanics*, 114(8), pp. 1335-1354

Yang, F., Fonder, G.A.1996, "An Iterative Solution Method for Dynamic Response of Bridge-Vehicles Systems", *Earthquake Engineering and Structural Dynamics*, Vol 25, pp.195–215

Yang, Y.B., Chang, C.H., Yau, J.D.1999, "An Element for Analysing Vehicle-Bridge Systems Considering Vehicle's Pitching Effect", *International Journal for Numerical Methods in Engineering*, Vol 46(7), pp.1031–1047

Yang, Y.B., Wu, Y.S.2001, "A Versatile Element for Analyzing Vehicle-Bridge Interaction Response", *Engineering Structures*, Vol 23(5), pp.452–469

Yang, Y.B., Wu, Y.S.2001, "A versatile Element for Analyzing Vehicle-Bridge Interaction Response", *Engineering Structures*, Vol 23(5), pp.452–469

Yu, L. and Chan, T.H.T. 2007, "Recent Research on Identification of Moving Loads on Bridges", *Journal of Sound and Vibration*, Vol 305, pp.3–21

Yu, L. 2002, Accounting for Bridge Dynamic Loads Using Moving Force Identification

System (MFIS), The Hong Kong Polytechnic University, Hong Kong

Zhai, W., Cai, Z.1997, "Dynamic Interaction Between a Lumped Mass Vehicle and a Discretely Supported Continuous Rail Track", *Computers and Structures*, Vol 63(5), pp.987–997

Zhai, W.M., Cai, C.B.2003, "Train/Track/Bridge Dynamic Interactions: Simulation and Applications", *Vehicle System Dynamics*, Vol 37, pp.653–665

Zhai, W.M.2007, *Vehicle-Track Coupling Dynamics*, Chinese Railway Press, Beijing, China

Zhang, Z.C., Lin, J.H., Zhang, Y.H. Howson, W.P. and Williams, F. W. 2010, "Non-Stationary Random Vibration Analysis of Three-Dimensional Train- Bridge Systems", *Vehicle System Dynamics*, 48 (4), pp. 457-480

Zhang,W.2012, Fatigue Performance of Existing Bridges under Dynamic Loads from Winds and Vehicles, PhD Thesis, Department of Civil and Environmental Engineering, Louisiana, State University

Appendix 1: Moving Force Modelling

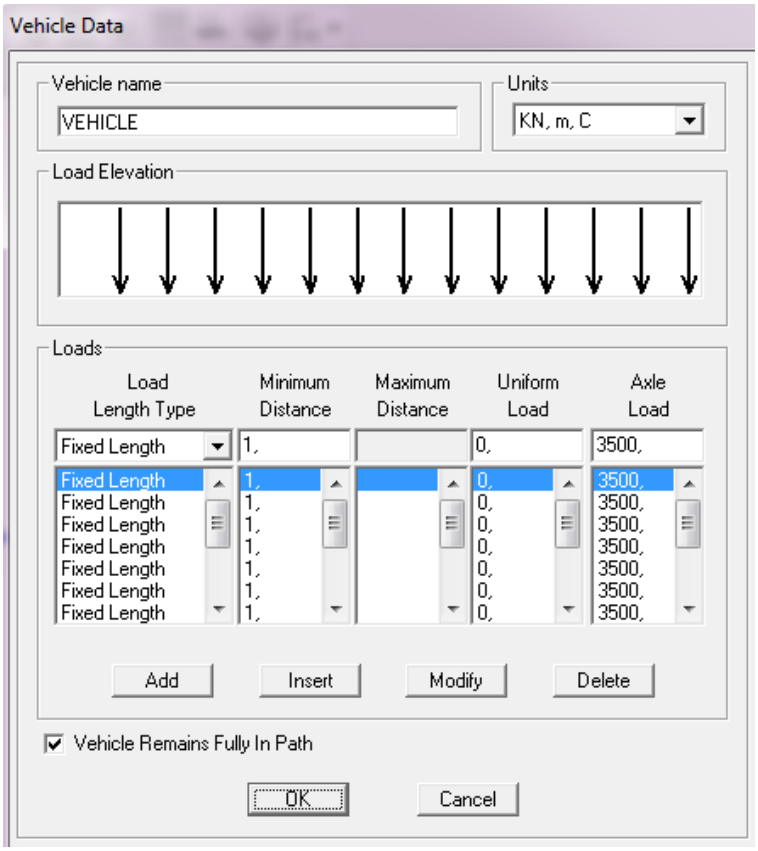

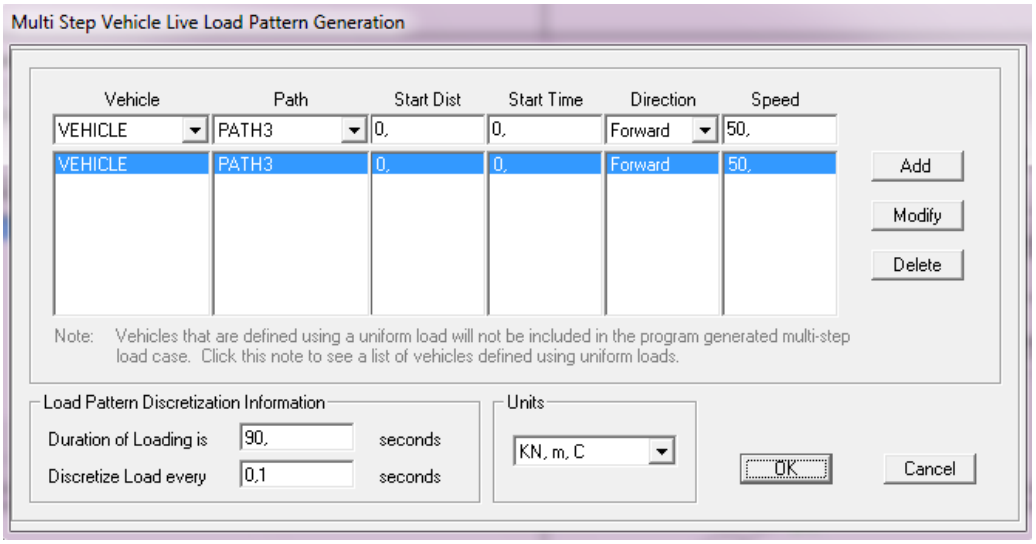

Appendix 2: Matlab Program for Vehicle PSD Plotting

```
Fs = 32e3;
t = 0:1/Fs:2.96;
x = cos(2*pi*t*1.24e3)+ cos(2*pi*t*10e3)+ randn(size(t));
nfft = 2^nextpow2(length(x));
Pxx = abs(fft(x,nfft)).^2/length(x)/Fs;

% Create a single-sided spectrum
Hpsd = dspdata.psd(Pxx(1:length(Pxx)/2),'Fs',Fs);
plot(Hpsd)
```

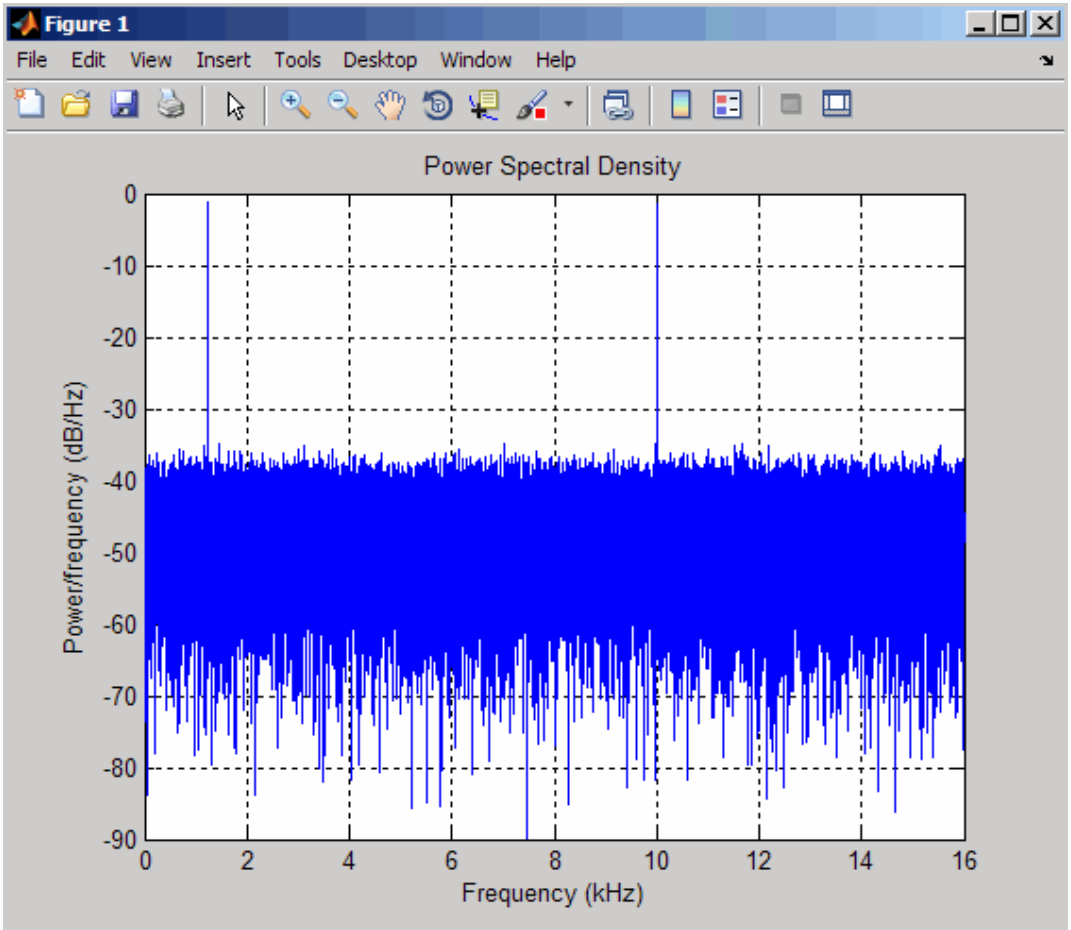


```
% Create a double-sided spectrum
Hpsd = dspdata.psd(Pxx,'Fs',Fs,'SpectrumType','twosided');
plot(Hpsd)
```

Appendix 3: Matlab Program for Wind Plotting

```
function [u,w,t,nodes] = windSim(filename)

% GOAL : Simulation of spatially correlated time series

% INPUT: text file .
% example: filename = 'INPUT.txt'

% OUTPUT:
% u: along wind turbulent component
% w: vertical turbulent component
% t: time vector
% nodes: structure variables that contains informations about mean wind
% speed, and coordinates of nodes

% example: [u,w,t,nodes] = windSim('INPUT.txt');

%% TIME DEFINITION
% import data from input file
[data] = importfile(filename, 7, 8,['%*s%f%*[^\n]'],'\t');
data=cell2mat(data);
fs=data(1); % sampling frequency
tmax=data(2); % duration of time series
dt=1./fs; % time step
N=tmax/dt+1; % number of time step for a whole wind histories
% build vector time and frequency
t = linspace(0,tmax,N);
f0 = 1./tmax;
f = [f0:f0:fs/2];
Nfreq = numel(f);
df = median(diff(f));

%% WIND DATA
[data] = importfile(filename, 12, 19,['%*s%f%*[^\n]'],'\t');
data=cell2mat(data);
Iu=data(1);
Iw=data(2);
Lux=data(3);
Lwx=data(4);
Cuy=data(5);Cuz=data(6);
Cwy=data(7);Cwz=data(8);

[typeWind] = importfile(filename, 25, 26,['%*s%s%*[^\n]'],'\t');
type=char(typeWind{1});
windProfile=char(typeWind{2}); % power or log

[data] = importfile(filename, 28, 32,['%*s%f%*[^\n]'],'\t');
data=cell2mat(data);
Uref=data(1);
zr = data(2);
a=data(3);
u_star=data(4);
roughness=data(5);
```

```
%% GRID GENERATION
clear data
[data] = importfile(filename, 36, 41,['%*s%f%*[^\n]'],'\t');
data=cell2mat(data);
Nyy = data(1);
Nzz     = data(2);
Zmin= data(3);
Zmax= data(4);
Ymin= data(5);
Ymax= data(6);

% Check compatibility between grid and node number
if and(Ymin==Ymax,Nyy>1),
    warning('Ymin = Ymax but Nyy > 1, Nyy is set to 1')
    Nyy=1;
end

if and(Zmin==Zmax,Nzz>1),
    warning('Zmin = Zmax but Nzz > 1, Nzz is set to 1')
    Nzz=1;
end

% Create the grid
clear nodes
y = linspace(Ymin,Ymax,Nyy);
z = linspace(Zmin,Zmax,Nzz);
[Z,Y] = meshgrid(z,y);
nodes.Y = Y(:);
nodes.Z = Z(:);

% Wind profile
if strcmp(windProfile,'power')==1,
    U= Uref.*(nodes.Z./zr).^(a);
elseif strcmp(windProfile,'log')==1,
    k=0.4; % Von karman constant
    U = u_star./k.*log(z./roughness);
else
    error('Wrong mean wind profile selected \n')
end
nodes.U = U(:);
% names affected at each nodes
for ii=1:Nyy*Nzz,
    nodes.name{ii} = strcat('N',num2str(ii));
end
% Standard deviation of wind speed at each nodes
stdU=0.01.*Iu.*nodes.U;
stdW=0.01.*Iw.*nodes.U;

%% Input data for wind coherence
dy = zeros(Nyy*Nzz,Nyy*Nzz); % matrix distance along y
dz = zeros(Nyy*Nzz,Nyy*Nzz); % matrix distance along z
meanU = zeros(Nyy*Nzz,Nyy*Nzz); % mean wind speed between two nodes
for kk= 1:Nyy*Nzz,
    for mm = 1:Nyy*Nzz,
        dy(kk,mm) = abs(nodes.Y(kk)-nodes.Y(mm));
        dz(kk,mm)  = abs(nodes.Z(kk)-nodes.Z(mm));
```

```
        meanU(kk,mm)  =  0.5.*(nodes.U(kk)+nodes.U(mm));
    end
end

%% GENERATION OF WIND HISTORIES
%preallocation
clear ii jj A G dummy*
dummySpeed = zeros(2*Nyy*Nzz,N);
tic
for jj = 1:Nfreq,
    %co-coherence
    DecY_u = dy.*Cuy*f(jj);
    DecY_w = dy.*Cwy*f(jj);
    DecZ_u = dz.*Cuz*f(jj);
    DecZ_w = dz.*Cwz*f(jj);
    coh_u = exp(-sqrt(DecY_u.^2+DecZ_u.^2)./meanU);
    coh_w = exp(-sqrt(DecY_w.^2+DecZ_w.^2)./meanU);
    % turbulence spectrum
    if strcmp(type,'Von Karman')==1,
        Su= VonKarmanSpectrum(f(jj),nodes.U,stdU,Lux,'u');
        Sw= VonKarmanSpectrum(f(jj),nodes.U,stdW,Lwx,'w');
    elseif strcmp(type,'Kaimal')==1,
        Su= KaimalSpectrum(f(jj),nodes.U,stdU,Lux,'u');
        Sw= KaimalSpectrum(f(jj),nodes.U,stdW,Lwx,'w');
    else
        error(' spectrum type is unknown \n')
    end
    % spectral matrix with correlation between u and w
    Suu = sqrt(Su*Su').*coh_u;
    Sww = sqrt(Sw*Sw').*coh_w;
    S = [Suu,zeros(size(Suu));zeros(size(Suu)), Sww];
    phi = 2*pi.*rand(2*Nyy*Nzz,1);
    phi=repmat(phi,[1,N]);
    wt =repmat(f(jj),[2*Nyy*Nzz,1])*t;
    A=cos(2.*pi.*wt+phi);
    G = chol(S,'lower');% cholesky decomposition of Svv
    dummySpeed = dummySpeed + sqrt(2*df).*abs(G)*A;
end
toc
% Output of the simulation
u = dummySpeed(1:Nyy*Nzz,:);
w=dummySpeed(Nyy*Nzz+1:2*Nyy*Nzz,:);



%% FUNCTIONS
    function [data] = importfile(filename, startRow,
endRow,formatSpec,delimiter)
        % GOAL
        % extract data from txt files or excel files to store them into
matrix

        %                                 INPUT
        %  filename:
        %           type: string with extension.
```

```
        %           definition: name of the file whose information are
extracted
        %  startRow:
        %           type: integer
        %           definition: first row of the file to be read
        %  endRow:
        %           type: integer
        %           definition: last row of the file to be read
        %  formatSpec:
        %           type: string
        %           definition: format of the data to be read.
        %           e.g. : formatSpec = ['%f%f%f%s%s%*[^\n]'];
        %  delimiter:
        %           type: string
        %           definition: symbol used to delimite the columns in the
file
        %           e.g. : delimiter = '\t'; or delimiter = ',';

        %                                OUTPUT
        %  data:
        %           type: matrix [N1 x N2] where N1 and N2 are integers.
        %           N1 = endRow-startRow or total number of rows if enRow
is not
        %           specified
        %           N2 = defined by formatSpec.
        %           definition: extracted data from the file, stored as a
matrix
        % Copyright (C) Etienne Cheynet, 2015.
        % last modification: 27/01/2015 10:56
        % Initialize variables.
        if nargin<=2
            startRow = 1;
            endRow = inf;
        end
        if endRow == [],
            endRow = inf;
        end
        %  open the text file.
        fileID = fopen(filename,'r');
        %Read columns of data according to format string.
        dataArray = textscan(fileID, formatSpec, endRow(1)-startRow(1)+1,
'Delimiter', delimiter, 'EmptyValue' ,NaN,'HeaderLines', startRow(1)-1,
'ReturnOnError', false);
        for block=2:length(startRow)
            frewind(fileID);
            dataArrayBlock = textscan(fileID, formatSpec, endRow(block)-
startRow(block)+1, 'Delimiter', delimiter, 'EmptyValue' ,NaN,'HeaderLines',
startRow(block)-1, 'ReturnOnError', false);
            for col=1:length(dataArray)
                dataArray{col} = [dataArray{col};dataArrayBlock{col}];
            end
        end
        % Close the text file.
        fclose(fileID);
        %% Create output variable
```

```
        dataArray = cellfun(@(x) num2cell(x), dataArray, 'UniformOutput',
false);
        data = [dataArray{1:end}];
        % if iscell(data)==1,
        %     data=cell2mat(data);
        % end
    end
    function [Sv] = VonKarmanSpectrum(f,V,stdV,L,component)
        % -----------------------------------------
        % INPUT
        % f: float; frequency is [1 x 1]
        % V: float; Mean wind speed Normal to the deck is [1x1]
        % std_speed : float; std of speed is [1 x 1]
        % L =  float; turbulence length scales is [1x1]
        % Iturb = ; float; turbulence intensity is [1x1]
        % component : string; is 'u' or 'w'
        % -----------------------------------------
        % OUTPUT
        % Sv: float; [1x1] value of Spectrum for a given frequency
        % -----------------------------------------
        % Von Karman coefficent
        coef=[-5/6, -11/6];
        % dimension of output
        Sv = zeros(size(V)); % is [Nzz,1]
        %calculation of S/std^2
        n = L.*V.^(-1).*f;
        if strcmp(component,'u')==1,
            Sv =  V.^(-1).*4.*L.*stdV.^2.*(1+70.7.*n.^2).^(coef(1));
        elseif strcmp(component,'w')==1,
            Sv=  V.^(-
1).*4.*L.*stdV.^2.*(1+70.7.*4.*n.^2).^(coef(2)).*(1+188.4.*4*n.^2);
        else
            fprintf('error: component unknown \n\n')
            return
        end
    end
    function [Sv] = KaimalSpectrum(f,V,stdV,L,component)
        % -----------------------------------------
        % INPUT
        % f: float; frequency is [1 x 1]
        % V: float; Mean wind speed Normal to the deck is [1x1]
        % std_speed : float; std of speed is [1 x 1]
        % Lturb =  float; turbulence length scales is [1x1]
        % Iturb = ; float; turbulence intensity is [1x1]
        % component : string; is 'u' or 'w'
        % -----------------------------------------
        % OUTPUT
        % Sv: float; [1x1] value of Spectrum for a given frequency
        % -----------------------------------------
        % -----------------------------------------
        %%
        n = f.*L./V;
        if strcmp(component,'u')==1,
            Sv = stdV.^2./f.*(4.*n)./(1+6.*n).^(5/3);
        elseif strcmp(component,'w')==1,
            Sv = stdV.^2./f.*(4.*n)./(1+6.*n).^(5/3);
```

```
        else
            fprintf(' spectrum type is unknown \n')
            return
        end
    end
end
```

Appendix 4: SAP2000 Vehicle Modelling

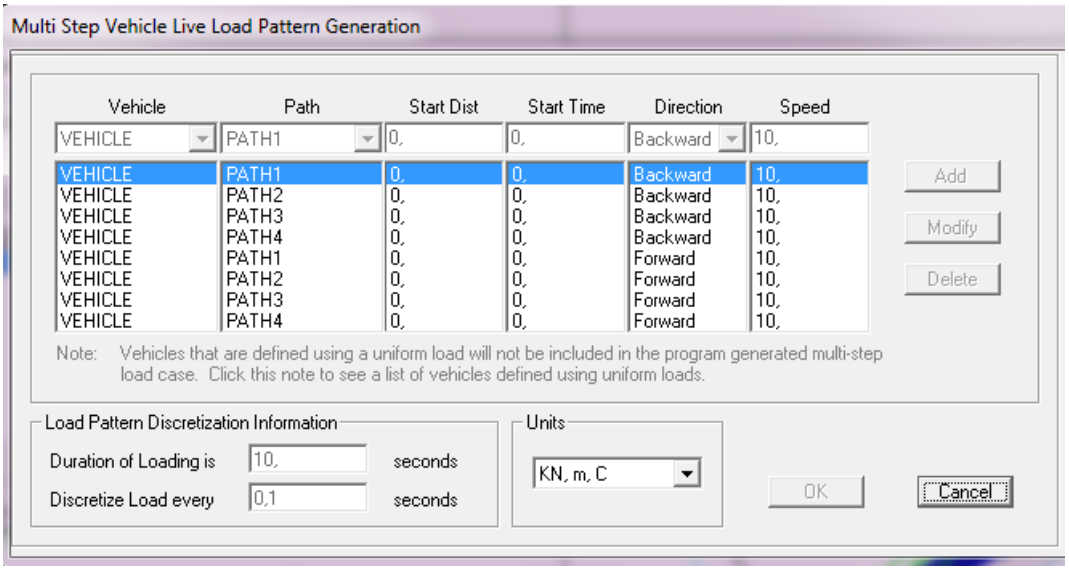

Appendix 5: SAP2000 LRB Bearing Modelling